2

PL-TR-91-2212(I)

TGAL-91-05

RECENT METHODOLOGICAL DEVELOPMENTS IN MAGNITUDE DETERMINATION AND YIELD ESTIMATION WITH APPLICATIONS TO SEMIPALATINSK EXPLOSIONS

Rong-Song Jih
Robert A. Wagner

Teledyne Geotech Alexandria Laboratory
3l4 Montgomery Street
Alexandria, VA 22314-1581

16 JULY 1991

FINAL REPORT (VOLUME I)
16 APRIL 1989 - 15 JULY 1991

APPROVED FOR PUBLIC RELEASE
DISTRIBUTION UNLIMITED

PHILLIPS LABORATORY
AIR FORCE SYSTEMS COMMAND
HANSCOM AIR FORCE BASE, MASSACHUSETTS 01731-5000

SPONSORED BY
Defense Advanced Research Projects Agency
Nuclear Monitoring Research Office
ARPA ORDER NO. 5307

MONITORED BY
Phillips Laboratory
Contract F19628-89-C-0063

This technical report has been reviewed and is approved for publication.

JAMES F. LEWKOWICZ
Contract Manager
Solid Earth Geophysics Branch
Earth Sciences Division

JAMES F. LEWKOWICZ
Branch Chief
Solid Earth Geophysics Branch
Earth Sciences Division

DONALD H. ECKHARDT, Director
Earth Sciences Division

REPORT DOCUMENTATION PAGE	Form Approved OMB No 0704-0188

1. AGENCY USE ONLY (Leave blank)	2. REPORT DATE	3. REPORT TYPE AND DATES COVERED
	16 July 1991	Final Report, 16 Apr 1989 - 15 Jul 1991

4. TITLE AND SUBTITLE

Recent Methodological Developments in Magnitude Determination and Yield Estimation with Applications to Semipalatinsk Explosions

5. FUNDING NUMBERS

Contract F19628-89-C-0063

PE 62714E
PR 9A10
TA DA
WU AZ

6. AUTHOR(S)

R.-S. Jih and R.A. Wagner

7. PERFORMING ORGANIZATION NAME(S) AND ADDRESS(ES)

Teledyne Geotech
314 Montgomery Street
Alexandria, VA 22314-1581

8. PERFORMING ORGANIZATION REPORT NUMBER

TGAL-91-05

9. SPONSORING/MONITORING AGENCY NAME(S) AND ADDRESS(ES)

DARPA/NMRO (Attn: Dr. A. Ryall)
3701 North Fairfax Drive
Arlington, VA 22209-1714

Phillips Laboratory
Hanscom AFB, MA 01731-5000

Contract Manager: J. Lewkowicz/LWH

10. SPONSORING/MONITORING AGENCY REPORT NUMBER

PL-TR-91-2212(I)

11. SUPPLEMENTARY NOTES

12a. DISTRIBUTION/AVAILABILITY STATEMENT

Approved for Public Release; Distribution Unlimited

12b. DISTRIBUTION CODE

13. ABSTRACT *(Maximum 200 words)*

Section I. An improved magnitude determination procedure is presented to account for the empirical near-source focusing/defocusing effects. This scheme provides more stable m_b measurements with a reduction in the fluctuational variation by a factor of up to 3. The events which do not show significant improvement could have been detonated in environments with different focusing patterns. The scatter in the network-averaged m_b based on the new scheme versus log(yield) is smaller than that for conventional GLM or LSMF m_b.

Section II. The research accomplished under this contract is summarized. Our major developments in the seismic yield estimation methodology include: [1] a refined m_b determination scheme (*cf.* Section I), [2] a regression algorithm "MLE-CY" which utilizes the bounded (*i.e.*, censored) yields in the m_b-yield calibration based on the maximum-likelihood approach, and [3] a regression algorithm "DWLSQ" which permits both variables to be imprecise due to either rounding or standard measurement errors, thus extending the ordinary weighted least-squares regression. These new techniques are fully tested with recently published Soviet yields (Bocharov *et al.*, 1989) of historical Semipalatinsk explosions and the WWSSN m_b database established at Geotech. The results all appear to be very encouraging in improving our remote monitoring capability.

14. SUBJECT TERMS	15. NUMBER OF PAGES
Magnitude Determination, Yield Estimation, Regression, Uncertainty, Least-squares, Maximum-likelihood, Rounding Error	104
	16. PRICE CODE

17. SECURITY CLASSIFICATION OF REPORT	18. SECURITY CLASSIFICATION OF THIS PAGE	19. SECURITY CLASSIFICATION OF ABSTRACT	20. LIMITATION OF ABSTRACT
Unclassified	Unclassified	Unclassified	UL

NSN 7540-01-280-5500 Standard Form 298 (Rev 2-89) Prescribed by ANSI Std Z39-18

Table of Contents

RECENT METHODOLOGICAL DEVELOPMENTS IN MAGNITUDE DETERMINATION AND YIELD ESTIMATION WITH APPLICATIONS TO SEMIPALATINSK EXPLOSIONS

R.-S. Jih and R. A. Wagner
Teledyne Geotech Alexandria Laboratory
314 Montgomery Street
Alexandria, VA 22314-1581

SUMMARY

This report includes two parts. The first section discusses in detail the research that was done since the submittal of our first annual report *(GL-TR-90-0107)*, and the second part gives a perspective overview of the whole project. Note that the same contract number (F19628-89-C-0063) is also used by two other totally independent tasks. This volume covers only the work performed under Task 1.

An improved magnitude determination procedure is described and tested in **Section I.** This procedure accounts for the near-source focusing/defocusing effects as well as the receiver effects with empirically determined correction terms. Although no *a priori* geophysical information is required in deriving these receiver and near-source terms, the inferred corrections turn out to show fair correlation with the tectonics underneath the receivers as well as the visible geological structures near the source region. For 79 out of 82 Semipalatinsk events in our WWSSN database, the new scheme provides more stable m_b measurements across the whole recording network with a reduction in the fluctuational variation by a factor of up to 3. The 3 events which do not show significant improvement could have been detonated in environments with different focusing patterns. The scatter in the network-averaged m_b based on the new scheme versus log(yield) is smaller than that for conventional GLM or LSMF m_b, if the standard and/or the rounding errors in the m_b and Soviet-published yields (Bocharov *et al.*, 1989) are included in the regressions.

Section II summarizes the research accomplished during the contract period, including those major results already reported in our first annual report *(GL-TR-90-0107)* as well as those discussed in Section I. The most important developments in the seismic yield estimation methodology under this project are:

- a refined m_b determination scheme (*cf.* Section I),
- an algorithm "MLE-CY" which utilizes the bounded yields in the m_b-yield regression based on the maximum-likelihood approach,
- an algorithm "DWLSQ" which permits both variables to be imprecise due to either rounding or standard measurement errors.

We have fully tested these techniques with Soviet-published yields and the WWSSN m_b database established at Geotech, and the results all appear to be very encouraging in improving our remote monitoring capability.

Also included in this report is a complete listing of 192 event m_b values measured off 21547 WWSSN recordings **(Appendix A)**. We have updated the "yield-dependent" test site bias estimate using these GLM91A m_b values **(Appendix B)**.

SECTION I

A REFINED NETWORK m_b DETERMINATION SCHEME INCORPORATING NEAR-SOURCE EFFECTS

Rong-Song Jih and Robert A. Wagner
Teledyne Geotech Alexandria Laboratories
314 Montgomery Street
Alexandria, VA 22314-1581

I.1 ABSTRACT

An improved magnitude determination procedure is presented to account for the empirical near-source focusing/defocusing effects. For 79 out of 82 Semipalatinsk events in our WWSSN database, the new scheme provides more stable m_b measurements across the whole recording network with a reduction in the fluctuational variation by a factor of up to 3. The standard error in the resulting network-averaged m_b is typically around 0.02 m.u., similar to that of *RMS* L_g based on in-country regional recordings. The 3 events which do not show significant improvement could have been detonated in environments with different focusing patterns. The scatter in the network-averaged m_b based on the new scheme versus log(yield) is smaller than that for conventional GLM or LSMF m_b, if the standard and/or the rounding errors in the m_b and Soviet-published yields are included in the regressions.

I.2 INTRODUCTION

The main problem with the conventional m_b is that it is a rather nebulous parameter; simply, it is a function of the largest peak-to-peak amplitude in the first few seconds of P wave motion with adjustment for the period of the arriving phase. The

parameter m_b was adapted from the need to order systematically the size of earthquakes. The measure itself has inherent impreciseness as the measure is not related to the physics of the source *per* se but is the largest constructive interference of waves originating at the source, source region, propagation path, receiver region, and receivers (Butler, 1981; Johnson, 1981). To relate the m_b to the seismic yield, all effects not due to the source must naturally be corrected. It is often difficult, however, to separate these effects. In fact, the effects of source and propagation are often indistinguishable, and unless one is known the other can not be uniquely determined (Johnson, 1981). Consequently, it was reported to be difficult to make m_b measurements that are internally consistent within 0.1 m_b with the conventional m_b (Bache, 1982), simply because some of the aforementioned effects are not accounted for accurately.

Von Seggern (1973) showed that including station corrections typically halves the standard deviation of m_b from North American LRSM stations recording NTS events. Even better results, with the standard deviation reduced by a factor of 3 or so, can be obtained for a network with all stations beyond 30°. Applying station corrections to the m_b determination or the network spectra averaging has become a standard procedure in this community (*e.g.*, Lilwall *et al.*, 1988; Murphy *et al.*, 1989; Sykes and Ekstrom, 1989; Jih and Shumway, 1989; and many others). The station effects are strongly dependent on azimuth (Chang and von Seggern, 1980), which led Bache (1982) and many others to believe that statistical station corrections will not be nearly so effective in reducing m_b variance in the multiple source region problem.

Marshall *et al.* (1979) attempted to correct several important factors that can bias m_b. They used bulletin log(A/T) data. These data are corrected for receiver-station attenuation differences, and the resulting magnitude is called m_2. Correcting m_2 for source-region attenuation gives m_3, and correcting m_3 for source depth gives m_Q. (The network averages of these m_bs are denoted by $\bar{m}_1$, $\bar{m}_2$, $\bar{m}_3$, and $\bar{m}_Q$, respectively.) The major change in this scheme is associated with the source-region

correction, which can be as different as 0.4 m.u. between sites or a factor of about 2.5 in yield estimates. Essentially this approach is based on the the discovery by Marshall and Springer (1976) and Douglas *et al.* (1981) that LRSM amplitude residuals correlate with P_n velocity near the stations, and under the assumption that such correlation between the attenuation and P_n is valid elsewhere as well. However, it turns out that the standard deviation of the m_Q is not less than that for the m_1 and m_2 from the same data set, indicating that the attenuation correction in Marshall *et al.* (1979) is not correlated with the residuals from these stations (Bache, 1982).

It is obvious that the only way to reduce the statistical fluctuation is to obtain fundamental causal knowledge of the focusing and defocusing beneath the source and receiver. We expect teleseismic P-wave amplitudes to vary as source location changes within a test site. The m_b residuals (with respect to the best-fitting m_b-yield curve) of NTS events show systematic trends that are consistent with local tectonics (Minster *et al.*, 1981). At Yucca Flat, the residuals are positive to the west and negative to the east of the north-south trending normal fault system that bisects the valley. At Pahute Mesa, the spatial pattern is less clear, but the residuals tend to be negative toward the center of the buried Silent Canyon Caldera and positive toward the edges. An attractive explanation is that these variations are due to focusing/defocusing effects that are not averaged out over the network, although the possibility of systematic source-coupling difference has not been eliminated.

Figure 1 illustrates the m_b residual patterns of E. Kazakh explosions as seen from various directions. For each event, the residual is the (maximum-likelihood) average of all station residuals (*viz*, with network m_b and the station term removed) in that quadrant. All three subsites exhibit very different azimuthal variation. For instance, Murzhik events are enhanced in the NE and SW directions and reduced in the NW and SE directions, whereas Degelen events are reduced towards the SW direction. There seems to be some weak distinction between NE and SW subregions of Balapan test site along SE and NW directions. Figure 2 gives the azimuthal pattern with the

four quadrants rotated by 45°. The initial P waves from the three adjacent test sites have virtually the same incident angle at any particular teleseismic station, and anything in common across all events (such as the crustal amplification as well as the upper mantle attenuation underneath the receiver) would have been lumped into the constant station term. Thus the station residuals averaged over all events from the same test site would correlate very little with the receiver. Instead, they should reveal more site-dependent information about the focusing/defocusing pattern underneath E. Kazakhstan.

In this study, we present an improved scheme to determine the network m_b with both the station terms and near-source focusing/defocusing effects corrected. Examples are given to illustrate that such procedure can reduce the random fluctuation in the station m_b values to about 0.15 m.u. or lower. It is shown that, by applying this scheme to worldwide explosions, it is possible to have a consistent base line in estimating the absolute magnitudes, which is crucial in estimating the test site bias, while the precision in the resulting network m_b values can be maintained as well as could be achieved by the single-test-site approach.

mb(Pmax) RESIDUALS AS SEEN FROM VARIOUS DIRECTIONS

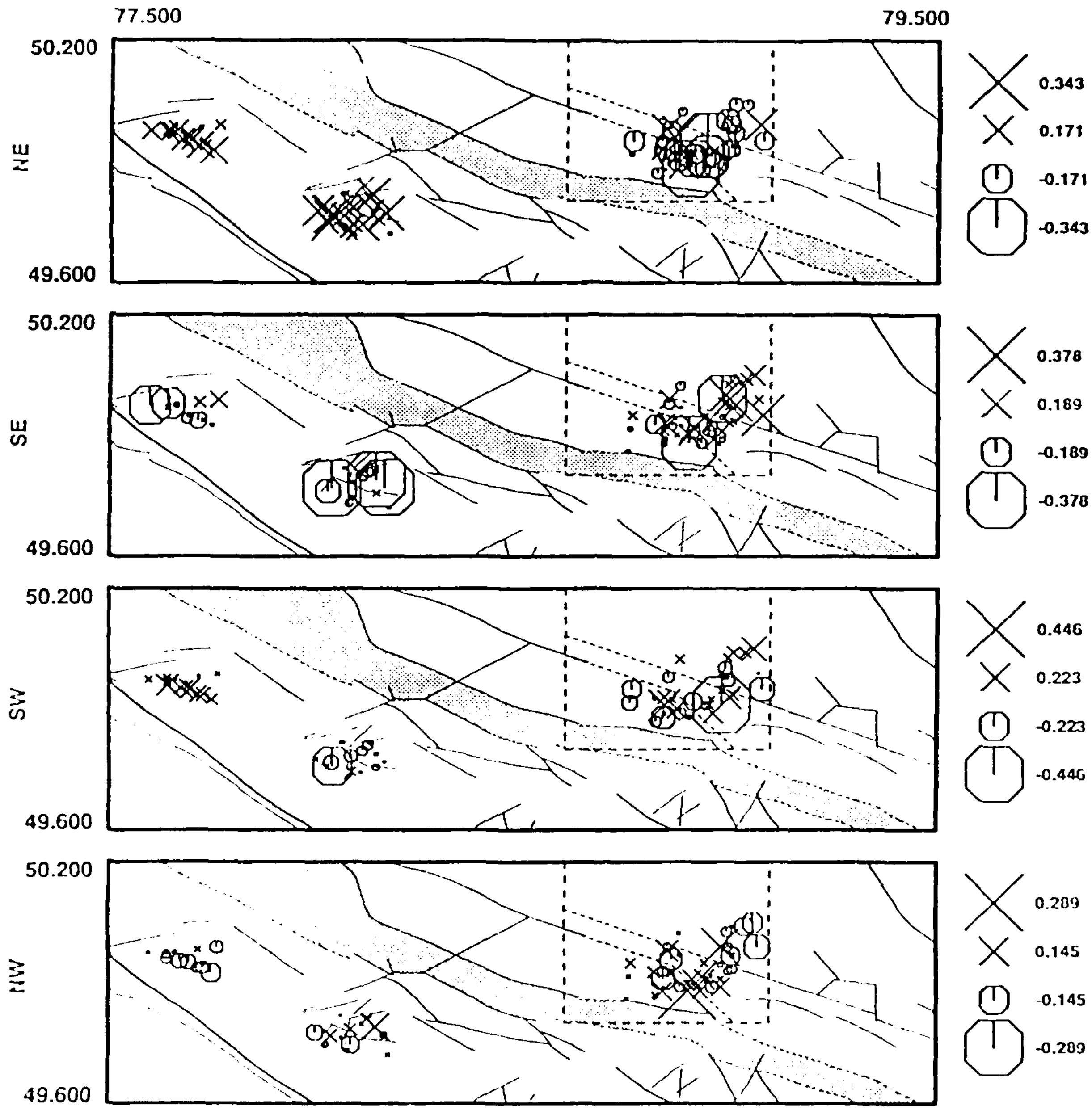

Figure 1. The m_b residuals of E. Kazakh explosions as seen from various directions. For each event, the residual is the (maximum-likelihood) average of all station residuals (viz with network m_b and the station term removed) in that quadrant. All three subsites exhibit very different azimuthal variation. For instance, Murzhik events are enhanced in the NE and SW directions, and reduced in the NW and SE directions, whereas Degelen events are reduced towards the SW direction. There seems to be some weak distinction between NE and SW subregions of Balapan test site along SE and NW directions.

mb(Pmax) RESIDUALS AS SEEN FROM VARIOUS DIRECTIONS

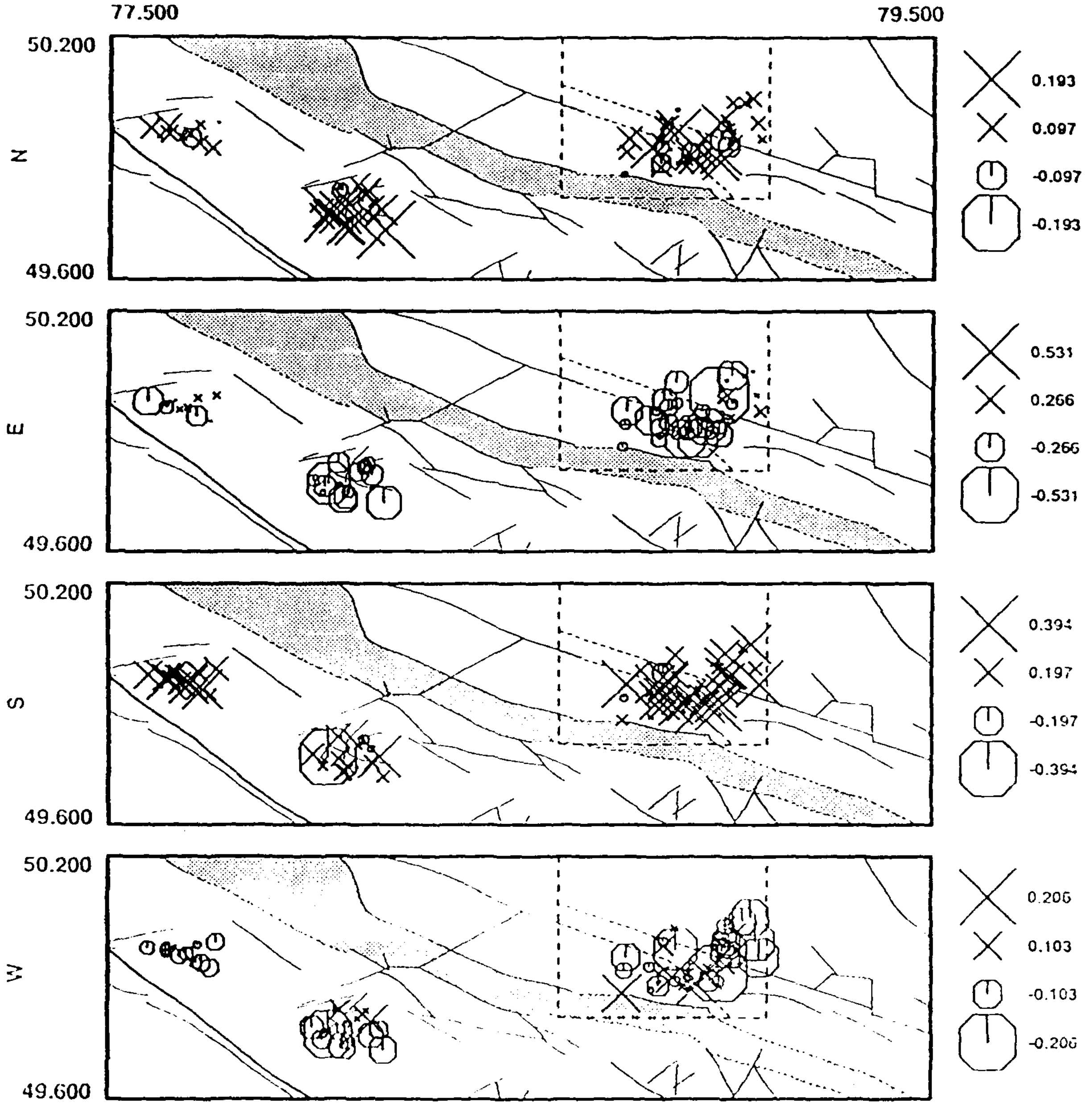

Figure 2. The azimuthal patterns with the four quadrants rotated by 45°. Most Semipalatinsk events are enhanced in the north, and reduced in the east.

I.3 DEFINITION OF A NEW MAGNITUDE, $m_{2.9}$

The conventional definition of station magnitude is computed as

$$m_b = \log_{10}(A/T) + B(\Delta) \qquad [1]$$

where A is the displacement amplitude (in nm) and T is the predominant period (in sec) of the *P* wave. The B(Δ) is the distance-correction term that compensates for the change of *P*-wave amplitudes with distance (*e.g.*, Gutenberg and Richter, 1956; Veith and Clawson, 1972). m_b in [1] is also denoted as m_1 in Marshall *et al.* (1979). The ISC bulletin m_b is just the network average of these raw station m_b values without any further adjustment.

Consider N_e explosions detonated at N_F source regions that are recorded at some or all of N_s stations. The GLM91A network m_b (*cf.* Appendix A) is the (maximum-likelihood) average of the "station-corrected" magnitudes:

$$m_{2.2}(i,j) \equiv m_1(i,j) - S(j) \qquad [2]$$

where S(j) is the "statistical" receiver correction at the j-th station. In Marshall *et al.* (1979), *a priori* information about the P_n velocity underneath each station is used to determine its associated "deterministic" receiver correction, S(j), and the resulting magnitude is called m_2. Our receiver corrections (Figure 3), however, are inferred jointly from a suite of event-station pairs, and no *a priori* geophysical or geological condition is assumed (and hence the different notation $m_{2.2}$). It turns out when the azimuthal coverage is broad enough, receiver corrections derived by such statistical approach do reveal the average tectonic structure underneath the recording stations, as many earlier studies have reported (*e.g.*, North, 1977): the station terms are positive in shields regions such as Australia, India, Canada, and Scandinavia; and they are negative in the east Africa rift valleys, island arcs (*e.g.*, Japan and Taiwan), and Indonesia. The high correlation between the tectonic type and the station terms suggests that the station corrections do reflect the upper mantle conditions underneath the receivers. The result also supports the claim of a marginal superiority of WWSSN

over ISC data. For instance, Pacific island arcs are believed to have high attenuation, low P_n velocities as well as negative station terms. However, North's (1977) station corrections based on 38316 ISC recordings of earthquakes around the world do not show this phenomenon because ISC does not have so wide an azimuthal coverage and uniform spatial sampling as does WWSSN.

WWSSN & ISC STATION CORRECTIONS

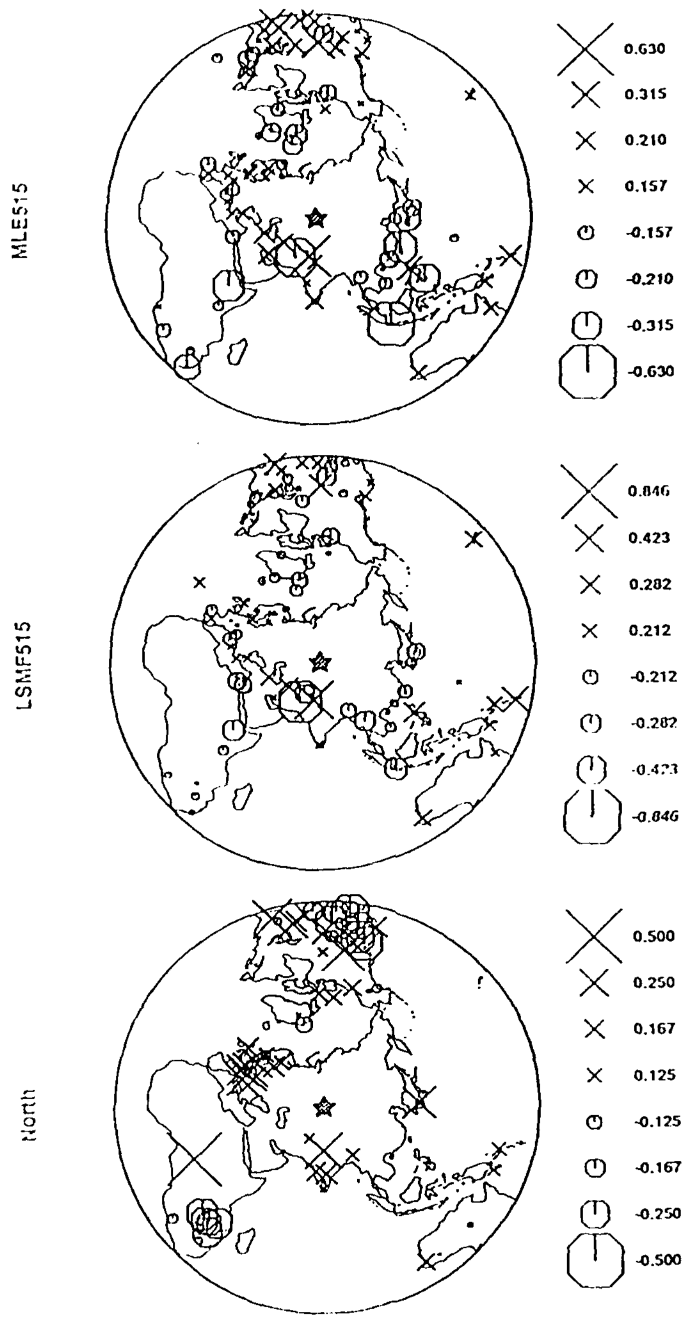

Figure 3. The station terms derived with WWSSN and ISC recordings. Our station terms (top; used in this study) are based on the GLM/MLE joint inversion of 192 worldwide explosions recorded at 122 "good" WWSSN stations. Only paths within 20 and 95 degrees are used. For each station, our GLM/LSMF joint inversion scheme puts any component constant across all events as the "station term", similar to the Douglas' (1966) LSMF approach. Both GLM (top) and LSMF (middle) station corrections exhibit a good correlation with the tectonics. The high correlation between the tectonic type and the station terms suggests that the station corrections do reflect the upper mantle conditions underneath the receivers. The result also supports the claim of a marginal superiority of WWSSN over ISC data, such as the 38316 ISC recordings used by North (1977) (bottom).

We now define a new magnitude, $m_{2.9}$, to account for the near-source focusing and defocusing effects:

$$m_{2.9}(i,j) \equiv m_1(i,j) - S(j) - F(k(i),j) = m_{2.2}(i,j) - F(k(i),j) \qquad [3]$$

At the j-th station, F(k(*),j) is a constant for all events detonated in the same k-th "geologically and geophysically uniform region". Partitioning a single nuclear test site into several "regions" may be necessary in order to account accurately for the focusing/defocusing effects. This $m_{2.9}$ is very similar to the m_3 in Marshall *et al.* (1979) except that, again, *a priori* attenuation information of the source region is used in Marshall *et al.* (1979) to determine the correction term, whereas we invert for the near-source effects from the data empirically. (The correlation between our statistical focusing/defocusing corrections and the geological structures will be verified in a later section.) As a result, the source-region corrections used by Marshall *et al.* (1979) are constants (for all explosions in the same source region) regardless of the location of the seismic stations, whereas our near-source corrections are dependent on the source-station paths.

Table 1 lists the station corrections (which are invariant for any explosion from any test site at any direction) as well as the near-source corrections associated with each subsite of Soviet's Semipalatinsk nuclear test ground.[1] Figure 4 plots out the lower-hemisphere equal-area projection of these "secondary corrections". The spatial map of these corrections are shown in Figure 5.

[1]The near-source corrections for other test sites can be similarly derived. Our explosion data set needs to be expanded, however, to warrant a reasonable partitioning at other source regions.

EQUAL-AREA PLOTS OF STATION MEAN mb(Pmax) ANOMALIES

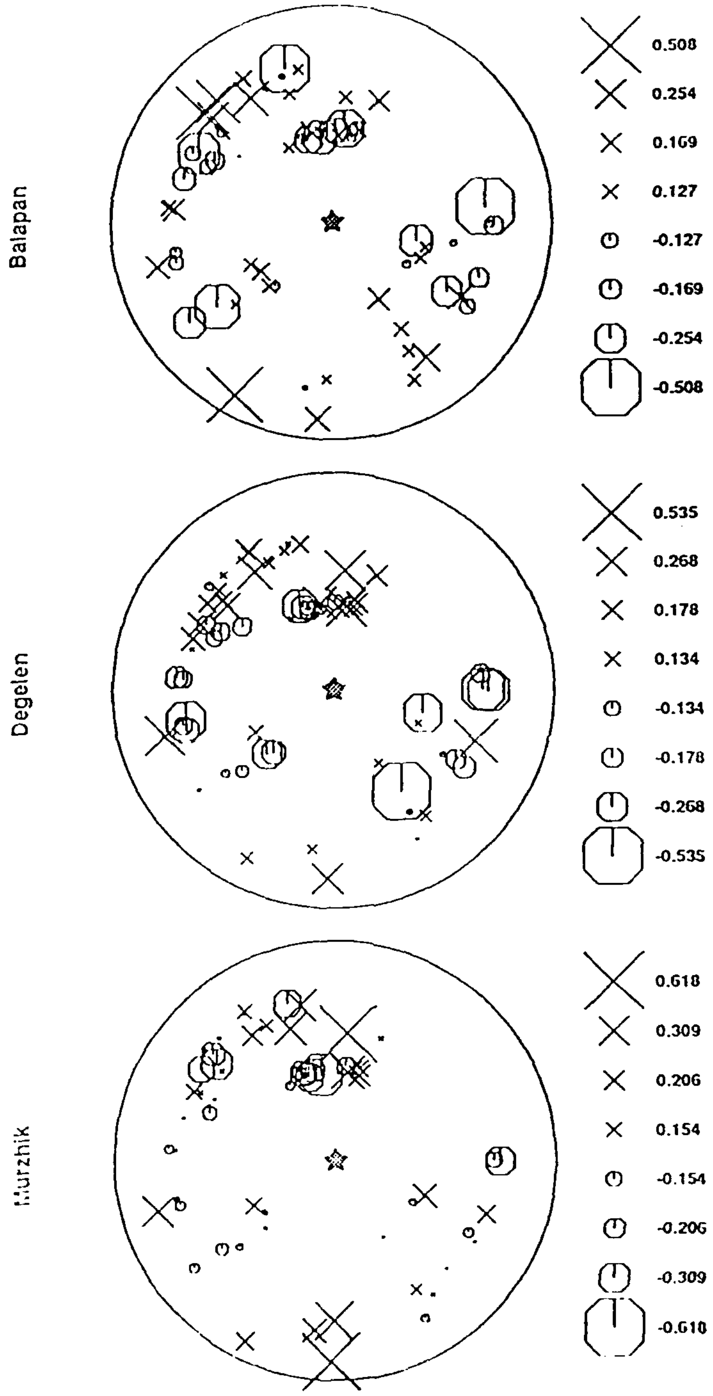

Figure 4. Lower-hemisphere equal-area projection of station-corrected $m_b(P_{max})$ anomalies for Soviet's 3 test sites in Eastern Kazakhstan. For each station, the mean m_b anomaly is defined as the mean residual averaged over all explosions from the same test site. The different patterns more or less reflect the focusing/defocusing underneath the source region.

MEAN STATION-CORRECTED mb(Pmax) ANOMALIES

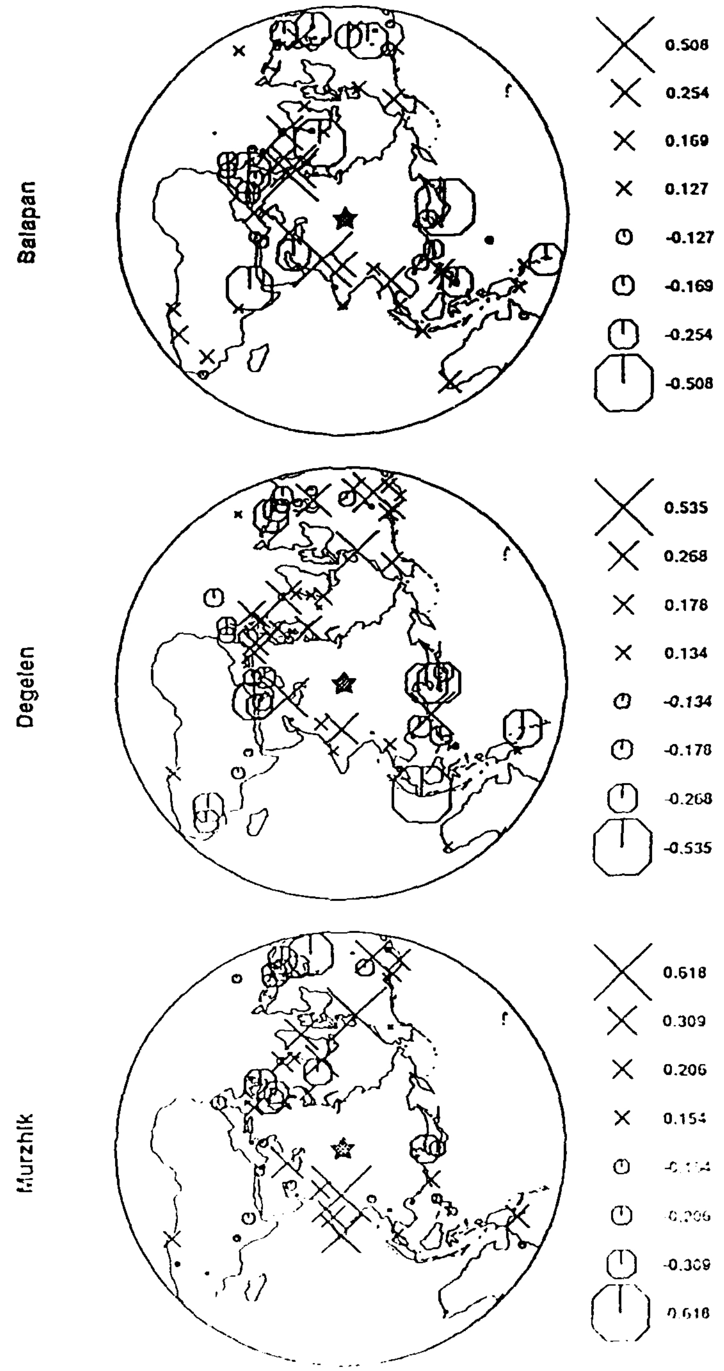

Figure 5. Same as Figure 4 except the mean m_b anomalies are superimposed by the map. We propose to regard these (site-dependent) mean station m_b anomalies as the "secondary corrections" to be applied in the procedure of magnitude determination.

Table 1. Receiver and Near-source Corrections of WWSSN Stations

Station Term		Near-source Term, F			Station		
Code	S	Balapan	Degelen	Murzhik	Longitude	Latitude	Description
AAE	-0.352	-0.387	-0.076	-0.127	38.766	9.029	Addis Ababa, Ethiopia
AAM	0.205	0.202	-0.073	-0.247	-83.656	42.300	Ann Arbor, Michigan
ADE	-0.044	____	____	____	138.709	-34.967	Adelaide, south Australia
AFI	-0.135	____	____	____	-171.777	-13.909	Afiamalu, Samoa Islands
AKU	-0.048	0.300	0.311	0.212	-18.107	65.687	Akureyri, Iceland
ALQ	-0.028	____	____	____	-106.457	34.943	Albuquerque, New Mexico
ANP	-0.349	-0.167	0.402	0.183	121.517	25.183	Anpu, Taiwan
ANT	0.040	____	____	____	-70.415	-23.705	Antofagasta, northern Chile
AQU	-0.133	-0.195	0.039	-0.024	13.403	42.354	Aquila, central Italy
ARE	0.223	____	____	____	-71.491	-16.462	Arequipa, southern Peru
ATL	0.141	____	____	____	-84.338	33.433	Atlanta, Georgia
ATU	0.128	0.191	-0.156	0.034	23.717	37.972	Athens Univ., Greece
BAG	-0.027	0.076	-0.009	-0.103	120.580	16.411	Baguio City, Luzon Island
BDF	0.067	____	____	____	-47.903	-15.664	Brasilia Array, Brazil
BEC	-0.114	0.090	0.058	-0.092	-64.681	32.379	Bermuda-Columbia, Atlantic
BHP	-0.219	____	____	____	-79.558	8.961	Balboa Heights, Panama
BKS	0.089	-0.014	0.101	0.229	-122.235	37.877	Byerly, central California
BLA	0.057	-0.233	-0.177	-0.299	-80.421	37.211	Blacksburg, West Virginia
BOG	0.032	____	____	____	-74.065	4.623	Bogota, Colombia
BOZ	0.188	-0.325	-0.025	-0.180	-111.633	45.600	Bozeman, Montana

Table 1. Receiver and Near-source Corrections of WWSSN Stations							
Station Term		Near-source Term, F			Station		
Code	S	Balapan	Degelen	Murzhik	Longitude	Latitude	Description
BUL	0.003	0.014	-0.266	-0.037	28.613	-20.143	Bulawayo, Rhodesia
CAR	0.190	____	____	____	-66.928	10.507	Caracas, Venezuela
CHG	-0.140	0.240	0.106	0.045	98.977	18.790	Chiengmai, southeast Asia
CMC	-0.178	0.114	0.375	0.602	-115.083	67.833	Copper Mine, Canada
COL	0.065	0.181	0.188	0.051	-147.793	64.900	College Outpost, Alaska
COP	0.127	-0.003	0.159	-0.276	12.433	55.683	Copenhagen, Denmark
COR	0.155	0.132	0.183	0.172	-123.303	44.586	Corvallis, Oregon
CTA	0.153	-0.072	0.003	-0.073	146.254	-20.088	Charters Towers, Australia
DAG	0.036	-0.052	0.086	____	-18.770	76.770	Danmarkshavn, Greenland
DAL	0.202	____	____	____	-96.784	32.846	Dallas, central Texas
DAV	-0.320	-0.264	-0.053	____	125.575	7.088	Davao, Mindanao Island
DUG	0.149	0.038	0.371	0.352	-112.813	40.195	Dugway, Utah
EIL	0.004	-0.117	-0.228	-0.103	34.950	29.550	Eilat, Arabic Peninsula
EPT	-0.023	____	____	____	-106.506	31.772	El Paso, Texas-Mexico border
ESK	0.048	-0.042	0.162	-0.327	-3.205	55.317	Eskdalemuir, Scotland
FLO	0.000	-0.294	-0.093	-0.446	-90.370	38.802	Florissant, eastern Missouri
FVM	0.034	-0.038	0.045	____	-90.426	37.984	French Village, eastern Missouri
GDH	-0.147	0.094	0.015	0.336	-53.533	69.250	Godhavn, western Greenland
GEO	-0.003	0.038	-0.016	-0.051	-77.067	38.900	Georgetown, Washington D.C.
GIE	-0.175	____	____	____	-90.300	-0.733	Galapagos Islands

Table 1. Receiver and Near-source Corrections of WWSSN Stations							
Station Term		Near-source Term, F			Station		
Code	S	Balapan	Degelen	Murzhik	Longitude	Latitude	Description
GOL	-0.204	0.114	0.199	-0.028	-105.371	39.700	Golden, Colorado
GRM	-0.285	-0.075	____	____	26.573	-33.313	Grahamstown, southern Africa
GSC	0.057	-0.072	0.131	-0.064	-116.805	35.302	Goldstone, central California
GUA	-0.088	-0.059	____	____	144.912	13.538	Guam, Mariana Islands
HKC	-0.188	-0.130	-0.200	-0.026	114.172	22.304	Hong Kong
HLW	-0.150	-0.096	-0.354	____	31.342	29.858	Helwan, Arabic Peninsula
HN-ME	0.175	____	____	____	-67.986	46.162	Houlton, New Brunswick
HNR	0.238	-0.278	____	____	159.947	-9.432	Honiara, Solomon Islands
IST	0.148	0.129	-0.195	-0.090	28.996	41.046	Istanbul, Turkey
JCT	0.133	____	____	____	-99.802	30.479	Junction City, central Texas
JER	0.011	-0.035	-0.159	-0.054	35.197	31.772	Jerusalem, Dead Sea region
KBL	0.023	____	____	____	69.043	34.541	Kabul, Afghanistan
KBS	-0.213	-0.429	0.043	-0.284	11.924	78.918	Kingsbay, Svalbard region
KEV	-0.119	0.139	0.122	-0.029	27.007	69.755	Kevoa, Finland
KIP	0.110	____	____	____	-158.015	21.423	Kipapa, Hawaii
KOD	0.196	0.075	0.015	0.402	77.467	10.233	Kodaikanal, India
KON	0.046	0.271	0.141	-0.243	9.598	59.649	Kongsberg, southern Norway
KRK	-0.004	____	0.233	0.150	30.062	69.724	Kirkenes, Sandinavia
KTG	-0.208	0.041	0.101	0.132	-21.983	70.417	Kap Tobin, eastern Greenland
LAH	0.469	____	____	____	74.333	31.550	Lahore, India-Pakistan border

Table 1. Receiver and Near-source Corrections of WWSSN Stations							
Station Term		Near-source Term, F			Station		
Code	S	Balapan	Degelen	Murzhik	Longitude	Latitude	Description
LEM	-0.499	0.123	-0.535	____	107.617	-6.833	Lembang, Java
LON	-0.044	-0.119	0.159	0.077	-121.810	46.750	Longmire, Washington
LOR	0.095	-0.362	-0.165	0.056	3.851	47.267	Lormes, France
LPA	0.357	____	____	____	-57.932	-34.909	La Plata, Uruguay
LPB	0.064	____	____	____	-68.098	-16.533	La Paz, Peru-Bolivia border
LPS	-0.068	____	____	____	-89.162	14.292	La Palma, Guatemala
LUB	0.191	____	____	____	-101.867	33.583	Lubbock, west Texas
MAL	-0.010	0.005	0.013	-0.145	-4.411	36.728	Malaga, Straits of Gibraltar
MAN	0.276	0.212	-0.181	____	121.077	14.662	Manila, Luzon island
MAT	-0.188	-0.508	-0.167	0.015	138.207	36.542	Matsushiro, Honshu, Japan
MDS	-0.043	-0.031	0.302	____	-89.760	43.372	Madison, Wisconsin
MNN	0.153	-0.037	____	____	-93.190	44.914	Minneapolis, Minnesota
MSH	0.202	____	____	____	59.588	36.311	Meshed, Iran-USSR border
MSO	-0.045	-0.019	-0.047	____	-113.941	46.829	Missoula, Montana
MUN	0.172	0.184	0.076	0.026	116.208	-31.978	Mundaring, western Australia
NAI	-0.112	0.075	-0.108	-0.075	36.804	-1.274	Nairobi, Kenya
NAT	0.118	____	____	____	-35.033	-5.117	Natal, Brazil
NDI	0.158	0.216	0.286	0.618	77.217	28.683	New Delhi, northern India
NHA	-0.134	____	-0.010	0.019	109.212	12.210	Nhatrang, southeast Asia
NIL	-0.030	____	____	____	73.252	33.650	Nilore, Pakistan

Table 1. Receiver and Near-source Corrections of WWSSN Stations							
Station Term		Near-source Term, F			Station		
Code	S	Balapan	Degelen	Murzhik	Longitude	Latitude	Description
NNA	-0.171	____	____	____	-76.842	-11.988	Nana, Peru
NOR	-0.240	0.086	0.154	0.335	-16.683	81.600	Nord, north coast of Greenland
NP-NT	0.107				-119.372	76.252	North Pole, Queen Elizabeth Islands
NUR	0.090	0.473	-0.076	0.041	24.651	60.509	Nurmijarvi, Finland
OGD	-0.167	-0.061	-0.214	-0.263	-74.596	41.088	Ogdensburg, New York
OXF	0.293	____	____	____	-89.409	34.512	Oxford, Mississippi
PDA	0.017	0.018	-0.167	____	-25.663	37.747	Ponta Delgada, Azores Islands
PEL	0.029	____	____	____	-70.685	-33.144	Peldehue, Chile-Argentina border
PMG	0.151	0.101	0.060	0.253	147.154	-9.409	Port Moresby, New Guinea
POO	0.076	-0.041	0.082	0.251	73.850	18.533	Poona, India
PRE	-0.089	0.118	-0.210	-0.017	28.190	-25.753	Pretoria, south Africa
PTO	-0.172	-0.163	-0.166	-0.029	-8.602	41.139	Porto, Serro Do Portugal
QUE	-0.446	0.484	0.107	0.190	66.950	30.188	Quetta, Pakistan
QUI	0.023	____	____	____	-78.501	-0.200	Quito, Ecuador
RAB	0.022	0.090	-0.347	-0.002	152.170	-4.191	Rabaul, New Britain region
RAR	-0.093	____	____	____	-159.773	-21.212	Rarotonga, Cook Islands region
RCD	0.370	-0.217	-0.139	____	-103.208	44.075	Rapid city, South Dakota
RIV	0.300	____	____	____	151.158	-33.829	Riverview, SE Australia
RK-ON	-0.013	____	____	____	-93.672	50.839	Red Lake, Ontario
SCP	-0.005	0.037	-0.129	-0.229	-77.865	40.795	State College Pennsylvania
SDB	0.053	0.114	0.130	0.172	13.572	-14.926	Sa Da Bandeira, Angola

Table 1. Receiver and Near-source Corrections of WWSSN Stations							
Station Term		Near-source Term, F			Station		
Code	S	Balapan	Degelen	Murzhik	Longitude	Latitude	Description
SEO	-0.132	-0.159	-0.377	-0.304	126.967	37.567	Seoul, South Korea
SHA	0.297	____	____	____	-88.143	30.694	Spring Hill, Mississippi
SHI	0.237	-0.273	-0.027	-0.105	52.520	29.638	Shiraz, southern Iran
SHK	-0.286	-0.063	-0.387	-0.160	132.678	34.532	Shiraki, southern Honshu, Japan
SHL	-0.001	0.106	0.024	-0.088	91.883	25.567	Shillong, India-Bangladesh border
SJG	-0.129	____	____	____	-66.150	18.112	San Juan, Puerto Rico
SNG	-0.003	0.099	-0.055	0.115	100.620	7.173	Songkhla, Malay Peninsula
SPA	-0.630	____	____	____	0.000	-90.000	South Pole, Antarctica
STU	0.067	-0.127	0.230	0.170	9.195	48.772	Stuttgart, Germany
TAB	0.234	0.189	0.363	0.325	46.327	38.068	Tabriz, Iran-USSR border
TAU	-0.137	____	____	____	147.320	-42.910	Tasmania Univ., Tasmania
TOL	0.169	-0.135	-0.143	-0.027	-4.049	39.881	Toledo, Spain
TRI	-0.144	0.027	0.215	0.016	13.764	45.709	Trieste, northern Italy
TRN	0.064	____	____	____	-61.403	10.649	Trinidad, Trinidad
TUC	0.008	____	____	____	-110.782	32.310	Tucson, eastern Arizona
UMF	0.144	0.385	0.058	0.040	20.237	63.815	Umea, Sweden
UNM	-0.266	____	____	____	-99.178	19.329	Nat Univ. of Central Mexico
VAL	-0.027	-0.070	0.237	0.050	-10.244	51.939	Valentia, Eire
WEL	0.107	____	____	____	174.768	-41.286	Wellington, New Zealand
WES	-0.216	-0.014	-0.309	-0.141	-71.322	42.385	Weston, New England
WIN	-0.154	0.151	0.009	-0.055	17.100	-22.567	Windhoek, South-West Africa

Table 2 lists the results of applying the receiver and near-source corrections (as shown in Table 1) to the 82 Semipalatinsk explosions in our database. For 79 out of 82 Semipalatinsk events used in this study, the final σ is typically around or below the same level that a "single-event MLE with primary correction only" could achieve. The only three events which do not show reduction in the variance are 770730D, 730723B, and 880914B (Table 2). A plausible explanation is that perhaps these three events are located in very different geological or geophysical environments from other events in the same testing area. Or, perhaps the 26 WWSSN stations for which the filmchips of JVE were available only cover a small portion of the focal sphere, and hence the focusing/defocusing effect is not fully accounted for. Most of the $\overline{m}_{2.9}$ in Table 2 have a standard error around 0.02 m.u., which is about the same as that for *RMS* L_g values inferred from an in-country regional network (*e.g.*, Israelson, 1991; Hansen *et al.*, 1990).

Another observation is that the resulting m_b values, $\overline{m}_{2.9}$ are essentially the same as those inferred from the GLM or the single-event MLE, $\overline{m}_{2.2}$. Figures 6 through 10 plot out the three different m_bs for five arbitrarily selected events. The solid line and the dashed lines represent the mean network-averaged m_b and the associated standard deviation of station m_b. The upward arrows represent the lower bounds of the station m_b, which came from those clipped measurements. The "Y" symbols are the upper bounds of the station m_b which are resulted from those noisy measurements. Both the "uncensored" (shown in filled circles) and "censored" station m_bs are used in computing the mean station residuals with the maximum-likelihood scheme described in Jih and Shumway (1989).

Table 2. Comparison of Network-Averaged m_b with Various Corrections				
Event	# of signals	Without correction	Station corrected	Near-source corrected
Date		$\overline{m}_1$, σ	$\overline{m}_{2.2}$, σ	$\overline{m}_{2.9}$, σ
661218M	51 2 1	5.747±0.038 0.281	5.753±0.033 0.239	5.738±0.022 0.161
670916M	36 18 2	5.097±0.041 0.305	5.110±0.036 0.268	5.095±0.018 0.137
670922M	35 20 1	5.033±0.036 0.271	5.048±0.029 0.214	5.029±0.017 0.125
671122M	7 52 0	4.169±0.054 0.413	4.318±0.039 0.299	4.231±0.013 0.099
690531M	30 21 0	4.965±0.050 0.357	5.006±0.039 0.276	5.026±0.015 0.110
691228M	45 2 3	5.666±0.043 0.306	5.665±0.035 0.250	5.660±0.018 0.125
700721M	38 12 1	5.182±0.043 0.307	5.199±0.033 0.236	5.184±0.018 0.125
701104M	38 12 1	5.267±0.042 0.303	5.279±0.032 0.232	5.249±0.020 0.145
710606M	38 6 2	5.323±0.040 0.272	5.341±0.031 0.210	5.319±0.015 0.099
710619M	41 6 0	5.294±0.040 0.278	5.311±0.030 0.208	5.287±0.013 0.086
711009M	27 9 3	5.165±0.037 0.233	5.187±0.028 0.174	5.136±0.016 0.100
711021M	32 6 0	5.348±0.049 0.301	5.383±0.036 0.224	5.341±0.021 0.127
720826M	29 10 2	5.168±0.045 0.290	5.186±0.030 0.193	5.163±0.017 0.111
720902M	15 25 0	4.615±0.049 0.312	4.635±0.038 0.243	4.602±0.017 0.107
651121D	48 12 1	5.384±0.035 0.271	5.394±0.024 0.188	5.381±0.019 0.152
660213D	51 2 10	6.073±0.038 0.305	6.092±0.027 0.218	6.088±0.014 0.114
660320D	49 6 8	5.848±0.041 0.322	5.865±0.030 0.239	5.853±0.009 0.074
660507D	9 23 1	4.517±0.043 0.250	4.559±0.031 0.181	4.456±0.014 0.078
661019D	51 8 5	5.534±0.035 0.276	5.542±0.025 0.201	5.525±0.014 0.111
670226D	48 7 6	5.826±0.044 0.341	5.843±0.035 0.274	5.854±0.011 0.086

Table 2. Comparison of Network-Averaged m_b with Various Corrections				
Event	# of signals	Without correction	Station corrected	Near-source corrected
Date		$\overline{m}_1$, σ	$\overline{m}_{2.2}$, σ	$\overline{m}_{2.9}$, σ
680929D	50 4 6	5.610±0.035 0.275	5.642±0.026 0.202	5.641±0.018 0.138
690723D	38 17 1	5.172±0.041 0.306	5.201±0.029 0.220	5.186±0.013 0.100
690911D	19 35 0	4.533±0.053 0.392	4.605±0.040 0.295	4.634±0.025 0.186
710322D	43 11 3	5.498±0.040 0.305	5.528±0.032 0.245	5.530±0.017 0.126
710425D	37 3 0	5.764±0.052 0.327	5.793±0.042 0.267	5.826±0.020 0.127
711230D	16 2 0	5.522±0.060 0.255	5.556±0.062 0.262	5.556±0.035 0.148
720328D	28 15 0	4.955±0.048 0.313	4.997±0.034 0.226	4.984±0.021 0.141
720816D	23 20 1	4.908±0.044 0.293	4.931±0.033 0.221	4.921±0.025 0.165
721210D	30 6 5	5.512±0.045 0.287	5.543±0.033 0.209	5.555±0.029 0.183
770329D	25 12 0	4.974±0.055 0.332	5.015±0.042 0.256	4.992±0.042 0.254
770730D	21 14 0	4.858±0.051 0.301	4.881±0.049 0.287	4.855±0.052 0.306
780326D	25 4 0	5.461±0.052 0.279	5.519±0.037 0.198	5.476±0.018 0.096
780422D	21 7 0	4.985±0.057 0.301	5.032±0.044 0.231	5.010±0.023 0.120
780728D	36 7 6	5.506±0.042 0.291	5.525±0.028 0.198	5.494±0.012 0.086
800522D	36 20 1	5.138±0.033 0.250	5.156±0.025 0.193	5.131±0.012 0.089
650115B	46 1 2	5.896±0.040 0.280	5.893±0.032 0.223	5.861±0.022 0.155
680619B	28 3 2	5.276±0.047 0.270	5.285±0.035 0.203	5.229±0.026 0.151
691130B	51 0 0	5.950±0.044 0.313	5.973±0.031 0.222	5.945±0.026 0.184
710630B	31 18 1	5.045±0.043 0.301	5.075±0.035 0.247	5.043±0.027 0.192
720210B	34 8 2	5.297±0.042 0.278	5.329±0.029 0.195	5.289±0.018 0.121

Table 2. Comparison of Network-Averaged m_b with Various Corrections				
Event	# of signals	Without correction	Station corrected	Near-source corrected
Date		m_1, σ	$m_{2.2}$, σ	$m_{2.9}$, σ
721102B	42 0 15	6.173±0.045 0.339	6.183±0.034 0.256	6.160±0.023 0.177
721210B	45 1 11	6.006±0.037 0.282	6.013±0.029 0.223	5.983±0.022 0.169
730723B	54 0 1	6.174±0.042 0.314	6.202±0.030 0.220	6.179±0.031 0.231
731214B	50 7 6	5.750±0.044 0.348	5.769±0.036 0.287	5.749±0.030 0.241
750427B	18 1 1	5.457±0.099 0.444	5.480±0.089 0.397	5.436±0.072 0.322
760704B	38 0 5	5.819±0.062 0.404	5.849±0.048 0.313	5.829±0.027 0.180
761207B	17 2 1	5.571±0.107 0.480	5.611±0.099 0.442	5.550±0.078 0.347
780611B	17 0 1	5.882±0.048 0.205	5.873±0.042 0.179	5.804±0.038 0.160
780915B	37 1 6	5.826±0.057 0.379	5.850±0.043 0.284	5.828±0.030 0.199
790623B	40 2 3	6.015±0.052 0.349	6.071±0.040 0.267	6.069±0.036 0.240
790804B	40 4 20	6.064±0.037 0.295	6.086±0.027 0.212	6.103±0.016 0.126
791028B	44 6 13	5.909±0.036 0.284	5.941±0.024 0.190	5.933±0.019 0.151
791223B	41 3 17	6.111±0.033 0.260	6.128±0.020 0.154	6.131±0.018 0.141
800914B	35 4 6	6.006±0.062 0.417	6.041±0.051 0.345	6.053±0.043 0.287
811018B	41 3 7	5.954±0.039 0.279	5.976±0.029 0.210	5.996±0.023 0.164
840526B	31 0 3	5.966±0.058 0.338	5.993±0.043 0.252	6.009±0.022 0.130
880914B	25 0 1	6.004±0.037 0.191	6.032±0.023 0.117	6.026±0.033 0.168
761123B	22 0 0	5.577±0.075 0.354	5.626±0.065 0.305	5.687±0.053 0.249
780829B	16 0 0	5.869±0.079 0.315	5.905±0.075 0.302	5.936±0.045 0.182
781129B	28 0 0	5.840±0.068 0.358	5.880±0.054 0.287	5.895±0.026 0.138
790707B	30 0 0	5.734±0.048 0.261	5.800±0.043 0.236	5.827±0.031 0.169

Table 2. Comparison of Network-Averaged m_b with Various Corrections				
Event	# of signals	Without correction	Station corrected	Near-source corrected
Date		$\overline{m}_1$, σ	$\overline{m}_{2.2}$, σ	$\overline{m}_{2.9}$, σ
790818B	28 0 0	6.023±0.065 0.344	6.087±0.052 0.273	6.088±0.031 0.166
791202B	15 0 0	5.807±0.112 0.435	5.874±0.089 0.344	5.892±0.067 0.259
801012B	23 0 0	5.804±0.087 0.417	5.828±0.070 0.334	5.872±0.047 0.228
801214B	29 0 0	5.873±0.053 0.288	5.911±0.047 0.252	5.935±0.030 0.162
801227B	24 0 0	5.855±0.056 0.273	5.896±0.042 0.208	5.892±0.034 0.165
810422B	25 0 0	5.826±0.070 0.350	5.865±0.057 0.287	5.922±0.035 0.174
810913B	17 0 0	6.014±0.093 0.383	6.024±0.064 0.265	6.060±0.023 0.096
811227B	23 0 0	6.187±0.079 0.380	6.207±0.060 0.287	6.189±0.036 0.174
820425B	14 0 0	5.924±0.099 0.372	5.944±0.072 0.269	5.982±0.040 0.150
820704B	21 0 0	6.073±0.053 0.245	6.089±0.048 0.222	6.095±0.032 0.145
821205B	26 0 0	6.043±0.064 0.325	6.093±0.053 0.271	6.109±0.037 0.191
830612B	16 0 0	5.921±0.091 0.365	5.943±0.069 0.276	5.934±0.046 0.186
831006B	25 0 0	5.885±0.064 0.318	5.942±0.048 0.238	5.935±0.032 0.162
831026B	18 0 0	5.933±0.070 0.298	5.941±0.053 0.225	5.998±0.034 0.146
840425B	21 0 0	5.850±0.099 0.453	5.892±0.082 0.374	5.905±0.043 0.196
840714B	23 0 0	5.920±0.088 0.424	5.999±0.074 0.357	6.054±0.043 0.207
841027B	19 0 0	6.141±0.078 0.340	6.150±0.066 0.289	6.191±0.034 0.146
841202B	22 0 0	5.630±0.065 0.305	5.693±0.057 0.266	5.720±0.044 0.206
841216B	15 0 0	5.911±0.107 0.415	5.993±0.070 0.272	6.043±0.035 0.135
841228B	19 0 0	5.853±0.077 0.335	5.916±0.053 0.230	5.945±0.037 0.162
850615B	15 0 0	6.016±0.078 0.301	6.069±0.049 0.191	6.060±0.035 0.134

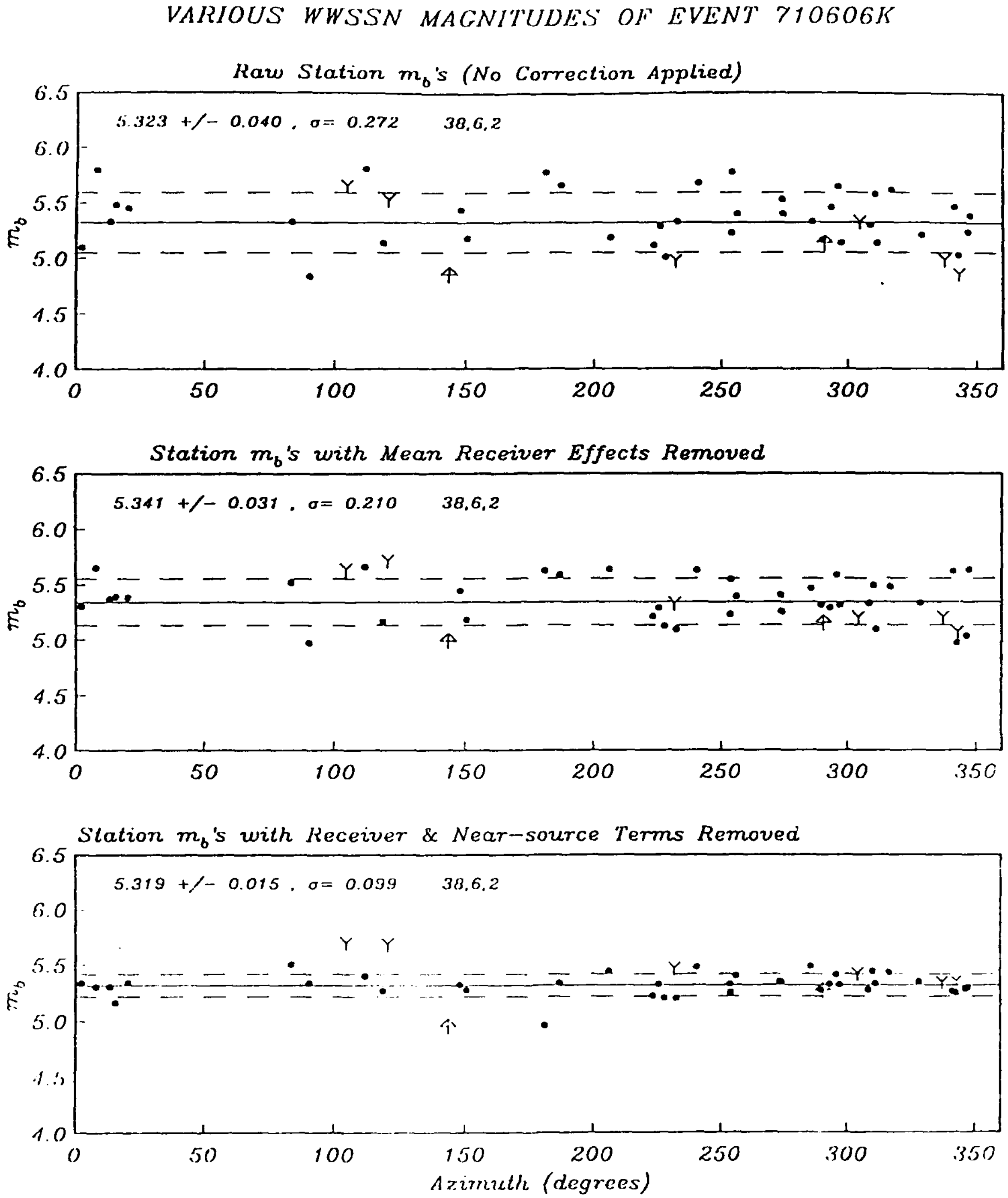

Figure 6. Scatter plot of 3 different types of station m_bs for Murzhik explosion 710606. The 38 good recordings, 6 noise, and 2 clips are shown with filled circles, Y-shaped downward arrows and upward arrows, respectively. The raw station m_bs (top) has a standard deviation of 0.27 m.u. Applying the "primary" station corrections reduces the scatter to 0.21 m.u. Applying the proposed "secondary" station corrections to count for the near-source focusing/defocusing effects would further reduce the scatter down to 0.1 m.u. The dashed lines around the network-averaged m_b clearly illustrate the remarkable reduction of fluctuation across the recording stations. The mean event m_b itself is not significantly changed, however.

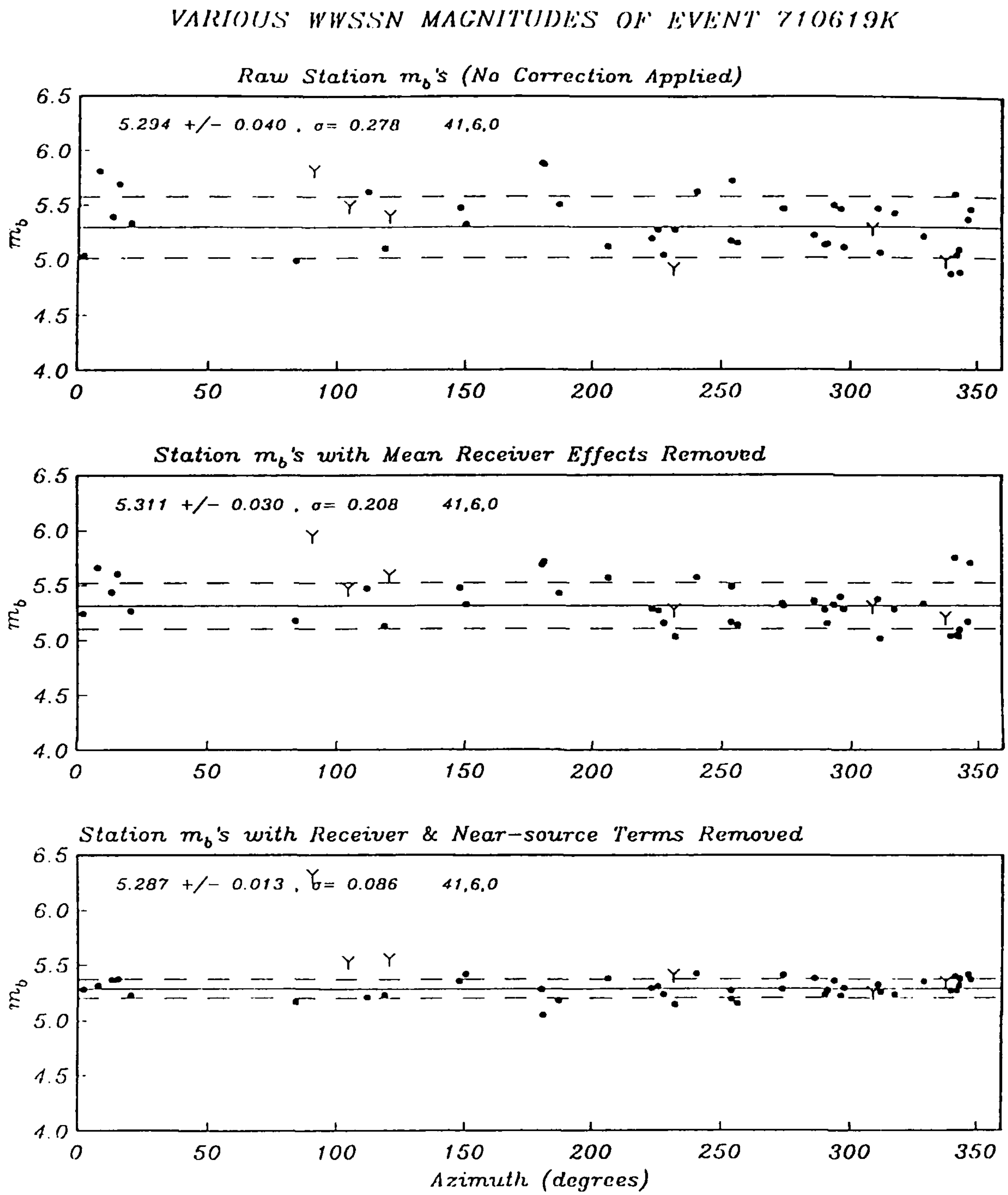

Figure 7. Same as Figure 6 except for Murzhik event 710619.

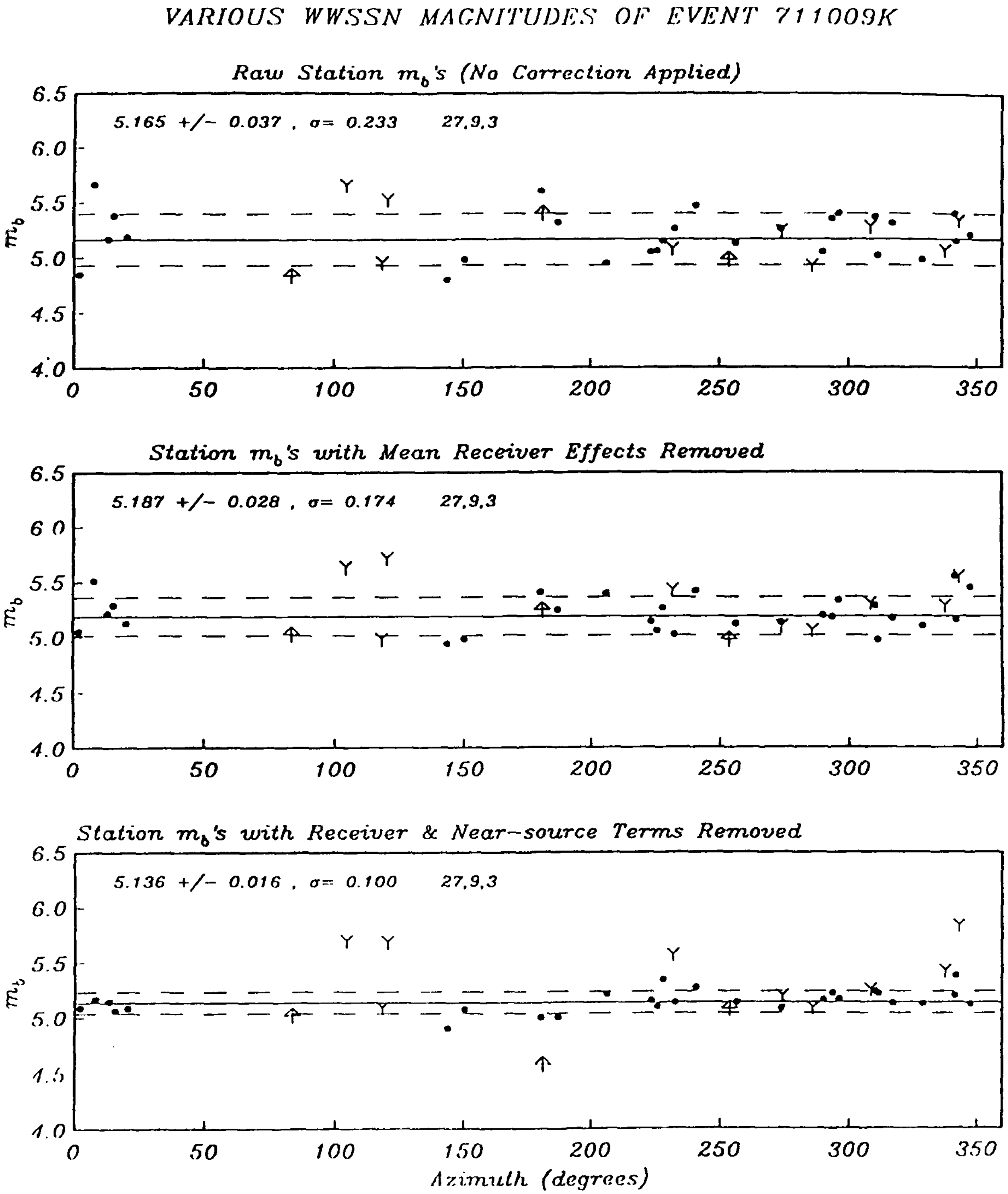

Figure 8. Same as Figure 6 except for Murzhik event 711009.

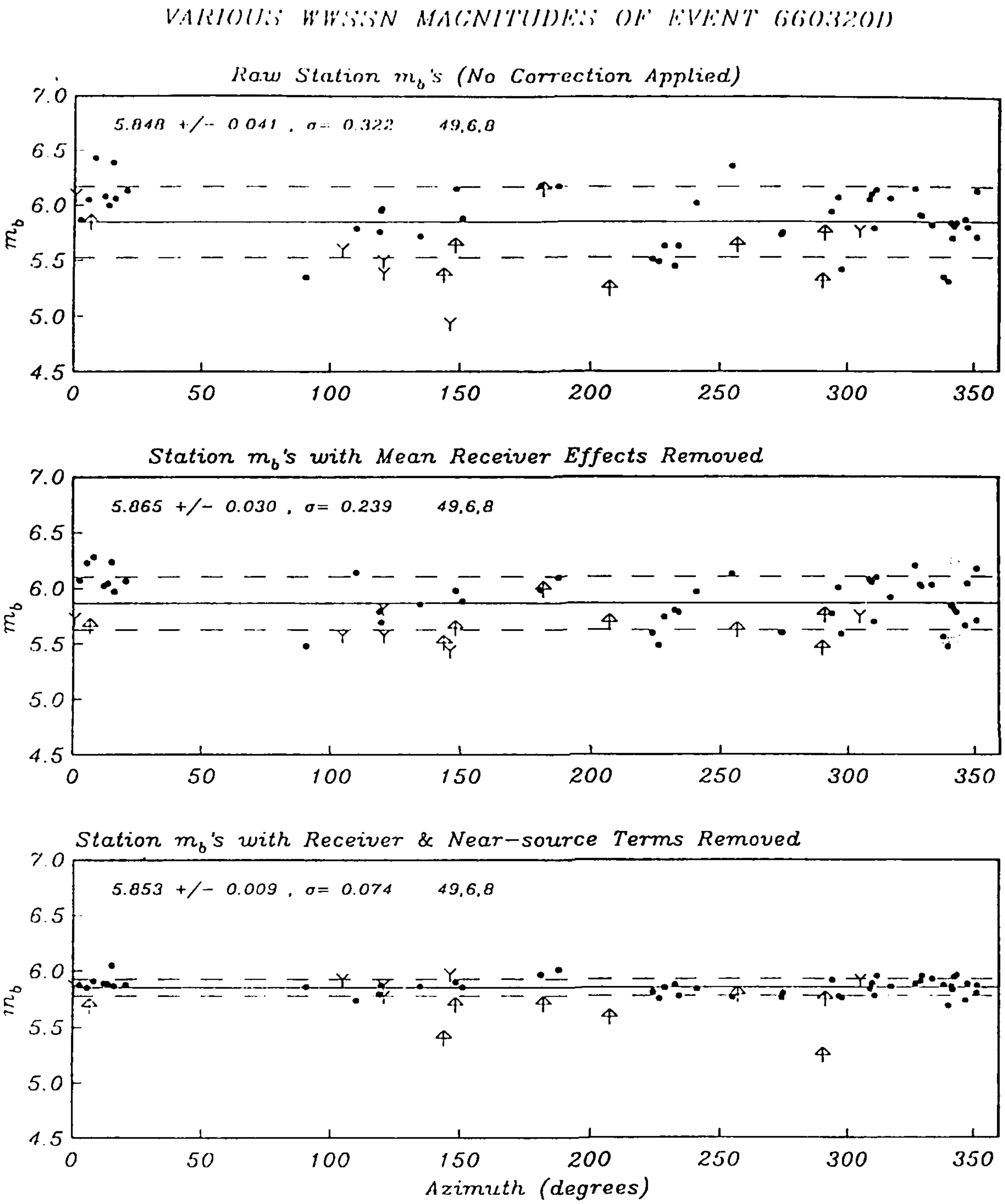

Figure 9. Same as Figure 6 except for Degelen event 660320. The near-source correction proposed in this study not only reduced the m_b scatter at stations that reported the good signals, but also improved the data consistence of the censored recordings.

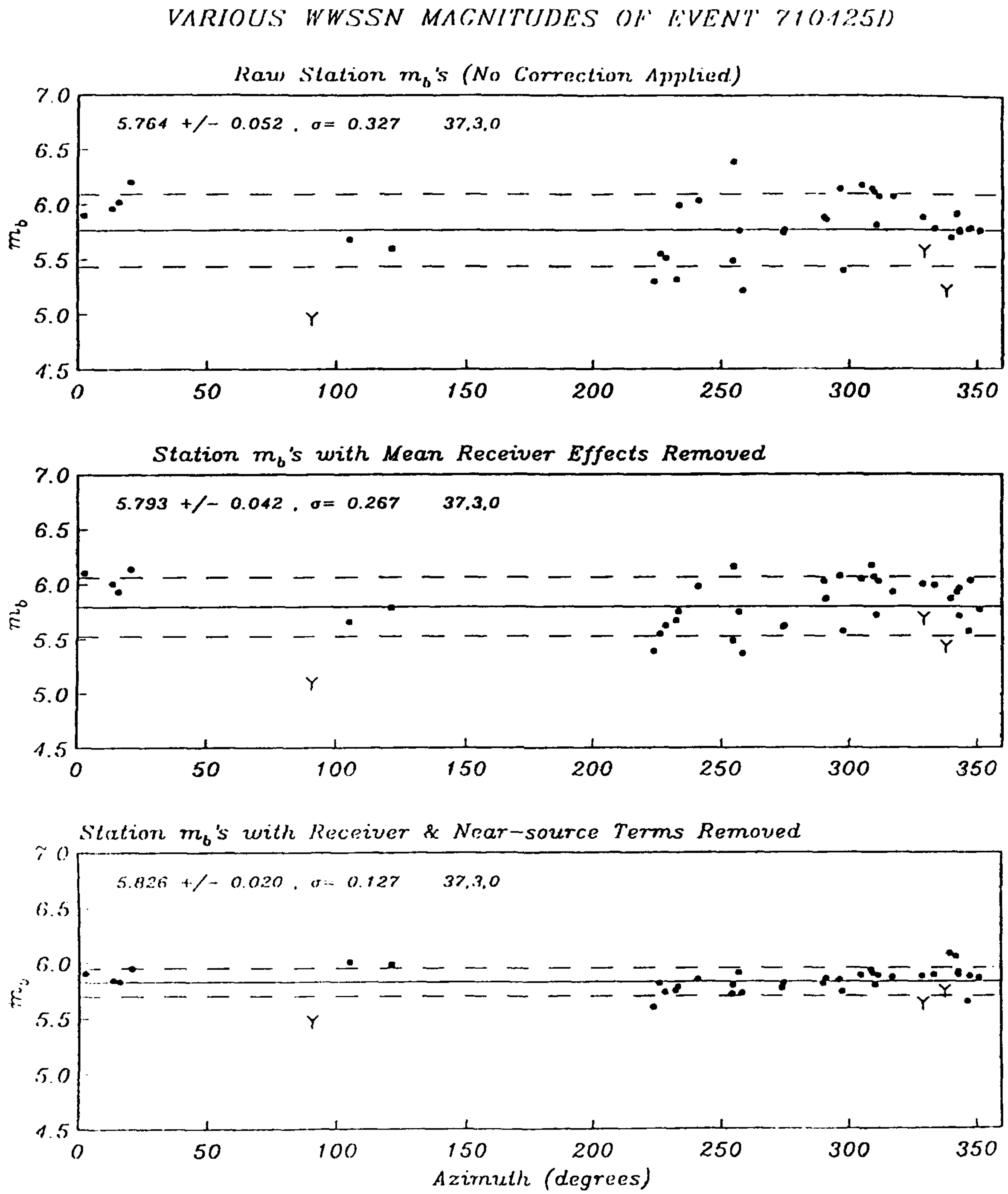

Figure 10. Same as Figure 6 except for Degelen event 710425.

I.4 UNDERLYING MODEL AND ADVANTAGES OF THE NEW MAGNITUDE

We now examine the fundamental difference between the present scheme and the previous ones. In LSMF and the standard GLM scheme (Douglas, 1966; Blandford and Shumway, 1982; Jih and Shumway, 1989; Murphy *et al.*, 1989), it is assumed that the observed station $m_b(i,j)$ is the sum of the true source size of the i-th event, E(i), the receiver term of the j-th station, S(j), and the random noise, v(i,j):

$$m_b(i,j) = E(i) + S(j) + v(i,j) \qquad [4]$$

The receiver term, S(j), is constant with respect to all explosions from many azimuths, and hence it would inherently reflect the "averaged" receiver effect --- provided the paths reaching the station have broad azimuthal coverage. These receiver corrections correlate with the upper mantle property underneath the receivers (North, 1977). When world-wide explosions are used, the standard deviation of the noise v in [4] is typically about 0.3 m.u. or larger.

If LSMF or GLM is applied to events within a smaller area of source region, then the σ could reduce to 0.15 or 0.2 m.u. Unfortunately, there are severe drawbacks associated with such "single-test-site GLM" approach. First of all, the station corrections will not necessarily represent the attenuation underneath the receiver side. They could be contaminated or even overwhelmed by the near-source effects shared by the explosions confined in a narrow azimuthal range. This explains the phenomenon Butler (1981) and Burdick (1981) reported that using Soviet explosions exclusively may fail to discern the attenuation differential between the eastern and western U.S. Secondly, when the "single-test-site GLM" inversion is applied to several test sites separately, there may not be a consistent baseline for magnitude comparison or absolute yield estimation, since the station terms are inherently inconsistent.

In the present scheme ([3]), however, we reformulate the whole model as

$$m_b(i,j) = E(i) + S(j) + F(k(i),j) + v(i,j) \qquad [5]$$

where F(k(i),j) is the correction term at the j-th station for the near-source

focusing/defocusing effect, which is constant for all events in the k-th "geologically and geophysically uniform region". For each seismic station, this F can be regarded as its azimuthal variation around the mean station term S. However, as we already explained, it would be more appropriate to consider F the near-source term because the back azimuths at the station could be nearly identical for adjacent test sites (such as Degelen and Murzhik), and yet the "F" terms could be very different. By incorporating the F term into the model, the σ for world-wide explosions is reduced to about 0.2, roughly the same level that which a "single-test-site GLM" could achieve. Intuitively, the present scheme (Equation [5]) provides a more detailed (and better) model than that of Equation [4] in describing the whole propagation path from the source towards the receiver. Simply put, Equation [4] yields a stronger fluctuation in the source terms, E, as well as a larger standard deviation of v because each term in the right-hand side of Equation [4] would have to "absorb" part of the missing F term in [5]. This is exactly the same reason why $m_{2.2}$ has smaller variation than m_1 since the latter would be interfered by the missing station term S in Equation [1].

For actual implementation, the present scheme can be replaced with an equivalent multi-stage procedure as follows. First, a set of station corrections (the so-called "primary corrections") is determined with one GLM. Then the "secondary correction" at each station is defined as the mean of all residuals of all events from the same test site (or the same geologic/geophysical regime) recorded at this particular station.

I.5 MAGNITUDE:YIELD RELATIONSHIP AT SEMIPALATINSK WITH $m_{2.9}$

To further demonstrate that $\bar{m}_{2.9}$ would provide more precise yield estimates, the 19 Semipalatinsk explosions for which the yields are published by Bocharov *et al.* (1989) are used as a test case. Table 3 gives the date, various m_b values, and the associated standard errors. Table 4 lists the Soviet-published yields and the

postulated uncertainties. We assume that these yields are subject only to 10% standard errors (S.E.) and/or the rounding. For each (m_b, yield) pair, we use a random number generator to produce a perturbed (m_b, yield) pair according to their uncertainty distribution. A standard least-squared regression is performed for each data set of perturbed samples. The procedure is repeated for several hundred iterations, and the resulting calibration curves (*i.e.*, the straight best-fitting lines) are shown as the darkened bundle in Figures 11 through 13. The detail of this generalized "doubly-weighted least-squares scheme" is discussed in Jih (1991). Here we only summarize the results to illustrate the advantages of $\overline{m}_{2.9}$ relative to the more conventional source measures. For comparison, regression result using RMS L_g reported at NORSAR (Ringdal, 1990) is also included in Tables 5 and 6 (Figure 14). Note that for the Soviet JVE shot (880914B), the yield is assumed to be 119 kt after Gordan (1988) (see also Sykes and Ekstrom, 1989; Priestley *et al.*, 1990). The regression result based on $\overline{m}_{2.9}$ has a smaller m_b scatter around the mean calibration curve (and hence a smaller uncertainty factor in the yield estimates) than those based on $\overline{m}_1$ and $\overline{m}_{2.2}$, as expected. It has a precision very close to that based on NORSAR RMS L_g over a wide range of yields. The precision is also very similar to what Patton (1988) found for 69 NTS explosions below the water table with L_g recorded at LLNL digital network. Note that the uncertainty factor in the yield estimates is yield dependent. It is smaller near the centroid of the data set (*i.e.*, around 50 kt in our case) and larger at both ends. This is contrary to a general perception that we might know yields much better at higher values around 150 kt. For yields below 10 kt there is no data point in NORSAR's RMS L_g data set, and hence there is a much larger uncertainty than that based on m_b.

Table 3. Various Network-Averaged m_b of 19 Special Events				
Event	# of signals	Without correction	Station corrected	Near-source corrected
Date		$\overline{m}_1$, σ	$\overline{m}_{2.2}$, σ	$\overline{m}_{2.9}$, σ
651121D	48 12 1	5.384±0.035 0.271	5.394±0.024 0.188	5.381±0.019 0.152
660213D	51 2 10	6.073±0.038 0.305	6.092±0.027 0.218	6.088±0.014 0.114
660320D	49 6 8	5.848±0.041 0.322	5.865±0.030 0.239	5.853±0.009 0.074
670922M	35 20 1	5.033±0.036 0.271	5.048±0.029 0.214	5.029±0.017 0.125
680929D	50 4 6	5.610±0.035 0.275	5.642±0.026 0.202	5.641±0.018 0.138
690723D	38 17 1	5.172±0.041 0.306	5.201±0.029 0.220	5.186±0.013 0.100
691130B	51 0 0	5.950±0.044 0.313	5.973±0.031 0.222	5.945±0.026 0.184
691228M	45 2 3	5.666±0.043 0.306	5.665±0.035 0.250	5.660±0.018 0.125
710425D	37 3 0	5.764±0.052 0.327	5.793±0.042 0.267	5.826±0.020 0.127
710606M	38 6 2	5.323±0.040 0.272	5.341±0.031 0.210	5.319±0.015 0.099
711009M	27 9 3	5.165±0.037 0.233	5.187±0.028 0.174	5.136±0.016 0.100
711021M	32 6 0	5.348±0.049 0.301	5.383±0.036 0.224	5.341±0.021 0.127
720210B	34 8 2	5.297±0.042 0.278	5.329±0.029 0.195	5.289±0.018 0.121
720816D	23 20 1	4.908±0.044 0.293	4.931±0.033 0.221	4.921±0.025 0.165
720902M	15 25 0	4.615±0.049 0.312	4.635±0.038 0.243	4.602±0.017 0.107
721102B	42 0 15	6.173±0.045 0.339	6.183±0.034 0.256	6.160±0.023 0.177
721210B	45 1 11	6.006±0.037 0.282	6.013±0.029 0.223	5.983±0.022 0.169
880914B	25 0 1	6.004±0.037 0.191	6.032±0.023 0.117	6.026±0.033 0.168

Table 6. 95% Confidence Scatter in m_b					
(assuming yields are subject to rounding and 10% S.E.)					
m_b used	1 kt	10 kt	50 kt	100 kt	150 kt
$\overline{m}_1$	0.27	0.16	0.14	0.15	0.17
$\overline{m}_{2.2}$	0.24	0.14	0.11	0.13	0.14
$\overline{m}_{2.9}$	0.21	0.11	0.09	0.11	0.13
NORSAR RMS L_g**	0.27	0.13	0.08	0.09	0.11
(assuming yields are subject to 10% S.E. only)					
$\overline{m}_1$	0.24	0.16	0.13	0.15	0.16
$\overline{m}_{2.2}$	0.21	0.13	0.11	0.13	0.14
$\overline{m}_{2.9}$	0.18	0.10	0.08	0.10	0.11
NORSAR RMS Lg	0.27	0.13	0.08	0.09	0.11

*) 19 Semipalatinsk shots in Table 3 used as calibration events.

**) 9 Semipalatinsk events with RMS L_g reported in Ringdal (1990) and Ringdal and Marshall (1989).

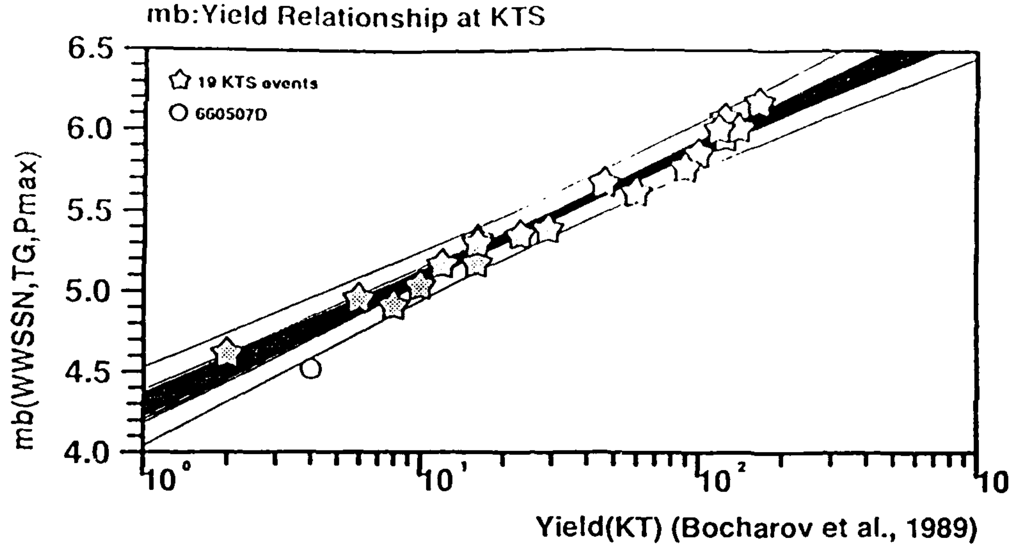

DWLS (uncertain X & Y): S=0.80(0.024), I=4.29(0.039), 19. data used,
95% error in mb at 1,10,50,100,150KT: 0.24, 0.15, 0.13, 0.15, 0.16,
95% factor in yield at 1,10,50,100,150KT: 3.96, 2.44, 2.13, 2.38, 2.57

OWLS (precise X assumed): S=0.82(0.032), I=4.26(0.052)

Standard LS: S=0.81(0.031), I=4.28(0.050)

10% s.e. in yields assumed; simple network-averaged mb used

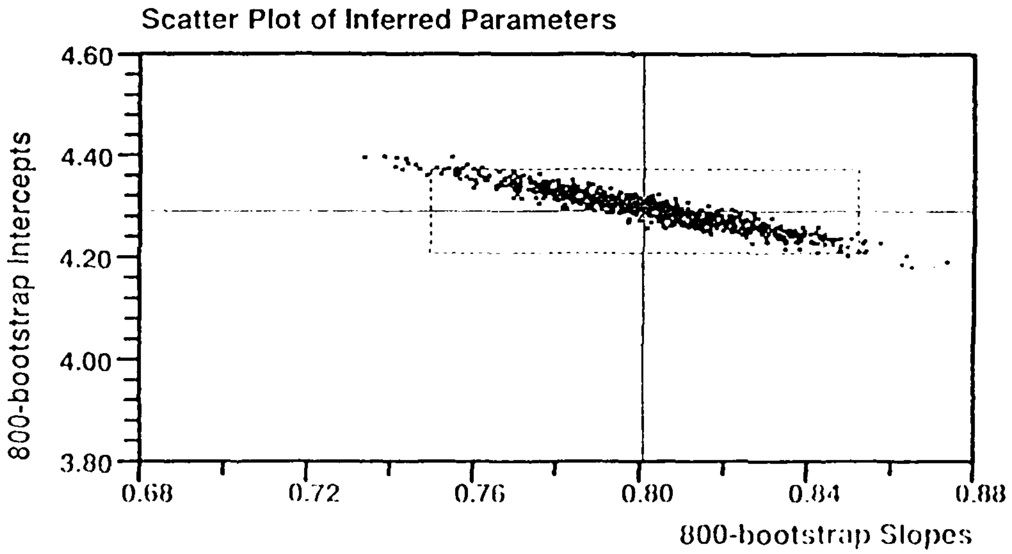

95% confidence interval of slope: 0.80+/-0.051
95% confidence interval of intercept: 4.29+/-0.082
[97.5% quantile of t(17. D.o.F.), 2.110, used]

Figure 11. Regressing the simple network-averaged m_b (*i.e.*, m_1) on the 19 Soviet-published yields. The yields are assumed to be subject to 10% standard errors. The uncertainties in the m_bs and the yields are taken into account through 800 bootstrap resamplings. The darkened bundle is actually the collection of all 800 regressions, each produced by a possible realization of 19 perturbed (m_b, yield) pairs. The 95% confidence band (shown as 2 curves around the darkened bundle) is narrower near the centroid and wider towards both ends, as expected. The individual 95% confidence intervals of the two inferred parameters (*i.e.*, the slope and the intercept of the calibration curve) are shown with the dashed line in the scatter plot (bottom). Note that the dashed rectangle is not the joint 90% confidence interval, however, due to the highly correlated nature of the two parameters.

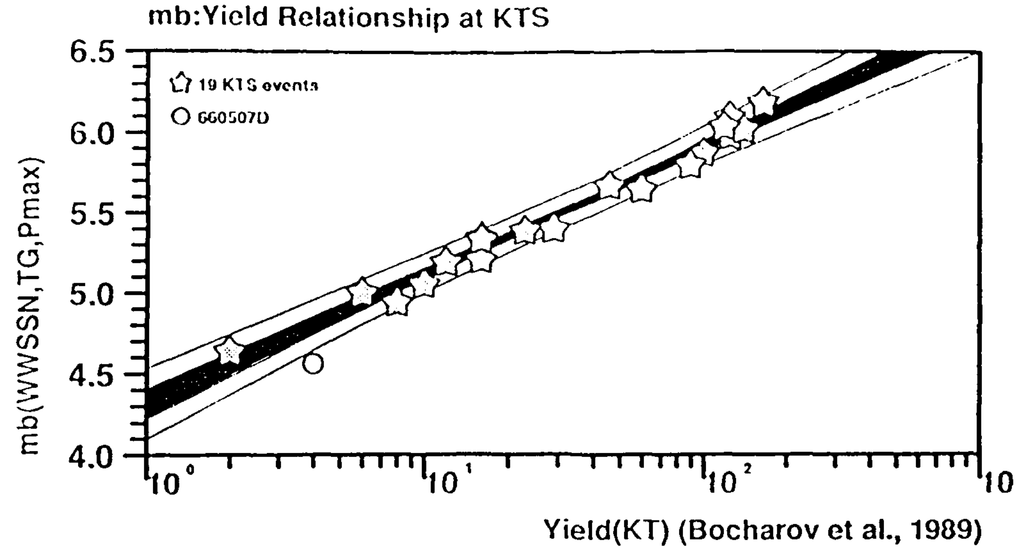

DWLS (uncertain X & Y): S=0.80(0.021), I=4.32(0.033), 19. data used,
95% error in mb at 1,10,50,100,150KT: 0.21, 0.13, 0.11, 0.13, 0.14,
95% factor in yield at 1,10,50,100,150KT: 3.45, 2.09, 1.86, 2.07, 2.23

OWLS (precise X assumed): S=0.82(0.032), I=4.28(0.053)

Standard LS: S=0.80(0.031), I=4.31(0.049)

10% s.e. in yields assumed; GLM station terms removed

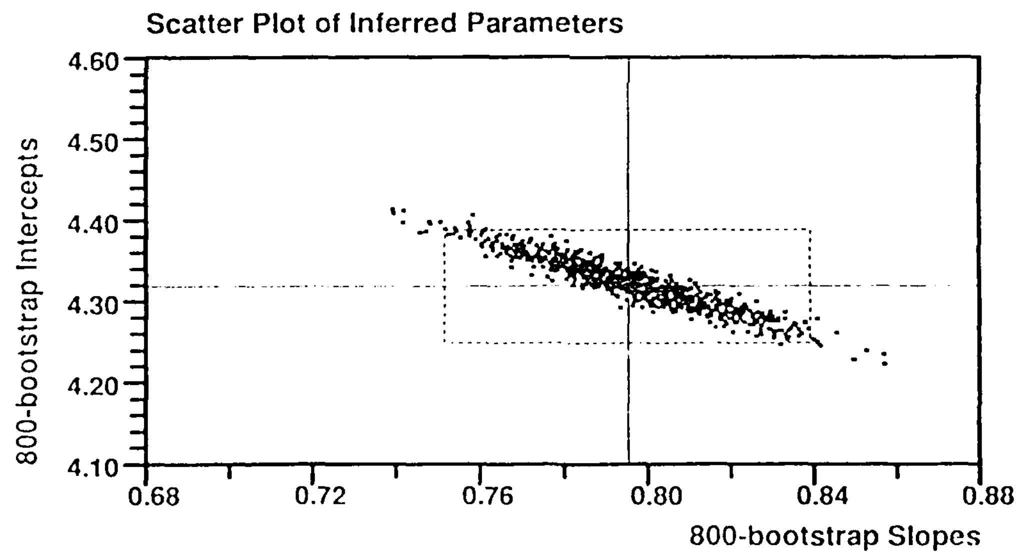

95% confidence interval of slope: 0.80+/-0.044
95% confidence interval of intercept: 4.32+/-0.070
[97.5% quantile of t(17. D.o.F.), 2.110, used]

Figure 12. Same as Figure 11 except the m_bs are those with station corrections applied, namely the m_{b2}. Note that the yields are assumed to have 10% standard error as in Figure 11, and the reduction in the scatter is due to the better precision of m_{b2}.

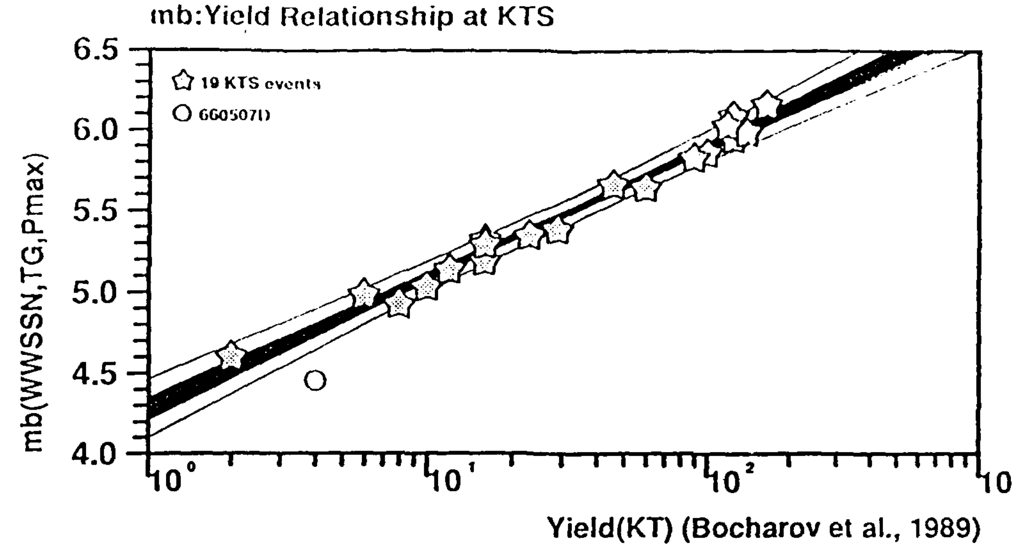

DWLS (uncertain X & Y): S=0.81(0.018), I=4.28(0.027), 19. data used,
95% error in mb at 1,10,50,100,150KT: 0.18, 0.10, 0.08, 0.10, 0.11,
95% factor in yield at 1,10,50,100,150KT: 2.83, 1.74, 1.60, 1.77, 1.91

OWLS (precise X assumed): S=0.80(0.030), I=4.29(0.047)

Standard LS: S=0.81(0.029), I=4.27(0.046)

10% s.e. in yields assumed; GLM station & near-source effects removed

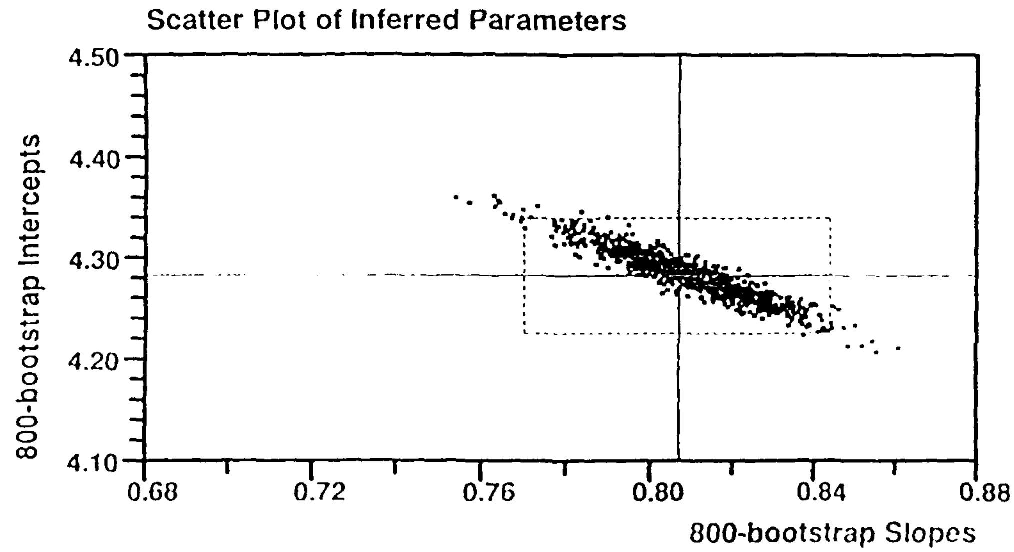

95% confidence interval of slope: 0.81+/-0.037
95% confidence interval of intercept: 4.28+/-0.057
[97.5% quantile of t(17. D.o.F.), 2.110, used]

Figure 13. Same as Figure 11 except the m_bs are those with both the station corrections and near-source focusing terms applied, namely the $m_{2.9}$. The improved m_b precision has direct impact on the regression, as compared to Figures 11 and 12. The yield of future Semipalatinsk explosions can be reliably predicted using this $m_{2.9}$:yield calibration curve for a precision similar to what RMS L_g could provide (*cf.* Figure 14).

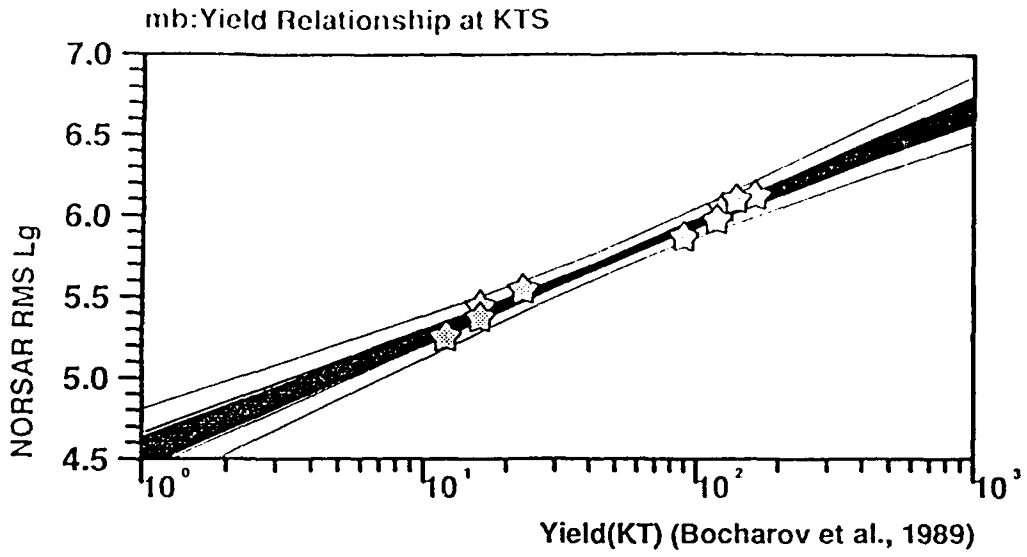

DWLS (uncertain X & Y): S=0.71(0.028), I=4.54(0.050), 9. data used,
95% error in mb at 1,10,50,100,150KT: 0.27, 0.13, 0.08, 0.09, 0.10,
95% factor in yield at 1,10,50,100,150KT: 5.74, 2.39, 1.65, 1.80, 1.98

OWLS (precise X assumed): S=0.71(0.035), I=4.53(0.063)

Standard LS: S=0.71(0.033), I=4.53(0.058)

10% s.e. in yields assumed

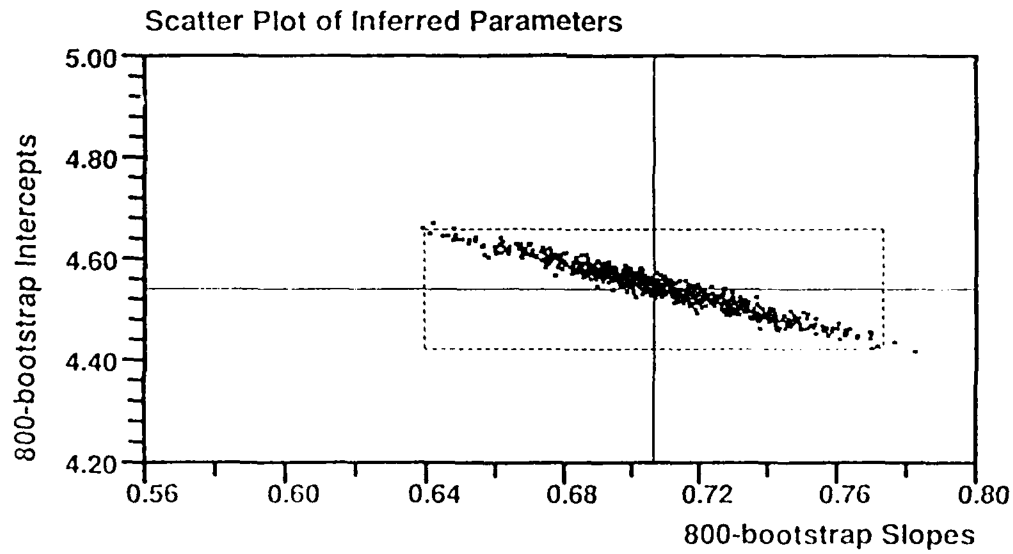

95% confidence interval of slope: 0.71+/-0.067
95% confidence interval of intercept: 4.54+/-0.118
[97.5% quantile of t(7. D.o.F.), 2.365, used]

Figure 14. Regressing 9 RMS L_g values (Ringdal, 1990) on Soviet-published yields. RMS L_g recorded at NORSAR has very high S/N ratio and hence very stable source measure for Semipalatinsk explosions above 10KT. There is no calibration data below 10KT and hence the extrapolation for future events with RMS L_g would have inherently larger uncertainty, as illustrated by the much wider 95% confidence band. Thus either teleseismic records based on P phases or L_g measured at in-state stations must be used for low-yield events.

I.6 GEOPHYSICAL INTERPRETATION OF OUR NEAR-SOURCE CORRECTIONS

If we remove the globally-averaged source sizes from the station-corrected magnitudes, all three test sites would exhibit different azimuthal and radial amplitude variations (Figure 5): Degelen and Murzhik events are systematically enhanced in the western U.S. and reduced in eastern U.S., whereas Balapan events are all reduced in the whole U.S. Degelen events are reduced in Indonesia and southeast Africa, whereas Balapan events are enhanced in these regions. Murzhik events are reduced in Scandinavia, but Balapan and Degelen events get enhanced there. Such highly direction-dependent, distance-dependent, and site-dependent patterns of the amplitude fluctuation could be a diagnostic for the path effects in the proximity of the test sites. Back projections (*e.g.*, Lynnes and Lay, 1990) of the m_b residuals onto the upper mantle and the lower crust reveal that similar m_b residuals come into alignment in several regions partitioned by known geological features (Figure 15). Murzhik events recorded in the western U.S. and in northeast Asia, Degelen events in the western U.S., and SW Balapan events at western European stations must pass through the area between Chinrau fault and Chingiz-Kalba shear zone. All these paths show positive m_b residuals. The north of Chinrau fault might have smaller P_n velocity and higher heat flow (Bonham *et al.*, 1980; Leith, 1987a, 1987b) and has negative mean m_b residuals on the back projections. Paths from NE Balapan to North America and many continental European stations must cross this area or even travel along the Chinrau fault before entering deeper mantle, and hence the complexity in the waveforms is inevitable. It seems that the mean m_b–L_g separation of 0.14±0.02 m.u. (*e.g.*, Ringdal and Hokland, 1987; Ringdal and Marshall, 1989; Richards *et al.*, 1990; Jih and Wagner, 1990) between the NE and SW subregions of Balapan could be due in part to the path effects --- in addition to the difference of source medium postulated previously by Marshall *et al.* (1984). Path effects can also explain why the SW Balapan waveforms tend to be more complex at YKA than those recorded at WRA, EKA, and GBA arrays (Jih and Wagner, 1991).

The initial P waves from the three adjacent test sites have virtually the same incident angle at each teleseismic station, and anything in common across all events (such as the crustal amplification as well as the upper mantle attenuation underneath the receiver) would have been lumped into the constant station term. Thus the station residuals averaged over all events from the same test site would correlate very little with the receiver. Instead, they should reveal more site-dependent information about the focusing/defocusing pattern underneath E. Kazakhstan (Figure 15).

The largest and prominent fault in the region is the southeast-trending Chingiz right-lateral strike-slip fault that passes about 10 km southwest of Degelen Mountain and right across the Murzhik test area (Rodean, 1979; Bonham *et al.*, 1980; Leith, 1987b). Soviets reported that this fault has a very steep dip, which is consistent with its linear expression over large distance as seen on Landsat imagery (Bonham *et al.*, 1980). A distinct fault-line scarp is developed along much of the oldest metamorphic rocks. Chingiz Fault extends for a total length of about 700 km. Soviet reports postulate that this fault extends down to the boundary of the granite layer of the crust and possibly into the upper mantle. For Murzhik explosions, the propagation of P_n and L_g waves could be affected by this fault significantly, which results in a radiation pattern such as we are observing. More specifically, the rays towards NW direction could be reflected or diffracted to other quadrants, due to its post-critical incidence angles. Such relatively distant crustal structure should have little impact on the first P waves of Balapan explosions at teleseismic distances, however.

GRIDDED LS-AVERAGED mb[Pmax] RESIDUALS OF E. KAZAKH SHOTS

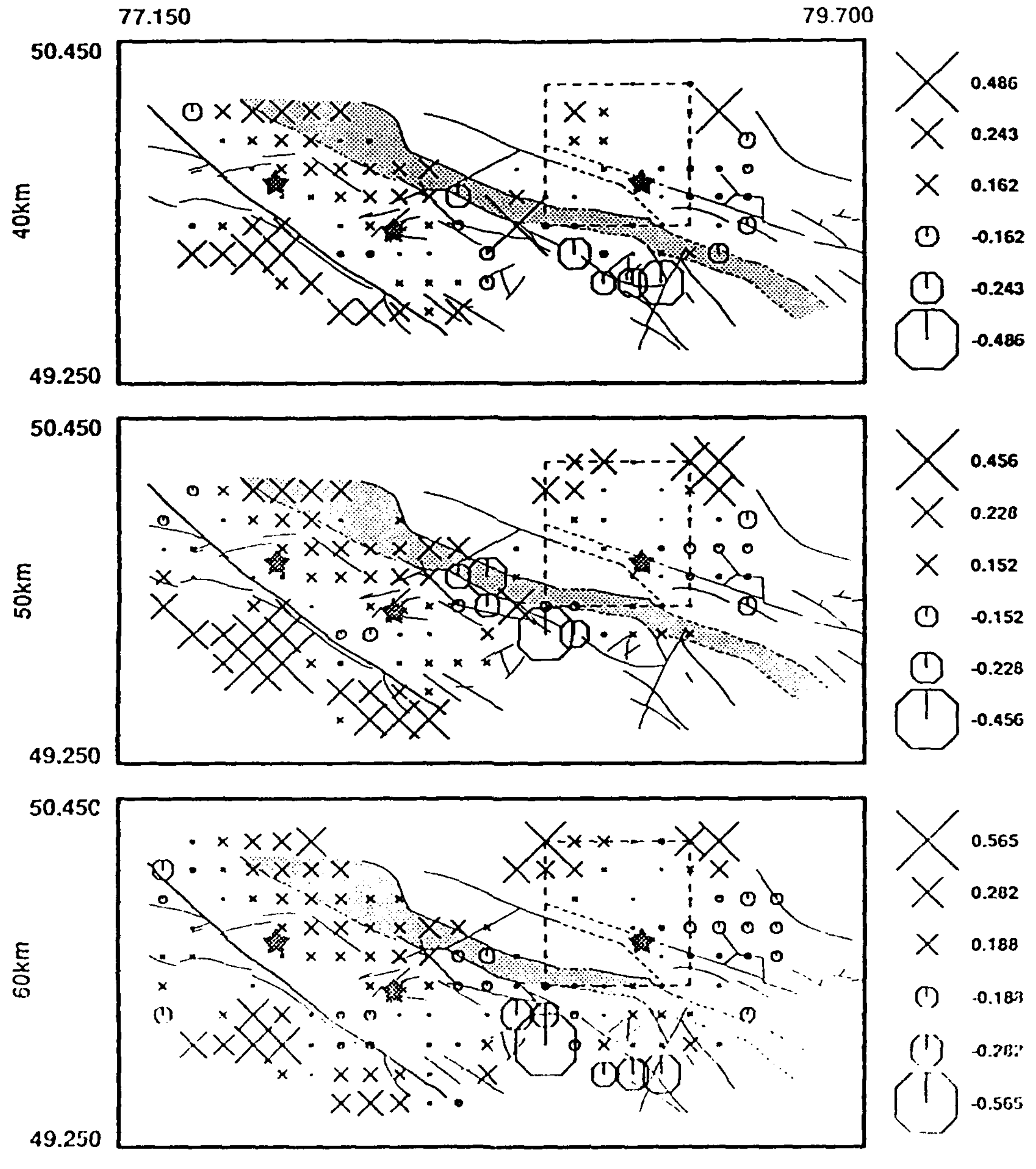

Figure 15. Back-projected m_b residuals averaged over a grid of every 0.2 degree by 0.2 degree underneath Soviet's Semipalatinsk nuclear test sites. The averaged residual pattern show some association with local geological features if the residuals are projected to depths down to the lower crust and the upper mantle. Thus even the teleseismic recordings might reveal some useful information about the path effects on the propagation of regional phases such as P_n and L_g

I.7 DISCUSSION AND CONCLUSIONS

The new magnitude determination scheme (Equation [3]) presented in this study significantly reduces the fluctuational variation across the recording stations. It is shown that, by applying this scheme to worldwide explosions, it is possible to have a consistent base line in estimating the absolute magnitudes (which is crucial in estimating the test site bias) while the precision in the resulting network m_b values can be maintained as well as could be achieved by the single-test-site approach. The standard error in most $\overline{m}_{2.9}$ values is 0.02 m.u., about the same as that for *RMS* L_g inferred from in-country regional network recordings reported by Israelson (1991) and Hansen *et al.* (1990). Most Murzhik events show nearly identical residual patterns, suggesting a common focusing/defocusing structure. Further partitioning of Balapan test site seems necessary, however.

The most detailed description of the wave propagation model would naturally suggest that yet another term could be added into Equation [3] to count for the source-region attenuation. So far such source region bias in m_b has always been inferred with other information such as the yields (as in this study), M_S (*e.g.*, Evernden and Marsh, 1987) or P_n velocity (*e.g.*, Marshall *et al.*, 1979) *etc.*. The hypothesis that such attenuation differential could be directly discerned from m_b alone by further improving Equation [3] is worth testing.

Digital signals recorded on seismic instruments at regional distance will be critical for monitoring low yield explosions below 10 kt. Obviously the regression routines developed in this study can well be applied to other source measures which are based on regional phases. On the other hand, teleseismic data such as the WWSSN data used in this study still carry invaluable information that is worthy of further exploitation, beyond simply calculating the "unified yield".

Throughout this study, our emphasis has been to reveal the site-dependent characteristics from the observations exclusively so that in the future the inferred results can be critically examined and compared with those derived by other means.

We suggest that the follow-up research be accompanied by well-constrained forward modeling studies using realistic structures. The upgraded linear finite-difference code which incorporates boundary conditions for topographical free-surface of arbitrary shape (Jih *et al.*, 1988) in addition to the "strain filter" and "marching grid" features as outlined in Jih *et al.* (1989) can be utilized in the future to improve our understanding of the fundamental issues of seismic energy partitioning on the focal sphere as well as their implications for yield determination.

I.8 ACKNOWLEDGEMENTS

Geotech's SPZ amplitudes of 111 events collected prior to this contract were all measured by Robert A. Wagner, Margaret E. Marshall, Russel O. Ahner, and James A. Burnetti under various DARPA-sponsored contracts. Abdul Mailk digitized the geologic map of Semipalatinsk region of Figure 17 based on Bonham *et al.* (1980). Figures 6 through 10 were plotted with the graphic routine "PLOTXY" originally designed by Robert Parker and Loren Shure, and installed on Geotech's computer by Robert K. Cessaro. D. Wilmer Rivers reviewed the manuscript. Discussions with Bob Blandford are gratefully acknowledged. This research was supported under DARPA contract F19628-89-C-0063, monitored by Phillips Laboratory. The views and conclusions contained in this paper are those of the authors and should not be interpreted as representing the official policies, either expressed or implied, of the Defense Advanced Research Projects Agency or the U.S. Government.

I.9 REFERENCES

Bache, T. C. (1982). Estimating the yield of underground nuclear explosions, *Bull. Seism. Soc. Am.*, **72-6**, S131-168.

Blandford, R. R., and R. H. Shumway (1982). Magnitude:yield for nuclear explosions in granite at the Nevada Test Site and Algeria: joint determination with station

effects and with data containing clipped and low-amplitude signals, *Report VSC-TR-82-12,* Teledyne Geotech, Alexandria, Virginia.

Bocharov, V. S., S. A. Zelentsoz, and V. Mikhailov (1989). Characteristics of 96 underground nuclear explosions at the Semipalatinsk test site, *Atomic Energy,* **67,** 210-214

Bonham, S., W. J. Dempsey, J. Rachlin (1980). Geologic environment of the Semipalatinsk area, U.S.S.R. *(Preliminary Report),* U.S. Geological Survey, Reston, VA 22092.

Burdick, L. J. (1981). The changing results on attenuation of *P* waves, in *"A technical assessment of seismic yield estimation", Report DARPA-NMR-81-01, Appendix,* DARPA, Arlington, VA.

Butler, R. (1981). Estimation of body wave magnitudes and site specific propagation effects, in *"A technical assessment of seismic yield estimation", Report DARPA-NMR-81-01, Appendix,* DARPA, Arlington, VA.

Butler, R. and L. Ruff (1982). Teleseismic short-period amplitudes: source and receiver variations, *Bull. Seism. Soc. Am.*, **70-3**, 831-850.

Chang, A. C. and D. H. von Seggern (1980). A study of amplitude anomaly and m_b bias at LASA subarrays, *J. Geophys. Res.*, **85**, 4811-4828.

DARPA (1981). *A technical assessment of seismic yield estimation, Report DARPA-NMR-81-02,* DARPA/NMRO, Arlington, VA.

Dahlman, O. and H. Israelson (1977). *Monitoring Underground Nuclear Explosions,* Elsevier Scientific Publishing Co., New York.

Douglas, A. (1966). A special purpose least squares programme, *AWRE Report No. O-54/66,* HMSO, London, UK.

Douglas, A. (1987). Differences in upper mantle attenuation between the Nevada and Shagan River Test Sites: Can the effects be seen in *P*-wave seismograms? *Bull. Seism. Soc. Am.*, **77,** 270-276.

Douglas, A., J. B. Young, and P. D. Marshall (1981). Some analyses of P_n and Rayleigh wave amplitudes observed at North American stations, *Geophysics J.,* **67,** 305-324.

Evernden, J. F. and G. E. Marsh (1987). Yields of U.S. and Soviet nuclear tests, *Physics Today,* **8-1,** 37-44.

Gordan, M. R. (1988). *New York Times,* October 30, 137 P.A15.

Gray, H. L., W. R. Schucany, W. A. Woodward, and G. P. McCartor (1990). Some effects of selection on the JVE data, *Report GL-TR-90-281*, Geophysics Laboratory, Hanscom Air Force Base, MA. **(ADA234287)**

Gutenberg, B. and C. F. Richter (1956). Magnitude and energy of earthquakes, *Annali Geofis*, **9,** 1-15.

Hansen, R. A., Ringdal, F. and P. G. Richards (1990). The stability of *RMS* L_g measurements and their potential for accurate estimation of yields of Soviet underground nuclear explosions, *Bull. Seism. Soc. Am.*, **80-6,** 2106-2126.

Israelson, H. (1991). RMS magnitude for Novaya Zemlya events (abstract), *EOS, Trans. A.G.U.*, **72-17,** 193.

Jih, R.-S. (1990). Geotech's magnitude:yield study during 1989-1990, in *Proceedings of the 12th DARPA/GL Seismic Research Symposium, (18-20 Sept 1990, Key West, FL.)* (Eds J. Lewkowicz and J. McPhetres), *Report GL-TR-90-0212,* Geophysics Laboratory, Hanscom Air Force Base, MA. **(ADA226635)**

Jih, R.-S. (1991). m_b-yield regression with uncertain data: a Monte-Carlo approach with applications to Semipalatinsk explosions *(preprint under clearance review).*

Jih, R.-S., C. S. Lynnes, D. W. Rivers, and I. N. Gupta (1989). Simultaneous modeling of teleseismic and near regional phases with linear finite-difference method (abstract), *EOS, Trans. A.G.U.*, **70-43,** 1189.

Jih, R.-S., K. L. McLaughlin and Z. A. Der (1988). Free boundary conditions of arbitrary polygonal topography in a 2-D explicit elastic finite difference scheme, *Geophysics,* **53,** 1045-1055.

Jih, R.-S. and R. A. Wagner (1990). m_b bias between Balapan and Degelen test sites, U.S.S.R., as revealed by direct regression of WWSSN data on Soviet-released censored and uncensored yields (abstract), *EOS, Trans. A.G.U.*, **71-43,** 1477.

Jih, R.-S. and R. A. Wagner (1991). Azimuthal variation of m_b residuals of E. Kazakh explosions and assessment of the path effects (abstract), *EOS, Trans. A.G.U.*, **72-17,** 193.

Jih, R.-S., R. A. Wagner, and T. W. McElfresh (1990). Magnitude-yield relationship at various nuclear test sites, in *Report GL-TR-90-0107 (=TGAL-90-03),* Geophysics Laboratory, Hanscom Air Force Base, MA. **(ADA223490)**

Jih, R.-S. and R. H. Shumway (1989). Iterative network magnitude estimation and uncertainty assessment with noisy and clipped data, *Bull. Seism. Soc. Am.*, **79,**

1122-1141.

Johnson, L. R. (1981) Near-source effects on P waves, in *"A technical assessment of seismic yield estimation", Report DARPA-NMR-81-01, Appendix,* DARPA, Arlington, VA.

Leith, W. (1987a). Geology of NRDC seismic stations sites in Eastern Kazakhstan, USSR. *Open-File Report 87-597,* U.S. Geological Survey, Reston, VA 22092.

Leith, W. (1987b). Tectonics of Eastern Kazakhstan and implications for seismic source studies in the Shagan River area, *Proceedings of 9th DARPA/AFGL Annual Seismic Research Symposium* (15-18 June, 1987, Nantucket, MA.) 34-37.

Lilwall, R. C., P. D. Marshall, and D. W. Rivers (1988). Body wave magnitudes of some underground nuclear explosions at the Nevada (USA) and Shagan River (USSR) Test Sites, *AWE Report O-15/88,* HMSO, London, UK.

Lynnes, C. S. and T. Lay (1990). Effects of lateral heterogeneity under the Nevada Test Site on short-period P wave amplitudes and travel times, *Pure and Applied Geophysics,* **132,** 245-267.

Marshall, P. D., D. L. Springer, and H. C. Rodean (1979). Magnitude corrections for attenuation in the upper mantle, *Geophys. J. R. astr. Soc.*, **57,** 609-638.

Marshall, P. D. and D. L. Springer (1976). Is the velocity of P_n an indicator of Q? *Nature,* **264**, 531-533.

Marshall, P. D., T. C. Bache, and R. C. Lilwall, R. C. (1984). Body wave magnitudes and locations of Soviet underground explosions at the Semipalatinsk Test Site, *AWE Report O-16/84,* HMSO, London, UK.

Minster, J. B., J. M. Savino, W. L. Rodi, T. H. Jordan, and J. F. Masso (1981). Three-dimensional velocity structure of the crust and upper mantle beneath the Nevada Test Site, *Report SSS-R-81-5138,* S-Cubed, La Jolla, California.

Murphy, J. (1981). Body wave coupling theory, in *"A technical assessment of seismic yield estimation", Report DARPA-NMR-81-01, Appendix,* DARPA/NMRO, Arlington, VA.

Murphy, J. R., B. W. Barker, and A. O'Donnell (1989). Network-averaged teleseismic P-wave spectra for underground explosions. Part I - Definitions and Examples, *Bull. Seism. Soc. Am.*, **79-1,** 141-155.

Nordyke, M. D. (1973), A review of Soviet data on the peaceful uses of nuclear explosions, *Report UCRL-51414-REV1,* Lawrence Livermore Laboratory, University of California, CA.

North, R. G. (1977). Station magnitude bias --- its determination, causes, and effects, *Lincoln Laboratory, Technical Report 1977-24,* Massachusetts Institute of Technology, Lexington, MA.

Patton, H. J. (1988). Application of Nuttli's method to estimate yield of Nevada Test Site explosions recorded on Lawrence Livermore National Laboratory's digital seismic system, *Bull. Seism. Soc. Am.*, **78,** 1759-1772.

Priestley, K. F., W. R. Walter, V. Martynov, and M. V. Rozhkov (1990). Regional seismic recordings of the Soviet nuclear explosion of the Joint Verification Experiment, *Geophys. Res. Lets.*, **17**, 179-182.

Richards, P. G., L. R. Sykes, and W. Tedards (1990). Evidence for reduced uncertainty in estimates of Soviet explosion yields, and for an increase in estimates of explosion detection capability (abstract), *EOS, Trans. A.G.U.*, **71-43**, 1477.

Ringdal, F. (1990). NORSAR detection and yield estimation studies, in *Proceedings of the 12th DARPA/GL Seismic Research Symposium, (18-20 Sept 1990, Key West, FL.)* (Eds J. Lewkowicz and J. McPhetres), *Report GL-TR-90-0212,* Geophysics Laboratory, Hanscom Air Force Base, MA. **(ADA226635)**

Ringdal, F. and B. K. Hokland (1987). Magnitude of large Semipalatinsk explosions using *P* coda and L_g measurements at NORSAR, Semiannual Technical Summary, 1 April 1987 - 30 Sept 1987, *NORSAR Scientific Report No. 1-87/88,* NTNF/NORSAR, Kjeller, Norway.

Ringdal, F. and P. D. Marshall (1989). Yield determination of Soviet underground nuclear explosions at the Shagan River Test Site, Semiannual Technical Summary, 1 Oct 1988 - 31 Mar 1989 (L. B. Loughran ed.), *NORSAR Scientific Report No.2-88/89,* NTNF/NORSAR, Kjeller, Norway.

Rodean, H. C. (1979), ISC events from 1964 to 1976 at and near the nuclear testing ground in eastern Kazakhstan, UCRL-52856, Lawrence Livermore Laboratory, University of California, CA.

Ryall, A. S. (1985). Note on m_b bias at selected Soviet seismic stations, *Proceedings of the 7th DARPA/GL Seismic Research Symposium,* (6-8 May 1985, Colorado Spring, CO.) 398-414.

Springer, D. L. and R. L. Kinaman (1971). Seismic source summary for U.S. underground nuclear explosions, 1961-1970, *Bull. Seism. Soc. Am.*, **61,** 1073-1098.

Springer, D. L. and R. L. Kinaman (1975). Seismic source summary for U.S. underground nuclear explosions, 1971-1973, *Bull. Seism. Soc. Am.*, **65,** 343-349.

Stump, B. W. (1991). Nuclear explosion seismology: verification, source theory, wave

propagation and politics, *Review of Geophysics (Supplement), 734-741, April 1991, U.S. National Report to International Union of Geodesy and Geophysics 1987-1990,* American Geophysical Union, Washington D.C.

Sykes, L. R. and D. M. Davis (1987). The yields of Soviet strategic weapons, *Scientific American,* **256-1**, 29-37.

Sykes, L. R. and G. Ekstrom (1989). Comparison of seismic and hydrodynamic yield determinations for the Soviet joint verification experiment of 1988, *Proc. Natl. Acad. Sci. USA,* **86,** 3456-3460.

U.S. Congress/Office of Technology Assessment (1988). Seismic verification of nuclear testing treaties, *OTA-ISC-361,* U.S. Government Printing Office, Washington, D.C.

Veith, K. F. and G. E. Clawson (1972). Magnitude from short-period P-wave data, *Bull. Seism. Soc. Am.*, **62,** 435-452.

Vergino, E. S. (1989). Soviet test yields, *EOS, Trans. A.G.U.*, Nov 28, 1989.

von Seggern, D. H. (1973). Joint magnitude determination and analysis of variance for explosion magnitude estimates, *Bull. Seism. Soc. Am.*, **63,** 827-845.

APPENDIX A

GEOTECH'S MAXIMUM-LIKELIHOOD NETWORK m_b, GLM91A

Short-period WWSSN vertical recordings (SPZ) of body waves from Soviet nuclear explosions detonated at the Semipalatinsk Test Site, Eastern Kazakhstan, USSR, are being measured and added to our database to determine the optimal network magnitudes using the maximum-likelihood estimator (MLE), which accounts for the effects of data censoring due to clipping and to noise (Blandford and Shumway, 1982; Jih and Shumway, 1989). As of now, our WWSSN database has been expanded to 192 events (totaling 515 usable "a", "b", and "max" event phases) from a variety of test sites. Only the stations at teleseismic distance (20 to 95 degrees) which recorded 7 or more good signals were used in the network m_b determination. Although we have also included some measurements made off LRSM tapes and CDSN recordings, most of those data failed to meet the criteria aforementioned. The 12170 good signals, 8047 noise measurements, and 1330 clipped recordings yield a $\hat{\sigma}_{MLE}$ of 0.300.

The 192 events in Table A.2 are grouped by test sites. 111 events were measured before 1/1/90 under various contracts during the past decade. 25 Balapan events (with prefix "SAF") were based on the raw WWSSN station magnitudes distributed by DARPA in 1988. The three numbers under the column "# of signals" represent the number of signals, noise, and clips associated with the P_{max} phase of each event. S.E.M. is the "standard error in the mean" of the event magnitudes. Except for the U.S. and French Sahara explosions which have specific code names, all the remaining events are identified with the dates and abbreviated test site codes shown below:

Table A.1. Geotech's m_b Database

Code	Number of Events		Nuclear Test Site
	1/1/90	7/15/91	
___	19	37	Nevada Test Site, U.S.A.
___	6	6	Outside Nevada Test Site, U.S.A.
___	3	3	Amchitka Island, Aleutians, U.S.A.
AZG	11	11	Azgir, U.S.S.R.
PNE	1	2	"PNE", U.S.S.R.
MEK	0	14	Murzhik (Konystan), E. Kazakh, U.S.S.R.
DEK	9	21	Degelen Mountain, E. Kazakh, U.S.S.R.
SEK	12	22	Balapan (Shagan River), E. Kazakh, U.S.S.R.
SAF	0	25	Balapan (Shagan River), E. Kazakh, U.S.S.R.
NNZ	18	18	Northern Novaya Zemlya, U.S.S.R.
SNZ	6	6	Southern Novaya Zemlya, U.S.S.R.
___	9	9	Ahaggar, French Sahara
TU	11	11	Tuamoto Islands, France
RAJ	1	1	Rajasthan, India
CH	6	6	Lop Nor, Sinkiang, China

Table A.2. Geotech's Maximum-Likelihood Network m_b					
Event	# of Signals	S.E.M.	$m_b(P_{max})$	$m_b(P_b)$	$m_b(P_a)$
ALMENDRO	26 0 2	0.057	6.229	6.021	5.732
BANEBERRY	14 30 0	0.045	4.869	4.547	4.373
BENHAM	42 1 7	0.042	6.392	6.140	5.829
BILBY	36 3 0	0.048	5.706	5.453	5.201
BOURBON	18 31 0	0.043	4.931	4.751	4.621
BOXCAR	32 0 4	0.050	6.443	6.220	5.887
CALABASH	36 17 0	0.041	5.551	5.357	5.180
CAMBRIC	14 35 0	0.043	4.576	4.310	4.012
CARPETBAG	37 7 1	0.045	5.806	5.585	5.352
CHANCELLOR	15 11 1	0.058	5.360	5.201	4.924
CHARTREUSE	31 16 1	0.043	5.260	5.029	4.909
CHATEAUGAY	17 28 2	0.044	5.080	4.898	4.509
COMMODORE	31 5 1	0.049	5.794	5.585	5.361
CORDUROY	18 14 0	0.053	5.324	5.131	5.013
DISCUSTHROWER	12 39 1	0.042	4.677	4.451	———
DURYEA	23 29 0	0.042	5.049	4.874	4.723
FLASK	36 8 0	0.045	5.509	5.221	5.038
GREELEY	49 2 2	0.041	6.340	6.143	5.909
HALFBEAK	43 2 2	0.044	6.113	5.811	5.583
HANDCAR	16 33 0	0.043	4.650	4.516	4.345

Table A.2. Geotech's Maximum-Likelihood Network m_b (Continued)					
Event	# of Signals	S.E.M.	$m_b(P_{max})$	$m_b(P_b)$	$m_b(P_a)$
HANDLEY	41 1 1	0.046	6.519	6.345	6.100
HARZER	31 5 1	0.049	5.549	5.327	5.031
KANKAKEE	24 27 0	0.042	4.875	4.624	4.390
KNICKERBOCKER	28 21 0	0.043	5.253	4.976	4.778
MAST	29 1 0	0.055	6.040	5.800	5.465
MINIATA	37 7 0	0.045	5.491	5.176	4.908
NASH	31 21 0	0.042	5.166	4.939	4.789
PALANQUIN	2 0 0	0.212	3.942	____	____
PILEDRIVER	40 12 2	0.041	5.480	5.243	4.996
PURSE	9 0 0	0.100	5.880	5.571	5.296
REX	16 35 1	0.042	4.778	4.442	3.952
SCAUP	2 1 0	0.173	4.625	4.305	4.247
SCHOONER	7 9 0	0.075	4.389	4.371	3.869
SCOTCH	38 8 1	0.044	5.643	5.386	5.133
SCROLL	2 0 0	0.212	4.077	3.642	____
STARWORT	21 6 0	0.058	5.474	5.162	4.937
STILTON	7 0 0	0.114	5.839	5.663	5.455
CANNIKIN	49 0 20	0.036	6.957	6.710	6.463
LONGSHOT	71 4 3	0.034	5.873	5.494	5.137
MILROW	52 0 4	0.040	6.544	6.245	6.000

Event	# of Signals	S.E.M.	$m_b(P_{max})$	$m_b(P_b)$	$m_b(P_a)$
FAULTLESS	47 1 3	0.042	6.497	6.193	5.869
GASBUGGY	11 37 0	0.043	4.690	4.438	4.197
RIOBLANCO	15 20 0	0.051	4.831	4.568	4.127
RULISON	9 37 0	0.044	4.595	4.287	4.161
SALMON	6 33 0	0.048	4.200	3.989	3.484
SHOAL	16 27 0	0.046	4.776	4.497	4.346
AZG22APR66	3 10 0	0.083	4.225	4.144	3.919
AZG01JUL68	44 10 3	0.040	5.542	5.245	4.932
AZG22DEC71	12 0 2	0.080	6.181	5.845	5.490
AZG25APR75	1 16 0	0.073	3.986	3.948	____
AZG29JUL76	41 5 7	0.041	5.877	5.594	5.133
AZG30SEP77	21 30 1	0.042	4.855	4.619	4.092
AZG17OCT78	7 0 5	0.087	6.108	5.733	5.294
AZG18DEC78	9 0 3	0.087	6.155	5.780	5.406
AZG17JAN79	10 0 4	0.080	6.170	5.881	5.524
AZG14JUL79	10 0 1	0.091	5.725	5.396	4.866
AZG24OCT79	3 0 6	0.100	5.942	5.678	4.865

Table A.2. Geotech's Maximum-Likelihood Network m_b (Continued)

Table A.2. Geotech's Maximum-Likelihood Network m_b (Continued)					
Event	# of Signals	S.E.M.	$m_b(P_{max})$	$m_b(P_b)$	$m_b(P_a)$
PNE21MAY68	41 9 1	0.042	5.301	5.089	4.858
PNE29AUG74	27 18 0	0.045	4.753	4.433	4.041
KON18DEC66	55 8 1	0.038	5.726	5.511	5.280
KON16SEP67	36 29 2	0.037	5.086	4.852	4.558
KON22SEP67	35 31 1	0.037	5.013	4.757	4.447
KON22NOV67	7 64 0	0.036	4.317	4.001	_____
KON31MAY69	30 31 0	0.038	4.990	4.775	4.398
KON28DEC69	45 9 3	0.040	5.652	5.468	5.192
KON21JUL70	38 21 1	0.039	5.178	4.933	4.592
KON04NOV70	38 22 1	0.038	5.242	5.053	4.844
KON06JUN71	38 12 2	0.042	5.321	5.119	4.793
KON19JUN71	41 13 0	0.041	5.297	5.076	4.783
KON09OCT71	27 12 3	0.046	5.165	4.977	4.742
KON21OCT71	32 9 0	0.047	5.359	5.139	4.795
KON26AUG72	29 15 2	0.044	5.155	4.934	4.606
KON02SEP72	15 29 0	0.045	4.602	4.330	4.079
DEK21NOV65	48 15 1	0.038	5.378	5.169	4.894
DEK13FEB66	51 4 10	0.037	6.089	5.898	5.652
DEK20MAR66	49 9 8	0.037	5.854	5.638	5.353
DEK07MAY66	9 26 1	0.050	4.495	4.243	4.016

Table A.2. Geotech's Maximum-Likelihood Network m_b (Continued)					
Event	# of Signals	S.E.M.	$m_b(P_{max})$	$m_b(P_b)$	$m_b(P_a)$
DEK19OCT66	51 10 5	0.037	5.539	5.370	5.112
DEK26FEB67	48 9 6	0.038	5.833	5.610	5.368
DEK29SEP68	50 8 6	0.038	5.631	5.439	5.138
DEK23JUL69	38 21 1	0.039	5.183	4.943	4.628
DEK11SEP69	19 39 0	0.039	4.603	4.265	4.013
DEK22MAR71	43 14 3	0.039	5.519	5.347	5.052
DEK25APR71	37 5 0	0.046	5.783	5.594	5.331
DEK30DEC71	16 3 0	0.069	5.553	5.377	5.020
DEK28MAR72	28 17 0	0.045	4.979	4.747	4.380
DEK16AUG72	23 23 1	0.044	4.905	4.650	4.361
DEK10DEC72	30 7 5	0.046	5.542	5.340	4.990
DEK29MAR77	25 14 0	0.048	5.004	4.723	4.329
DEK30JUL77	21 16 0	0.049	4.877	4.630	4.230
DEK26MAR78	25 6 0	0.054	5.507	5.284	4.963
DEK22APR78	21 9 0	0.055	5.020	4.771	4.480
DEK28JUL78	36 9 6	0.042	5.524	5.313	5.002
DEK22MAY80	36 23 1	0.039	5.129	4.926	4.671
SEK15JAN65	46 1 2	0.043	5.894	5.746	5.511
SEK19JUN68	28 3 2	0.052	5.282	5.022	4.651
SEK30NOV69	50 0 0	0.042	5.965	5.787	5.401

Table A.2. Geotech's Maximum-Likelihood Network m_b (Continued)					
Event	# of Signals	S.E.M.	$m_b(P_{max})$	$m_b(P_b)$	$m_b(P_a)$
SEK30JUN71	31 19 1	0.042	5.062	4.794	4.499
SEK10FEB72	34 8 2	0.045	5.319	5.089	4.825
SEK02NOV72	42 1 15	0.039	6.185	5.944	5.608
SEK10DEC72	44 2 11	0.040	6.020	5.794	——
SEK23JUL73	53 1 1	0.041	6.191	6.006	5.763
SEK14DEC73	49 8 6	0.038	5.760	5.564	5.261
SEK27APR75	18 1 1	0.067	5.494	5.254	4.917
SEK04JUL76	38 0 5	0.046	5.848	5.601	5.236
SEK07DEC76	17 2 1	0.067	5.615	5.420	4.976
SEK11JUN78	17 0 1	0.071	5.879	5.572	5.294
SEK15SEP78	37 1 6	0.045	5.851	5.698	5.447
SEK23JUN79	40 3 3	0.044	6.060	5.860	5.631
SEK04AUG79	40 5 20	0.037	6.093	5.861	5.594
SEK28OCT79	44 5 13	0.038	5.946	5.706	5.467
SEK23DEC79	41 3 17	0.038	6.145	5.894	5.599
SEK14SEP80	34 5 6	0.045	6.033	5.771	5.459
SEK18OCT81	41 4 7	0.042	5.979	5.754	5.478
SEK26MAY84	30 0 3	0.052	6.002	5.915	5.590
SEK14SEP88	25 0 1	0.059	6.034	5.762	5.509

Event	# of Signals	S.E.M.	$m_b(P_{max})$	$m_b(P_b)$	$m_b(P_a)$
SAF23NOV76	22 0 0	0.064	5.626	—	—
SAF29AUG78	16 0 0	0.075	5.905	—	—
SAF29NOV78	28 0 0	0.057	5.880	—	—
SAF07JUL79	30 0 0	0.055	5.799	—	—
SAF18AUG79	28 0 0	0.057	6.087	—	—
SAF02DEC79	15 0 0	0.078	5.874	—	—
SAF12OCT80	23 0 0	0.063	5.828	—	—
SAF14DEC80	29 0 0	0.056	5.911	—	—
SAF27DEC80	24 0 0	0.061	5.896	—	—
SAF22APR81	25 0 0	0.060	5.865	—	—
SAF13SEP81	17 0 0	0.073	6.024	—	—
SAF27DEC81	23 0 0	0.063	6.207	—	—
SAF25APR82	14 0 0	0.080	5.944	—	—
SAF04JUL82	21 0 0	0.066	6.089	—	—
SAF05DEC82	26 0 0	0.059	6.093	—	—
SAF12JUN83	16 0 0	0.075	5.943	—	—
SAF06OCT83	25 0 0	0.060	5.942	—	—
SAF26OCT83	18 0 0	0.071	5.941	—	—
SAF25APR84	21 0 0	0.066	5.892	—	—
SAF14JUL84	23 0 0	0.063	5.999	—	—

Table A.2. Geotech's Maximum-Likelihood Network m_b (Continued)

Event	# of Signals	S.E.M.	$m_b(P_{max})$	$m_b(P_b)$	$m_b(P_a)$
SAF27OCT84	19 0 0	0.069	6.150	____	____
SAF02DEC84	22 0 0	0.064	5.693	____	____
SAF16DEC84	15 0 0	0.078	5.993	____	____
SAF28DEC84	19 0 0	0.069	5.916	____	____
SAF15JUN85	15 0 0	0.078	6.069	____	____
NNZ27OCT66	56 0 14	0.036	6.447	6.305	6.075
NNZ21OCT67	53 5 3	0.038	5.783	5.611	5.424
NNZ07NOV68	59 1 5	0.037	6.042	5.847	5.602
NNZ14OCT69	59 2 7	0.036	6.144	5.972	5.778
NNZ14OCT70	35 0 22	0.040	6.820	6.640	6.436
NNZ27SEP71	23 0 21	0.045	6.629	6.487	6.276
NNZ28AUG72	32 0 11	0.046	6.383	6.261	6.008
NNZ12SEP73	23 0 21	0.045	6.770	6.677	6.356
NNZ29AUG74	25 0 18	0.046	6.583	6.402	6.141
NNZ21OCT75	23 0 17	0.048	6.548	6.344	6.110
NNZ23AUG75	27 0 12	0.048	6.495	6.376	6.128
NNZ20OCT76	25 34 0	0.039	4.680	4.369	4.056
NNZ01SEP77	25 2 2	0.056	5.572	5.433	5.126
NNZ10AUG78	39 3 18	0.039	5.867	5.637	5.414
NNZ11OCT80	42 4 6	0.042	5.674	5.460	5.202

Table A.2. Geotech's Maximum-Likelihood Network m_b (Continued)

Event	# of Signals	S.E.M.	$m_b(P_{max})$	$m_b(P_b)$	$m_b(P_a)$
NNZ01OCT81	43 4 5	0.042	5.666	5.505	5.251
NNZ18AUG83	30 4 5	0.048	5.721	5.542	5.339
NNZ25OCT84	22 3 4	0.056	5.610	5.439	5.174
SNZ27SEP73	32 3 1	0.050	5.754	5.518	5.227
SNZ27OC73A	14 0 24	0.049	7.082	6.864	6.645
SNZ27OC73B	9 28 0	0.049	4.189	4.037	____
SNZ27OC73C	4 34 0	0.049	3.951	3.928	3.587
SNZ02NOV74	12 0 29	0.047	7.001	6.784	6.502
SNZ18OCT75	21 0 21	0.046	6.838	6.527	6.245
BERYL	11 6 0	0.073	5.017	4.815	4.455
CORUNDON	11 41 0	0.042	4.247	3.951	3.852
EMERAUDE	14 25 0	0.048	4.596	4.269	____
GRENAT	32 31 1	0.038	4.787	4.524	4.332
OPALE	3 50 0	0.041	3.950	3.909	3.827
RUBIS	45 5 0	0.042	5.434	5.185	4.863
SAPHIR	55 5 5	0.037	5.725	5.479	5.196
TOURMALINE	27 39 0	0.037	4.671	4.463	4.158
TURQUOISE	11 53 0	0.038	4.258	3.986	____

Table A.2. Geotech's Maximum-Likelihood Network m_b (Continued)

Table A.2. Geotech's Maximum-Likelihood Network m_b (Continued)					
Event	# of Signals	S.E.M.	$m_b(P_{max})$	$m_b(P_b)$	$m_b(P_a)$
TU19FEB77	16 27 0	0.046	4.665	4.413	—
TU19MAR77	20 5 1	0.059	5.682	5.475	5.175
TU24NOV77	32 0 0	0.053	5.702	5.437	5.102
TU30NOV78	38 7 2	0.044	5.635	5.251	4.862
TU25JUL79	18 0 0	0.071	5.917	5.624	5.158
TU23MAR80	27 14 3	0.045	5.394	5.141	4.713
TU19JUL80	38 2 2	0.046	5.559	5.202	4.939
TU03DEC80	31 10 0	0.047	5.371	5.020	4.739
TU25JUL82	22 13 0	0.051	5.252	5.078	4.717
TU19APR83	21 1 0	0.064	5.533	5.228	5.011
TU25MAY83	18 0 0	0.071	5.764	5.446	5.163
RAJ18MAY74	7 23 0	0.055	4.595	4.341	4.081
CH22SEP69	30 12 0	0.046	5.190	4.801	4.409
CH27OCT75	12 24 0	0.050	4.655	4.467	4.223
CH17OCT76	12 33 0	0.045	4.610	4.298	4.134
CH06OCT83	16 12 1	0.056	5.207	4.997	4.740
CH03OCT84	10 12 0	0.064	5.020	4.769	4.489
CH19DEC84	3 10 0	0.083	4.424	4.077	4.101

APPENDIX B

ESTIMATES OF TEST SITE BIAS WITH m_b(GLM91A)

Since the near-source correction procedure presented in this study has not been applied to regions other than Semipalatinsk, some experiments using the more complete m_b(GLM91A) values may be interesting. The event m_b values in Table A.2 are corrected for the station terms, and hence are very similar to the $\overline{m}_{2.2}$ discussed in Section I.3. The only difference is that $\overline{m}_{2.2}$ is computed as the (maximum-likelihood) averaged $m_{2.2}$ across those and only those stations which reported the amplitude, whereas m_b(GLM91A) is inverted jointly with all 515 events and 122 stations simultaneously, and hence the missing stations are also included in the (maximum-likelihood) averaging. The discrepancy in the two m_b values is insignificant, however (*cf.* Tables 2 and A.2).

Figure 16 shows the results of regressing m_b(GLM91A) on the published yields of Semipalatinsk and NTS high-coupling explosions with 10% S.E. in yields assumed. U.S. and U.S.S.R. have released the yields of roughly equally many events (Springer and Kinaman, 1971, 1975; Bocharov *et al.*, 1989; Vergino, 1989). Note that the NTS calibration curve based on P_{max} phase of m_b(GLM91A) (top of Figure 16) has the same slope and intercept as those based on $\overline{m}_{2.9}$ (Figure 13). Also note that the NTS curve based on the first arrivals (*i.e.*, P_a phase) has a smaller slope, and there seems to be a lot of scatter for the low yields. Blandford (written communication, 1991) pointed out that this might occur if the low-yield $m_b(P_a)$ were biased high and had a lot of scatter due to the noise wavelets interfering with signal wavelets.

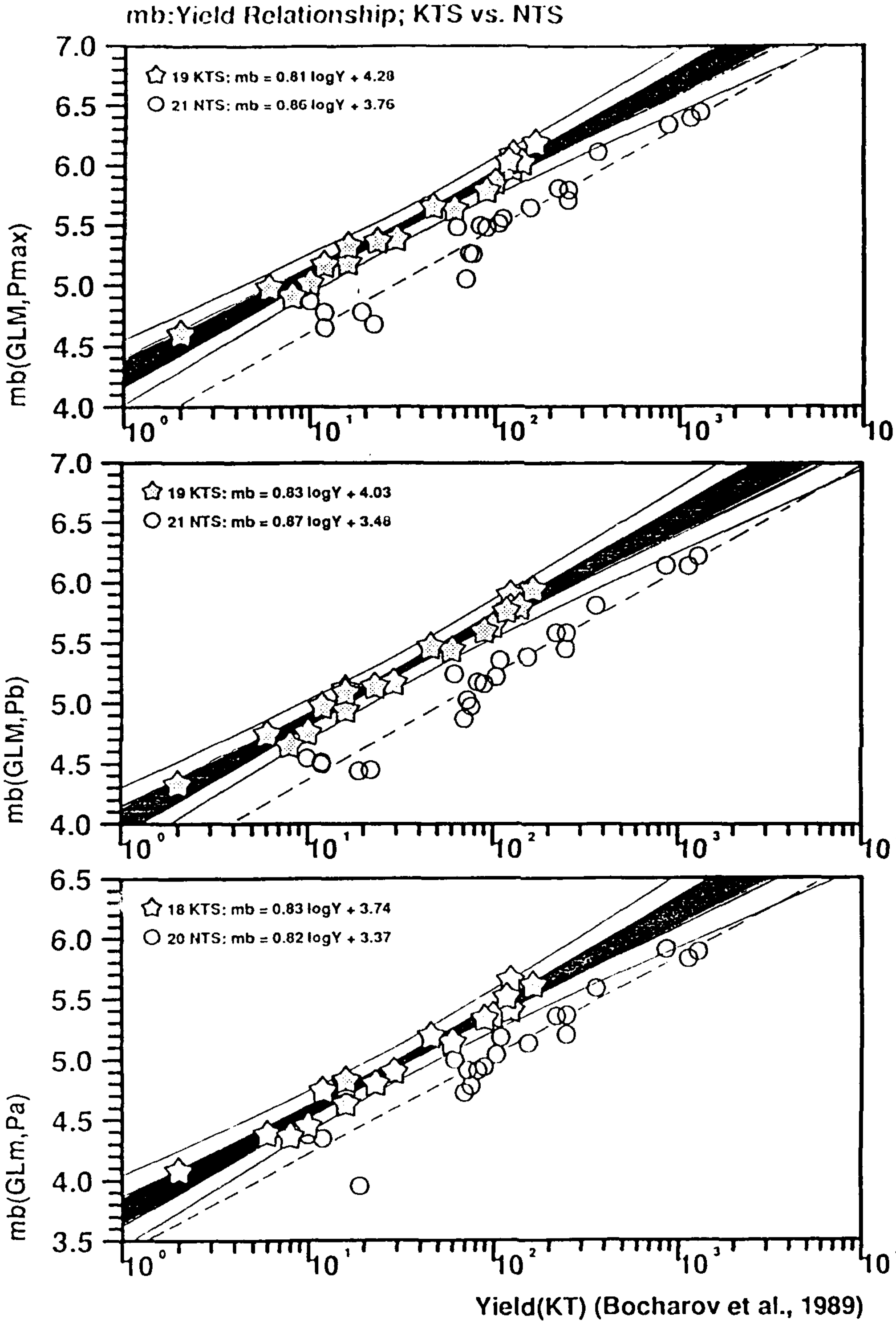

Figure 16. m_b(GLM) versus published yields of Semipalatinsk and NTS high-coupling explosions (with 10% S.E. in yields assumed). U.S. and U.S.S.R. have released the yields of roughly equally many events. The mean KTS-NTS test site bias is larger than 0.35 m.u. if P_{max} or P_b is used, and the larger scatter in NTS calibration curve is ignored. The bias would be about 0.15-0.2 m.u. if only granitic shots at NTS are used.

Table B.1 lists the mean KTS-NTS test site bias at three different yield levels. Results based on "b" and "max" phases suggest that the bias is yield-dependent and appears to be larger at the lower yield end. The "mean" KTS-NTS m_b bias is slightly larger than 0.35 m.u., although Figure 16 also indicates that the NTS granite events would seem to be about 0.15-0.2 m.u. below the Semipalatinsk curve.

Table B.1. Estimated Test Site Bias (from Nuttli's earlier studies)

Test Sites	Magnitude	Description	10kt	100kt	150kt
Balapan - NTS	m_b(ISC), L_g	Nuttli (1987)	0.35	0.35	0.35
Degelen - NTS	m_b(ISC), L_g	Nuttli (1987)	0.58	0.58	0.58
Estimated Test Site Bias (from this study)					
Test Sites	Magnitudes	Description	10kt	100kt	150kt
KTS* - NTS**	$m_b(P_{max})$	Marshall	0.55	0.50	0.48
KTS - NTS	$m_b(P_a)$	TG	0.38	0.39	0.40
KTS - NTS	$m_b(P_b)$	TG	0.51	0.47	0.47
KTS - NTS	$m_b(P_{max})$	TG	0.47	0.42	0 41
KTS - NTS***	$m_b(P_{max})$	TG, S-Cubed***	0.36	0.36	0.36

*) Combining all UK/AWE's Balapan, Degelen, and Murzhik m_b values as listed in Vergino (1989)

**) UK/AWE's NTS m_b as distributed in 1987

***) Murphy (1981): m_b(S-Cubed) = 3.92 + 0.81 log(W) for NTS high-coupling events

That NTS granite events might lie above typical wet-tuff or rhyolite events on the m_b-yield calibration curve can be further illustrated by some simple calculations with the three events Dougals (1987) analyzed. The announced yields of events 680619B, 710630B, and PILEDRIVER are <20 kt, <20 kt, and 56 kt, respectively. Our yield estimates (*cf.* the P_{max} calibration curves shown in Figure 16), however, are 17 kt, 9 kt,

and 100 kt, respectively, based on their corresponding m_b(GLM91A, P_{max}) of 5.282, 5.062, and 5.480. (Note that the m_b discrepancy between $\bar{m}_{2.9}$ and m_b(GLM91A) is insignificant.) At NTS, a high-coupling 17-kt shot has an expected m_b of 4.82, which is 0.46 m.u. below that of 680619B at Balapan. Likewise, a 9-kt high-coupling shot at NTS would be expected to have a m_b around 4.58, about 0.48 m.u. smaller than that of 710630B. At KTS, the expected m_b for 100 kt and 56 kt would be 5.9 and 5.69, respectively; which are 0.42 and 0.43 m.u. larger than typical NTS shots at the corresponding yields. The KTS-NTS bias of 0.48 (9 kt), 0.46 (17 kt), 0.43 (56 kt), and 0.42 (100 kt) resemble that yield dependency as shown in Table B.1, as expected. PILEDRIVER's m_b(GLM91A), 5.480, is about 0.22 m.u. larger than that of a 56-kt shot at NTS, *i.e.*, 5.26. This result seems to match very well with Ryall's (1985) inference of the attenuation differential between Semipalatinsk and NTS using earthquake data recorded at seismic stations in these two region.

Murphy (1981) points out that the "statistically significant" m_b-yield relationship for the wet tuff/rhyolite explosions at Pahute Mesa and Yucca Flat is

$$m_b = 3.92 + 0.81 \log(W) \qquad [1]$$

which happens to be about 0.36 m.u. below our inferred calibration curve for historical Semipalatinsk explosions. This could be simply accidental. Nevertheless, an interesting speculation can be offered to explain the coincidence. It is not impossible that the Soviets are fully aware of Equation [1] and the commonly quoted KTS-NTS bias of 0.35 m.u. (*e.g.*, OTA, 1988). Perhaps the Soviets have purposefully released a subset of their historical explosions which would fit a prescribed curve roughly 0.35 m.u. above Equation [1]. If this was indeed the case, probably the released 19 Eastern Kazakhstan events were not "fudged" otherwise --- although whether they are truly representative of the whole explosion population would still remain open (*cf.* the discussion in Gray *et al.*, 1990). We could also argue that, if the aforementioned speculation were valid, then Geotech's m_b measurements of Soviet events must correlate very well with the magnitudes which the Soviet seismologists have used in determining

their own yields.

Using 20 NTS tuff/rhyolite events, Marshall *et al.* (1979)'s $\overline{m}_2$ give

$$\overline{m}_2 = 3.71 + 0.89 \log(W). \qquad [2]$$

This is not significantly different from our result for 21 NTS tuff/rhyolite events (Figure 16):

$$m_b(\text{GLM91A}) = 3.76 + 0.86 \log(W) \qquad [3]$$

Combining our GLM/MLE-derived WWSSN m_b with RMS L_g values measured at NORSAR (Ringdal and Marshall, 1989), the m_b-L_g residuals for E. Kazakh explosions show a strong difference among these three test sites (Figure 17). The SW subregion of Balapan test site excites slightly larger m_b (relative to L_g), whereas all the remaining regions of E. Kazakh test site have negative residuals. All studies of the intrasite m_b–L_g bias of Balapan explosions lead to a very consistent estimate, namely 0.14±0.02 m.u. (Table B.2 and Jih and Wagner, 1991).

As noted in Appendix A, DARPA distributed the WWSSN station m_b values of 39 large Balapan explosions furnished by AFTAC in the spring of 1988. Lilwall *et al.* (1988) supplemented this data set with some ISC recordings in their analysis, and they found that the event m_b values based on Blacknest's Joint Maximum-Likelihood (JML) method are not significantly different from those based on LSMF. We have incorporated these AFTAC's m_b values into our database (*cf.* pages 58-59), with a compensating correction for the different B(Δ) factors. The LSMF results of the 39 AFTAC-measured Balapan events show a mean m_b-L_g bias of 0.14 between SW and NE subregions of Balapan test site (Table B.2).

Table B.2. Mean m_b-L_g of Balapan Explosions				
Reference	SW	TZ	NE	SW-NE
Ringdal and Hokland (1987)	0.112±0.009(?)	___	-0.059±0.014(?)	0.17
Marshall (1987) + NORSAR	0.116±0.009(26)	0.041±0.012(10)	-0.042±0.014(14)	0.16
Ringdal and Marshall (1989)	0.05±0.007(46)	-0.02±0.009(20)	-0.10±0.012(30)	0.15
TGAL + NORSAR	0.020±0.015(20)	-0.071±0.017(8)	-0.112±0.017(8)	0.13
AFTAC + NORSAR	-0.012±0.010(18)	-0.113±0.020(6)	-0.153±0.018(7)	0.14
Marshall (1987) + Nuttli	-0.012±0.015(17)	-0.060±0.026(4)	-0.118±0.014(14)	0.11

Table B.3 lists the mean m_b–L_g values at three test sites of Eastern Kazakhstan. Murzhik events have smaller relative m_b excitation, as compared to Balapan and Degelen explosions. Since Balapan and Murzhik events essentially followed the same depth-yield scaling (Jih and Shumway, 1991; Jih, 1990), the relatively strong L_g excitation at Murzhik could probably be due to the smaller size (and hence shallower depth of burial) at Murzhik, or due to the source medium (Figure 17).

Table B.3. Mean m_b-L_g of Eastern Kazakh Explosions			
Reference	SR	DM	MK
TGAL + NORSAR	-0.030±0.014(36)	-0.047±0.034(5)	-0.128±0.034(3)
AFTAC + NORSAR	-0.063±0.014(31)	___(?)	___(?)

SPATIAL PATTERN OF mb-Lg RESIDUALS OF E. KAZAKH SHOTS

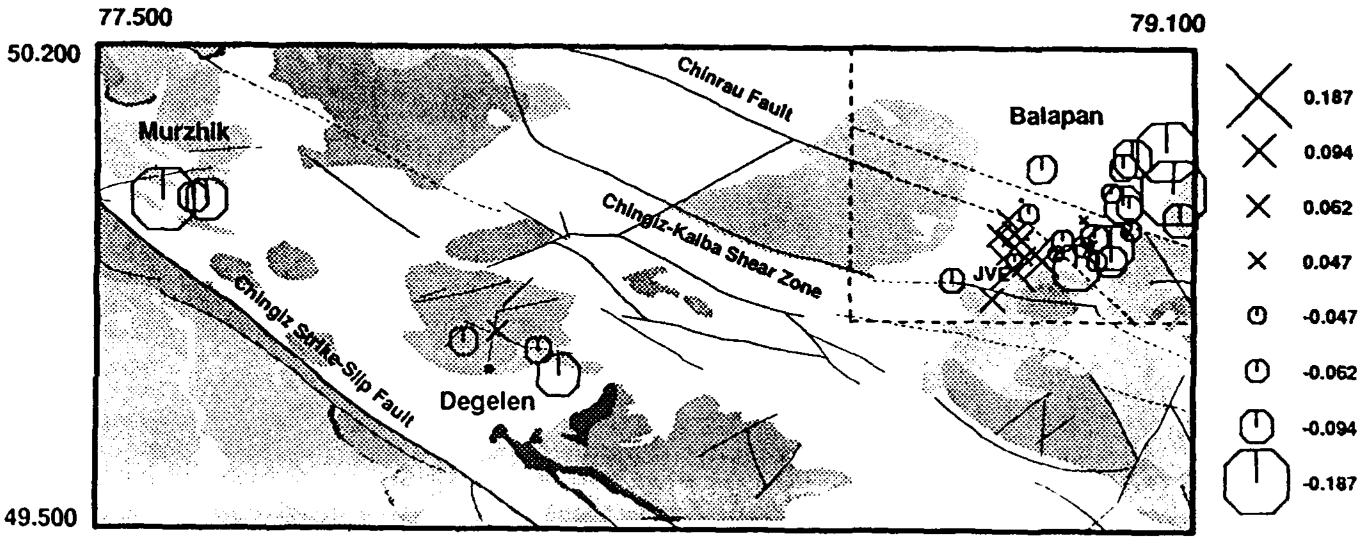

Figure 17. The spatial pattern of m_b-L_g residuals of Semipalatinsk explosions with TG's m_b(GLM) and RMS L_g values reported at NORSAR. The residual pattern of Balapan events strongly indicates significant difference in the source medium across the Chinrau fault separating the northeastern and southwestern portion of the test site, as reported by Ringal and Marshall (1989) and Marshall *et al.* (1984). The mean m_b-L_g bias between SW and NE Balapan is about 0.13 m.u.

mb: Geotech's WWSSN GLM/MLE Pmax (GLM91A, 515 events)
(122 stations, each recorded 7 signals or more)
NORSAR RMS Lg (Ringdal, 1990; Ringdal and Marshall, 1989)
Surface geology: Bonham et al. (1980), Leith (1987).
Balapan, SW region, 20 events: mb(TG)= mb(Lg) + 0.020(0.015)
Balapan, TZ region, 8 events: mb(TG)= mb(Lg) - 0.071(0.017)
Balapan, NE region, 8 events: mb(TG)= mb(Lg) - 0.112(0.017)
Balapan, 36 events: mb(TG)= mb(Lg) - 0.030(0.014)
Degelen, 5 events: mb(TG)= mb(Lg) - 0.047(0.034)
Murzhik, 3 events: mb(TG)= mb(Lg) - 0.128(0.034)
Sedimentary & volcanic rocks
Devonian & Carboniferous rock
Granitic rocks
Limestone

SECTION II PROJECT OVERVIEW

RECENT METHODOLOGICAL DEVELOPMENTS IN MAGNITUDE DETERMINATION AND YIELD ESTIMATION WITH APPLICATIONS TO SEMIPALATINSK EXPLOSIONS

Rong-Song Jih
Teledyne Geotech Alexandria Laboratories
314 Montgomery Street
Alexandria, VA 22314-1581

II.1 CONTRACT NO.: F19628-89-C-0063, Task 1 (expired July 1991)

II.2 OBJECTIVES

The primary objective is to study the technical issues relating to the seismic estimation of the yield of remote underground explosions. Our approach is to improve both the numerical and statistical modeling tools as much as we can, and then apply the upgraded numerical tools to the excitation/propagation study of the teleseismic and regional phases, and apply the upgraded statistical tools to the magnitude determination as well as the yield estimation problems with emphasis on Soviet explosions.

II.3 RESEARCH ACCOMPLISHED DURING CONTRACT PERIOD

II.3.1 Upgrading of Unbiased Network m_b Estimator

The body wave magnitudes used in developing and applying the magnitude-yield relationship are network m_b values which are some "average" of the station m_b.

Previously a major objective of magnitude-calculation research was to determine the network m_b that is not biased by the sample truncation due to the limited range of the seismometers. Ringdal (1976) introduced the maximum-likelihood estimator [MLE] to correct for the statistical bias introduced by data censoring from non-detection. Von Seggern and Rivers (1978) pointed out the importance of accounting for the data censoring due to signal clipping. Blandford and Shumway (1982) derived the general linear model [GLM] in the presence of data censoring using the Expectation Maximization [EM] algorithm. They simultaneously estimated event magnitudes and station corrections in a maximum-likelihood sense. Jih and Shumway (1989) re-examined and documented the GLM algorithms, and they discussed the uncertainty assessment in the censoring situation. It is concluded that in the multi-parameter linear regression problem with censored data, the scaling of $\sigma/\sqrt{\text{degrees of freedom}}$ still provides an extremely good approximation of the uncertainty associated with each parameter. In the case of non-censoring, such approximation can be proved to be "exact". The methodological similarities and differences between the iterative least squares [ILS] and the maximum-likelihood estimator [MLE] were also identified in Jih and Shumway (1989).

A recent breakthrough in magnitude determination is the development of a procedure to account for the near-source focusing/defocusing effects. Jih and Wagner (1991b) propose to compute the new station magnitude $m_{2.9}$ for the i-th event recorded at the j-th station as

$$m_{2.9}(i,j) = \log_{10}[A(i,j)/T(i,j)] + B(\Delta(i,j)) - S(j) - F(k(i),j) \quad [1]$$

where A(i,j) is the displacement amplitude (in millimicrons) and T(i,j) is the period (in seconds) of the *P* wave. The $B(\Delta)$ is the distance-correction term. S(j) is the station correction, and F(k(i),j) is the near-source focusing correction for explosions from the k(i)-th source region. Some of the S terms for explosions from any test site and the F terms for the Semipalatinsk area are listed in Table 1. A complete list can be found in Jih and Wagner (1991b). This new magnitude is called $m_{2.9}$ to avoid confusion with

the m_3 defined in Marshall *et al.* (1979) that corrects for the source-region attenuation and station terms solely based on published P_n velocity.

Table 1. Receiver and Near-source Corrections for WWSSN Stations (partial listing)

Station Term		Near-source Term, F			Station		
Code	S	Balapan	Degelen	Murzhik	Longitude	Latitude	Description
AAE	-0.352	-0.387	-0.076	-0.127	38.766	9.029	Addis Ababa, Ethiopia
AAM	0.205	0.202	-0.073	-0.247	-83.656	42.300	Ann Arbor, Michigan
AKU	-0.048	0.300	0.311	0.212	-18.107	65.687	Akureyri, Iceland
ANP	-0.349	-0.167	0.402	0.183	121.517	25.183	Anpu, Taiwan
AQU	-0.133	-0.195	0.039	-0.024	13.403	42.354	Aquila, central Italy
ATU	0.128	0.191	-0.156	0.034	23.717	37.972	Athens Univ., Greece
BAG	-0.027	0.076	-0.009	-0.103	120.580	16.411	Baguio City, Luzon Island
BEC	-0.114	0.090	0.058	-0.092	-64.681	32.379	Bermuda-Columbia, Atlantic
BKS	0.089	-0.014	0.101	0.229	-122.235	37.877	Byerly, central California
BLA	0.057	-0.233	-0.177	-0.299	-80.421	37.211	Blacksburg, West Virginia
BOZ	0.188	-0.325	-0.025	-0.180	-111.633	45.600	Bozeman, Montana
BUL	0.003	0.014	-0.266	-0.037	28.613	-20.143	Bulawayo, Rhodesia
CHG	-0.140	0.240	0.106	0.045	98.977	18.790	Chiengmai, southeast Asia
CMC	-0.178	0.114	0.375	0.602	-115.083	67.833	Copper Mine, Canada
COL	0.065	0.181	0.188	0.051	-147.793	64.900	College Outpost, Alaska
COP	0.127	-0.003	0.159	-0.276	12.433	55.683	Copenhagen, Denmark
COR	0.155	0.132	0.183	0.172	-123.303	44.586	Corvallis, Oregon
CTA	0.153	-0.072	0.003	-0.073	146.254	-20.088	Charters Towers, Australia
DAG	0.036	-0.052	0.086	_____	-18.770	76.770	Danmarkshavn, Greenland
DAV	-0.320	-0.264	-0.053	_____	125.575	7.088	Davao, Mindanao Island
DUG	0.149	0.038	0.371	0.352	-112.813	40.195	Dugway, Utah
EIL	0.004	-0.117	-0.228	-0.103	34.950	29.550	Eilat, Arabic Peninsula
ESK	0.048	-0.042	0.162	-0.327	-3.205	55.317	Eskdalemuir, Scotland
FLO	0.000	-0.294	-0.093	-0.446	-90.370	38.802	Florissant, eastern Missouri

Testing results indicate that the procedure described in [1] has the following advantages:

[A] For 79 out of 82 Semipalatinsk events we have tested, Equation [1] provides more stable m_b measurements across the whole recording network, as compared to the conventional GLM or LSMF procedure which only corrects for the station terms (*cf.* Table 2). The reduction in the standard deviation of network m_b from $\overline{m}_1$ to $\overline{m}_{2.9}$ could reach a factor of 3 (*cf.* Table 2). Events which do not show improvements in precision could have been detonated in environments with different focusing patterns.

[B] The resulting network m_b values are not significantly different from the GLM results. Thus if the mean network m_b values derived by GLM or LSMF are unbiased, so are the refined results.

[C] The scatter in $\overline{m}_{2.9}$ versus log(yield) is smaller than that for other m_b (*cf.* Table 3).

Table 2. Various Network-Averaged m_b of 19 Special Events*				
Event	# of signals	Without correction	Station corrected	Near-source corrected
Date		$\overline{m}_1$, σ	$\overline{m}_{2.2}$, σ	$\overline{m}_{2.9}$, σ
651121D	48 12 1	5.384±0.035 0.271	5.394±0.024 0.188	5.381±0.019 0.152
660213D	51 2 10	6.073±0.038 0.305	6.092±0.027 0.218	6.088±0.014 0.114
660320D	49 6 8	5.848±0.041 0.322	5.865±0.030 0.239	5.853±0.009 0.074
670922M	35 20 1	5.033±0.036 0.271	5.048±0.029 0.214	5.029±0.017 0.125
680929D	50 4 6	5.610±0.035 0.275	5.642±0.026 0.202	5.641±0.018 0.138
690723D	38 17 1	5.172±0.041 0.306	5.201±0.029 0.220	5.186±0.013 0.100
691130B	51 0 0	5.950±0.044 0.313	5.973±0.031 0.222	5.945±0.026 0.184
691228M	45 2 3	5.666±0.043 0.306	5.665±0.035 0.250	5.660±0.018 0.125
710425D	37 3 0	5.764±0.052 0.327	5.793±0.042 0.267	5.826±0.020 0.127
710606M	38 6 2	5.323±0.040 0.272	5.341±0.031 0.210	5.319±0.015 0.099
711009M	27 9 3	5.165±0.037 0.233	5.187±0.028 0.174	5.136±0.016 0.100
711021M	32 6 0	5.348±0.049 0.301	5.383±0.036 0.224	5.341±0.021 0.127
720210B	34 8 2	5.297±0.042 0.278	5.329±0.029 0.195	5.289±0.018 0.121
720816D	23 20 1	4.908±0.044 0.293	4.931±0.033 0.221	4.921±0.025 0.165
720902M	15 25 0	4.615±0.049 0.312	4.635±0.038 0.243	4.602±0.017 0.107
721102B	42 0 15	6.173±0.045 0.339	6.183±0.034 0.256	6.160±0.023 0.177
721210B	45 1 11	6.006±0.037 0.282	6.013±0.029 0.223	5.983±0.022 0.169
880914B	25 0 1	6.004±0.037 0.191	6.032±0.023 0.117	6.026±0.033 0.168

*) 19 Semipalatinsk explosions for which the yields were published.

**) $\overline{m}_1$ = network average of raw m_b without any correction --- equivalent to ISC bulletin m_b. $\overline{m}_{2.2}$ = network average of m_b with GLM station corrections applied. $\overline{m}_{2.9}$ = network average of m_b with both station terms and near-source focusing terms removed.

Table 3. 95% Confidence Factor of Semipalatinsk Yield Estimate					
(assuming yields are subject to rounding and 10% S.E.)					
m_b used	1 kt	10 kt	50 kt	100 kt	150 kt
$\overline{m}_1$	4.74	2.58	2.19	2.42	2.61
$\overline{m}_{2.2}$	3.98	2.20	1.89	2.12	2.29
$\overline{m}_{2.9}$	3.23	1.82	1.67	1.88	2.04
Ringdal's *RMS* L_g[1]	5.74	2.39	1.65	1.80	1.98
Israelson's *RMS* L_g[2]	2.82	1.81	1.72	1.87	1.97
(assuming yields are subject to 10% S.E. only)					
$\overline{m}_1$	3.96	2.44	2.13	2.38	2.57
$\overline{m}_{2.2}$	3.45	2.09	1.86	2.07	2.23
$\overline{m}_{2.9}$	2.83	1.74	1.60	1.77	1.91
Ringdal's *RMS* L_g	5.74	2.39	1.65	1.80	1.98
Israelson's *RMS* L_g	2.70	1.84	1.78	1.86	1.95

1) RMS L_g of 9 Semipalatinsk events furnished by Ringdal (1990) with NORSAR and GRF data.

2) RMS L_g of 16 Semipalatinsk events furnished by Israelson (1991b) with hand-digitized Soviet analog seismograms.

II.3.2 m_b-Yield Regression Routine with Censored Yields: MLE-CY

In general there are four types of yield data available: [0] the yield, W, is known as y_0 kt, [1] W is left censored, *i.e.*, the exact value of W is only known to be less than certain level, [2] W is right censored, *i.e.*, the exact value of W is only known to be larger than certain level, and [3] W is only known to lie between two bounds. The majority of Soviet yields recently published by Bocharov *et al.* (1989) and Vergino (1989) are of type 3.

The problem of estimating the yield of an explosion from the estimated seismic magnitude has been handled traditionally using the linear or piecewise linear model

$$X = \alpha + \beta \log(W) + v = \alpha + \beta Y + v \qquad [2]$$

where X is the measured magnitude (*e.g.*, m_b or M_S), α and β are intercept and slope estimators, W is the yield in kiloton [kt], and v is an error term. v is assumed to be a Gaussian random variable with mean zero and standard deviation σ. One may then collect a number of "calibration events", estimating α and β by least squares using a number of known yields and measured magnitudes. This classical calibration approach leads to predicting a future log-yield Y at magnitude = $\hat{X}$ by inverting Equation [2], *i.e.*, $\hat{Y} = (\hat{X} - \hat{\alpha})/\hat{\beta}$.

The geometrical interpretation of "regressing X on Y" is that the $(\hat{\alpha}, \hat{\beta})$ thus estimated will be the optimal solution that minimizes the sum of the squared X residuals, $\sum (X - \hat{\alpha} - \hat{\beta}Y)^2$. Implicitly, here we have made an assumption that the independent variable Y has nearly perfect accuracy and precision as compared to X. Alternately, one can estimate λ and η in the inverse regression model

$$Y = \lambda + \eta X + v' \qquad [3]$$

and then predict a future log-yield directly as $\hat{Y} = \hat{\lambda} + \hat{\eta}\hat{X}$. Likewise, here one is implicitly assuming that X has perfect accuracy and precision, and hence the optimal estimate $(\hat{\lambda}, \hat{\eta})$ is the one that minimizes the sum of squared Y residuals, $\sum (Y - \hat{\lambda} - \hat{\eta}X)^2$. Thus either the yield or the magnitude must be regarded as an error-free independent variable in these two models. Symbolically, these two conventional regression models are based on the following two extreme assumptions: $\sigma(X)/\sigma(Y) = \infty$ and $\sigma(X)/\sigma(Y) = 0$, respectively.

In reality, both the m_b and the yield measurements are subject to error. At NTS, $\sigma(m_b) >> \sigma(\log \text{yield})$ could be a reasonable assumption to justify the regression of m_b on the yields. However, this may not be the case in general. Note that [3] can be rewritten in a form similar to [2]: $X = \alpha' + \beta' Y + v''$ with the transformations $\alpha' = -\lambda/\eta$,

$\beta' = 1/\eta$.

Elegant maximum-likelihood theory can be derived for "regressing censored Y on X" (Jih *et al.*, 1990a). Suppose there are n_0, n_1, n_2, and n_3 events for each type, respectively. The conditional likelihood function of the censored observations ($\mathbf{y}_0$, $\mathbf{t}_1$, $\mathbf{t}_2$, $\mathbf{t}_3$) given the intercept α, slope β, and σ is

$$L(\mathbf{y}_0, \mathbf{t}_1, \mathbf{t}_2, \mathbf{t}_3 \mid \alpha, \beta, \sigma) = \prod_{j=1}^{n_0} P(Y_j = y_{0j} \mid \alpha, \beta, \sigma) * \prod_{j=1}^{n_1} P(Y_j < t_{1j} \mid \alpha, \beta, \sigma) * \quad [4]$$

$$\prod_{j=1}^{n_2} P(Y_j > t_{2j} \mid \alpha, \beta, \sigma) * \prod_{j=1}^{n_3} P(t_{aj} < Y_j < t_{bj} \mid \alpha, \beta, \sigma)$$

and the log-likelihood function is

$$\ln L(\mathbf{y}_0, \mathbf{t}_1, \mathbf{t}_2, \mathbf{t}_3 \mid \alpha, \beta, \sigma) = -\frac{n_0}{2}\ln(2\pi\sigma^2) - \frac{1}{2\sigma^2}\sum_{j=1}^{n_0}(y_{0j} - \frac{x_{0j}-\alpha}{\beta})^2 + \quad [5]$$

$$\sum_{j=1}^{n_1}\ln\Phi(z_{1j}) + \sum_{j=1}^{n_2}\ln\Phi(-z_{2j}) + \sum_{j=1}^{n_3}\ln[\Phi(z_{bj}) - \Phi(z_{aj})]$$

where $z_i \equiv (\alpha + \beta\, t_i - x_i)/\beta\sigma$; $\mathbf{y}_0$, $\mathbf{t}_1$, $\mathbf{t}_2$, and $\mathbf{t}_3$ are the collection of announced yields.

Solving $\frac{\partial \ln L}{\partial \sigma} \equiv 0$ implies immediately that the $\hat{\sigma}$ must satisfy the following necessary condition:

$$\sigma^2 = \frac{\sum_{j=1}^{n_0}(y_{0j} - \frac{x_{0j}-\alpha}{\beta})^2}{n_0 + \sum_{j=1}^{n_1}\frac{\phi(z_{1j})}{\Phi(z_{1j})}z_{1j} - \sum_{j=1}^{n_2}\frac{\phi(z_{2j})}{\Phi(-z_{2j})}z_{2j} + \sum_{j=1}^{n_3}\frac{\phi(z_{bj})z_{bj} - \phi(z_{aj})z_{aj}}{\Phi(z_{bj}) - \Phi(z_{aj})}} \quad [6]$$

Solving $\frac{\partial \ln L}{\partial A} \equiv 0$ implies that the sum of the "refined residuals" should be zero. Solving $\frac{\partial \ln L}{\partial B} \equiv 0$ implies that the vector of refined residuals should be orthogonal to the vectors of means. It follows that the optimal estimate of A and B can be obtained by the "standard least squares" inversion with the censored data all replaced by their

conditional expectations, *i.e.*, the "refined observations". Thus σ can be solved iteratively with [6] along with α and β using the EM algorithm. In the non-censored case, this "MLE-CY" code gives results identical to those derived by the standard least squares.

II.3.3 A General m_b-Yield Regression Routine with Uncertain Data: DWLSQ

Even the 19 Semipalatinsk explosions for which the "exact" yields were published would inevitably be subject to many sources of error. The Soviets might have rounded 8 of the announced 19 yields to the nearest 5 kt or 10 kt. An announced yield of 100 kt (*e.g.*, 660320D) could mean something actually measured between 95 kt and 104 kt. It could also indicate that 100 kt was the designed energy release, and the actual yield was somewhere nearby. Likewise, the "real yield" of 2 kt (*e.g.*, 720902M) could be something between 1.5 kt and 2.4 kt. Below 100 kt, the rounding errors could overwhelm the presumed standard measurement error --- assuming the announced yields are not otherwise "fudged".

A more general regression routine has been developed to take the rounding and standard errors in the yields into account (Jih, 1991). For each (m_b, yield) pair, we use a random number generator to produce a perturbed (m_b, yield) pair according to their uncertainty distribution. A standard least-squared regression is then performed for each data set of 19 perturbed pseudo-observations. The procedure is repeated for several hundred iterations, and all the resulting calibration curves are then used to infer the ensemble behavior. This "doubly-weighted least-squares scheme" is an extension to the "ordinary weighted least-squares" in which only errors in the m_b would be used to adjust the inferred parameters.

The "upper 95% confidence limit" of the predicted m_b at a given log(yield) level (say, Y_0) can be computed as follows:

$$\hat{m}_b(\max) + t(\text{D.O.F.},0.975)[\sigma^2(m_b) + \sigma^2(\text{regression})(\frac{1}{N} + \frac{(Y_0 - \bar{Y})^2}{\sum(Y_i - \bar{Y})^2})]^{0.5} \quad [7]$$

where N = number of data points used in the regression, D.O.F. = N-2, $\sigma(m_b)$ = the mean S.E. in the network m_b used in the regression, σ(regression) = the σ of residuals, $\hat{m}_b(\max)$ = estimate of the largest possible mean m_b at the given log(yield) level, $\bar{Y}$ is the mean log(yield) used in the regression, and t(D.O.F., 0.975) is the 97.5 percentile of Student's *t* distribution at "D.O.F." degrees of freedom. The "lower 95% confidence limit" can be computed in a similar way.

II.3.4 Expansion of Geotech's WWSSN m_b Database

Our database of station m_b values based on the short-period vertical-component (SPZ) WWSSN [World Wide Standard Seismograph Network] recordings of body waves has been expanded to 192[1] events from a variety of regions including the N.T.S. (U.S.), French Sahara, Azgir (U.S.S.R.), Urals (U.S.S.R.), Murzhik (E. Kazakh, U.S.S.R.), Degelen Mountain (E. Kazakh, U.S.S.R.), Balapan (E. Kazakh, U.S.S.R.), Novaya Zemlya (U.S.S.R.), Tuamoto Islands (France), Rajasthan (India), and Lop Nor (Sinjiang, China). This database consists of 515 usable "a" (*i.e.*, zero-crossing to first peak), "b" (*i.e.*, first peak to first trough), and "max" (*i.e.*, max peak-to-trough or trough-to-peak in the first 5 seconds) event phases. Jih *et al.* (1990b) reported evidences which indicate that the GLM network m_b values inferred from these WWSSN recordings are better than many other magnitude measurements.

[1] 111 events were measured by R. A. Wagner, M. E. Marshall, R. O. Ahner, and J. A. Burnetti under previous contracts during the past decade. R. A. Wagner added 56 more events to Geotech's m_b database during FY90-91. The remaining 25 events were adapted from the data that DARPA distributed in 1988.

II.3.5 Magnitude-Yield Relationship at Semipalatinsk Area

A systematic comparative analysis of the magnitude-yield relationship at three regions (Balapan [= Shagan River] , Degelen, and Murzhik [= Konystan]) of Semipalatinsk, Eastern Kazakhstan, U.S.S.R. has been conducted using miscellaneous unclassified magnitudes as well as the recently published yields of 96 Soviet explosions. Only the most noteworthy observations are summarized here:

- 1 **MLE-CY and DWLSQ vs. Ericsson's code.** Including the censored yields in the regression does generally improve the accuracy of the yield estimates slightly, if the magnitudes are "consistent". The "MLE-CY" code is robust in detecting the inherent inconsistency of the magnitudes by utilizing the censored information.

  In reality, both the magnitude and the yield measurements are subject to error. Pending the determination as to which of the two extreme hypotheses, namely $\sigma(m_b)/\sigma(Y) = 0$ and $\sigma(m_b)/\sigma(Y) = \infty$, is closer to the real situation, we also applied Ericsson's (1971) curve-fitting method[2] to the regressions of non-censored yields using various $\sigma(m_b)/\sigma(Y)$ ratios. As expected, we can see the smooth transition of estimated parameters (*i.e.*, the slope and the intercept) as $\sigma(m_b)/\sigma(Y)$ varies. Thus the censored cases with nontrivial $\sigma(m_b)/\sigma(Y)$ values could also be "interpolated" accordingly (Jih *et al.*, 1990b). Note that Ericsson's (1971) method allows different variances in both the independent and the dependent variables in the regression. However, it can be applied to the non-censored case only. "MLE-CY" and Ericsson's methods represent two different directions in extending the standard least squares. "DWLSQ" is even more flexible than Ericsson's code in that it permits the errors in each (m_b, yield) pair to be arbitrary.

- 2 **Rounding Errors vs. Gaussian Errors in the Yields.** There has been some concern about the accuracy and precision of the Soviet published yields. It turns out that, so long as the best m_b (such as $\overline{m}_{2.9}$) is used, the uncertainty factor in the predicted yield of future Semipalatinsk events is not very sensitive to the

[2] Code provided by R. H. Shumway and T. M. McElfresh

postulated uncertainty (precision) in the published yields of the 19 events. Also, the yields of future underground explosions in the Semipalatinsk area can be estimated seismically with a capability much better than the factor-of-2 uncertainty that is commonly reported. For instance, a factor of 1.5 could be a reasonable uncertainty estimate at around the 50-kt level if $\overline{m}_{2.9}$ is used as the source measure. At yields below 10 kt small variations of the physical environment may produce greater uncertainty. Therefore, the uncertainty may be inherently greater at such low yield level.

Table 4. Inferred Calibration Parameters and Associated Uncertainty Factors

Uncertainty in yield	Slope	Intercept	1kt	10kt	50kt	100kt	150kt
R.E. + 20% S.E.	0.793±0.031	4.308±0.050	4.14	2.04	2.09	2.55	2.89
R.E. + 10% S.E.	0.804±0.022	4.288±0.038	3.23	1.82	1.67	1.88	2.04
R.E. + 5% S.E.	0.805±0.020	4.286±0.035	3.11	1.78	1.53	1.64	1.77
R.E. + 2% S.E.	0.806±0.020	4.285±0.035	3.33	1.81	1.53	1.69	1.82
R.E. + 1% S.E.	0.805±0.020	4.287±0.035	3.04	1.80	1.49	1.60	1.75
R.E. Only	0.807±0.019	4.284±0.034	3.04	1.83	1.54	1.60	1.72
20% S.E.	0.794±0.031	4.306±0.049	4.08	2.16	1.88	2.23	2.50
10% S.E.	0.807±0.018	4.282±0.027	2.83	1.74	1.60	1.77	1.91
5% S.E.	0.811±0.012	4.277±0.018	2.41	1.62	1.51	1.61	1.71
2% S.E.	0.811±0.009	4.276±0.014	2.33	1.57	1.48	1.57	1.64
1% S.E.	0.812±0.009	4.275±0.014	2.32	1.57	1.49	1.57	1.64
0.1% S.E.	0.812±0.009	4.275±0.014	2.32	1.57	1.49	1.57	1.64

R.E.: Rounding Error ; S.E.: Standard Error

- 3 **Yield estimates of recent Balapan explosions.** Ringdal and Hokland (1987) noted that, for Balapan explosions detonated after 1976, the largest peak of clustered NORSAR *RMS* L_g values was 6.06. It corresponds to 138 kt on the calibration curve derived with "DWLSQ":

$$RMS\ L_g = 4.54(\pm 0.050) + 0.71(\pm 0.028)\ \log(W) \qquad [8]$$

which is almost identical to the mean yield of 139±7 kt computed by Sykes and Ruggi (1989) using the 9 largest Balapan shots during 1976-1985.

- 4 **Depth-yield scaling at Eastern Kazakhstan.** The Soviet-announced burial depths [DOB] indicate a strong tendency to detonate Semipalatinsk explosions at a "scale depth", Ds, (*i.e.*, the DOB scaled to a yield of 1 kt) of 117 meters, based on the relation

$$\text{DOB (meters)} = 117 \cdot [\text{W(kt)}]^{0.25} \qquad [9]$$

[9] is determined using 18 Semipalatinsk events (4 Balapan, 6 Murzhik, and 8 Degelen) of known yields and DOB. The yields are assumed to be perturbed by 10% standard error, and the DOB are subject to 0.1% error. Deleting the 8 Degelen events gives very similar result with smaller scatter and slightly larger Ds:

$$\text{DOB (meters)} = 145 \cdot [\text{W(kt)}]^{0.24} \qquad [10]$$

For explosions from Murzhik and Balapan test sites, the focal depths correlate with the announced yields even better than m_b(NEIS), m_b(EKA), m_b(4 UK arrays), and log(M_o, 4 UK arrays) (*cf.* Table 5D of Jih *et al.*, 1990b). Both [9] and [10] strongly suggest that the DOBs of historical Semipalatinsk explosions appeared to be proportional to the **quartic root** of the yields instead of the **cubic root** as observed at NTS. Degelen explosions tend to be underburied except the event 660507. The Soviets seem to have been pushing the DOBs to the shallow limit (and thereby accepting the possible containment risks) at Degelen Mountain during the period 1961-1972.

• 5 **Test site bias.** There have been several studies which indicate that Nuttli's (1987) "Degelen puzzle" (Table 5) could be invalid because of the relatively poorer quality m_b(ISC) used (jih *et al.*, 1990). The updated m_b bias estimate between Eastern Kazakhstan and NTS is systematically larger than 0.35 if m_b values reported by TG, S-cubed, or UK/AWE are used (Table 6; see also Evernden and Marsh, 1987). The WWSSN data reveal a m_b bias of 0.13 m.u. (relative to NORSAR's *RMS* L_g) between the SW and NE subregions of Balapan Test Site, which confirms what Ringdal and Marshall (1989) found with ISC and NORSAR data. Relative to m_b, L_g-yield relationship does appear to be more transportable, as indicated by the insignificant difference between KTS and NTS calibration curves using *RMS* L_g (Table 6).

Table 5. Nuttli's (1987) Estimates of m_b Bias (Relative to $m_b(L_g)$)

Test Sites	Magnitude Used	10 kt	100 kt	150 kt
Balapan - NTS	m_b(ISC), $m_b(L_g)$	0.35	0.35	0.35
Degelen - NTS	m_b(ISC), $m_b(L_g)$	0.58	0.58	0.58

Table 6. Updated Estimates of Test Site Bias				
Magnitudes Used		KTS-NTS Bias		
KTS	NTS	10 kt	100 kt	150 kt
Marshall *et al.*[1]	Marshall *et al.*[2]	0.55	0.48	0.46
Jih and Wagner[3]	Jih and Wagner[4]	0.47	0.42	0.41
Jih and Wagner[3]	Murphy[5]	0.36	0.36	0.36
Murphy[6]	Murphy[5]	0.47	0.41	0.40
Ringdal[7]	Patton[8]	0.09	0.05	0.04
Israelson[9]	Patton[8]	0.04	0.06	0.07

1) Combining all UK/AWE's Balapan, Degelen, and Murzhik m_b values as listed in Vergino (1989).

2) UK/AWE's NTS m_b values as distributed in 1987.

3) m_b = 0.81 log(W) + 4.28 using 19 KTS explosions with published yields (Jih and Wagner, 1991).

4) m_b = 0.86 log(W) + 3.76 for NTS high-coupling events (Jih and Wagner, 1991).

5) m_b(S-cubed) = 0.75 log(W) + 4.45 based on the network-averaged spectra (Murphy, 1990).

6) m_b(S-Cubed) = 3.92 + 0.81 log(W) for NTS high-coupling events (Murphy, 1981).

7) RMS L_g = 0.71 log(W) + 4.54 with NORSAR RMS L_g furnished by Ringdal (1990).

8) $m_b(L_g)$ = 0.76 log(W) + 4.40 with LLN data (Patton, 1988).

9) RMS L_g = 0.78 log(W) + 4.42 based on RMS L_g values furnished by Israelson (1991b) (Jih, 1991).

- 6 **Cratering to non-cratering correction.** The new calibration curve for Balapan explosions also provides an alternative and straightforward approach to derive the m_b adjustment converting cratering shots to contained explosions of the same yield (*cf.* Table 8A of Jih *et al.*, 1990b). The correction derived by this approach matches that by other studies rather well.

- 7 **Distinct features of Degelen and Balapan sites.** Degelen Mountain is the only test site that has a decreasing $\log(P_{max}/P_a)$ and $\log(P_b/P_a)$ with increasing yields (*cf.* Table 8A of Jih *et al.*, 1990b). It is also the only test site for which the phase "a" shows the smallest scatter around the calibration curve, as compared to the phases "b" and "max" (*cf.* Table 6C of Jih *et al.*, 1990b). Both the mountainous topography (which causes complex pP interference) as well as the testing practice (*e.g.*, the abnormally shallow shot depths and the usage of tunnels) could be responsible. At Balapan, the phase "b" has the smallest scatter around the

calibration curve (*cf.* Table 5C of Jih *et al.*, 1990b). These observations confirm the conjecture that the first cycle could give better results than does the "max" phase in a proper environment.

- 8 **Benchmark of various magnitudes.** For Balapan events, *RMS* L_g reported at NORSAR (Ringdal and Marshall, 1989; Ringdal and Hansen, 1989) and $\overline{m}_{2.9}$ based on WWSSN provide the smallest scatter around the calibration curve. In fact, even $\overline{m}_{2.2}$ would seem to be better than almost all other unclassified magnitudes based on the teleseismic P waves or $\log(\Psi_\infty)$ in terms of yield estimation as well as the m_b scaling against Ringdal's *RMS* L_g.
- 9 **Abnormal events detected by MLE-CY.** The Balapan cratering event 650115 (100-150 kt, 178 meters) and four events at Degelen Mountain (641116, 194 meters; 660629, 187 meters; 661019, 185 meters; and 671017, 181 meters) were rejected by the "MLE-CY" code as outliers. All 4 of these Degelen events were said to have yields between 20 and 150 kt. However, a fully contained explosion at Balapan or Murzhik regions with a shallow DOB of 180 meters or so would be expected to have a yield near 2 kt (*e.g.*, Murzhik event 720902) rather than any value between 20 and 150 kt. Another interesting event is Degelen event 660507 which has an announced yield of 4 kt and a remarkably deep DOB (as compared to Balapan and Murzhik explosions). Perhaps an experiment with a much larger yield was planned for that explosion.

II.3.6 REPORTS, PRESENTATIONS, AND PUBLICATIONS

The publications and presentations generated during the contract period are listed as follows:

(1989) Iterative network magnitude estimation and uncertainty assessment with noisy and clipped data, *Seism. Res. Let.*, **60-1**, 28, presented at 1989 Annual SSA Meeting, Victoria, British Columbia, Canada.

(1989) Finite-difference simulations of near-regional propagation --- preliminary results, presented at *MIT/ERL 3rd Annual Workshop on Seismic Wave Propagation and Inversion in Heterogeneous Media* (July 31 - August 3, 1989, Boston, MA.)

(1989) Iterative network magnitude estimation and uncertainty assessment with noisy and clipped data, *Bull. Seismo. Soc. Am.*, **79,** 1122-1141.

(1989) Iterative network magnitude estimation and uncertainty assessment with noisy and clipped data, presented at *Mid-Atlantic Regional Probability and Statistics Meeting* (October 21, 1989, N.I.S.T., Gaithersburg, MD.)

(1989) Simultaneous modeling of teleseismic and near regional phases with linear finite-difference method, *EOS, Trans. Am. Geophys. Union,* **70-43,** 1189 (1989 Fall AGU Meeting, San Francisco, CA.)

(1990) Magnitude-yield relationship at various nuclear test sites --- a maximum-likelihood approach using heavily censored explosive yields, *Report GL-TR-90-0107 (=TGAL-90-03),* Geophysics Laboratory, Hanscom AFB, MA. **(ADA223490)**

(1990) Maximum-likelihood magnitude-yield regression with heavily censored data, *EOS, Trans. Am. Geophys. Union,* **71-17,** 566 (1990 Spring AGU Meeting, Baltimore, MD.)

(1990) Geotech's magnitude-yield study during 1989-1990, *Proceedings of 12th DARPA/AFGL Seismic Research Symposium,* 281-287 (18-20 Sept 1990, Key West, FL.) (Eds J. Lewkowicz and J. McPhetres), *Report GL-TR-90-0212,* Geophysics Laboratory, Hanscom Air Force Base, MA. **(ADA226635)**

(1990) m_b bias between Balapan and Degelen Test Sites, U.S.S.R, as revealed by direct regression of WWSSN data on Soviet-published censored and uncensored yields, *EOS, Trans. Am. Geophys. Union,* **71-43,** 1477 (1990 Winter AGU Meeting, San Francisco, CA.)

(1991) Azimuthal variation of m_b residuals of E. Kazakh explosions and assessment of the path effects, *EOS, Trans. Am. Geophys. Union,* **72-17**, 193 (1991 Spring AGU Meeting, Baltimore, MD.)

(1991) A refined network m_b determination scheme incorporating near-source effects, in *Report PL-TR-91-2212 (=TGAL-91-05),* Phillips Laboratory, Hanscom Air Force base, MA.

(1991) Recent methodological developments in magnitude determination and yield estimation with applications to Semipalatinsk explosions (Section A of *"Explosion source size determination, discrimination, and spectral characteristics"), Proceedings of 13th DARPA/PL Seismic Research Symposium,* (8-10 Oct 1991, Keystone,

CO.) (Eds J. Lewkowicz and J. McPhetres), *PL-TR-91-2208,* Phillips Laboratory, Hanscom Air Force base, MA. **(ADA241325)**

II.4. CONCLUSIONS AND RECOMMENDATIONS

The new magnitude determination scheme (Equation [1]) significantly reduces the fluctuational variation across the recording stations, as illustrated in this study. It is shown that, by applying this scheme to worldwide explosions, it is possible to have a consistent base line in estimating the absolute magnitudes (which is crucial in estimating the test site bias) while the precision in the resulting network m_b values can be maintained as well as could be achieved by the single-test-site approach. The standard error in most $\overline{m}_{2.9}$ values is 0.02 m.u., about the same as that for *RMS* L_g inferred from in-country regional recordings reported by Israelson (1991a) and Hansen *et al.* (1990).

The most detailed description of the wave propagation model would naturally suggest that yet another term could be added into the Equation [1] to count for the source-region attenuation. So far such source region bias in m_b has always been inferred with other information such as the yields (as in this study), M_S (*e.g.*, Evernden and Marsh, 1987) or P_n velocity (*e.g.*, Marshall *et al.*, 1979) *etc.*. The hypothesis that such attenuation differential could be directly discerned from m_b alone by further improving Equation [1] is worth testing.

The two regression routines developed in this study (*i.e.*, "MLE-CY" and "DWLSQ") represent two very different directions in extending the standard least-squares regression. They should be merged together for a more general and robust tool.

Digital signals recorded on in-country seismic instruments at regional distance will be critical for monitoring low yield explosions below 10 kt. Obviously the regression routines developed in this study can well be applied to other source measures which are based on regional phases. On the other hand, teleseismic data such as the

WWSSN data used in this study still carry invaluable information that are worthy of further exploitation, beyond simply calculating the "unified yield".

Throughout this study, our emphasis has been to reveal the site-dependent characteristics from the observations exclusively so that in the future the inferred results can be critically examined and compared with those derived by other means. We suggest that the follow-up research be accompanied by well-constrained forward modeling studies using realistic structures. The upgraded LFD code which incorporates boundary conditions for topographical free-surface of arbitrary shape (Jih *et al.*, 1988) in addition to the "strain filter" and "marching grid" features as outlined in Jih *et al.* (1989) can be utilized in the future to improve our understanding of the fundamental issues of seismic energy partitioning on the focal sphere as well as their implications for yield determination.

II.5 ACKNOWLEDGEMENTS

Many Geotech staff and outside scholars have contributed to this research. I am indebted to many useful discussions with Robert R. Blandford, Paul G. Richards, Peter D. Marshall, Alan S. Ryall, Frode Ringdal, William Leith, Robert Herrmann, and Chris S. Lynnes. The SPZ amplitudes of 111 events collected prior to this contract were measured by Robert A. Wagner, Margaret E. Marshall, Russel O. Ahner, and James A. Burnetti under various DARPA-sponsored contracts. Robert Wagner alone measured all of those amplitudes added during FY90-91. Robert H. Shumway and Tom McElfresh provided Ericsson's code which was used in the report *GL-TR-90-0107*. Chris S. Lynnes installed a graphic library which translates all the figures into PostScript-formatted outputs. Robert K. Cessaro installed the graphic routine "PLOTXY" originally designed by Robert Parker and Loren Shure. I find this utility routine to be very handy and easy to use (*cf.* Figures 6 through 10 of Section I, this volume). Abdul Mailk digitized the geologic map of Semipalatinsk region based on

Bonham *et al.* (1980). Wilmer Rivers ported the code "MLE-CY" to classified computer facility at CSS, and he also reviewed all manuscripts generated under this project. Richard Baumstark, Tom McElfresh, and Mary Ann Brennan always provide prompt answers and assistance on our questions about more efficient use of UNIX software. This research was supported under DARPA contract F19628-89-C-0063, monitored by Phillips Laboratory. The views and conclusions contained in this paper are those of the author and should not be interpreted as representing the official policies, either expressed or implied, of the Defense Advanced Research Projects Agency or the U.S. Government.

II.6. REFERENCES

Bache, T. C. (1982). Estimating the yield of underground nuclear explosions, *Bull. Seism. Soc. Am.*, **72-6**, S131-168.

Blandford, R. R., and R. H. Shumway (1982). Magnitude:yield for nuclear explosions in granite at the Nevada Test Site and Algeria: joint determination with station effects and with data containing clipped and low-amplitude signals, *Report VSC-TR-82-12,* Teledyne Geotech, Alexandria, Virginia.

Bocharov, V. S., S. A. Zelentsoz, and V. Mikhailov (1989). Characteristics of 96 underground nuclear explosions at the Semipalatinsk test site, *Atomic Energy,* **67,** 210-214

DARPA (1981). *A technical assessment of seismic yield estimation, Report DARPA-NMR-81-02,* DARPA/NMRO, Arlington, VA.

Ericsson, U. (1971). Maximum-likelihood linear fitting when both variables have normal and correlated error, *Report C4474-A1,* Research Institute of National Defense, Stockholm, Sweden.

Evernden, J. F. and G. E. Marsh (1987). Yields of U.S. and Soviet nuclear tests, *Physics Today,* **8-1,** 37-44.

Hansen, R. A., Ringdal, F. and P. G. Richards (1990). The stability of *RMS* L_g measurements and their potential for accurate estimation of yields of Soviet underground nuclear explosions, *Bull. Seism. Soc. Am.*, **80-6**, 2106-2126.

Israelson, H. (1991a). RMS magnitude for Novaya Zemlya events (abstract), *EOS, Trans. A.G.U.*, **72-17**, 193.

Israelson, H. (1991b). Analysis of historical USSR seismograms - RMS magnitudes, yields, and depths of explosions at the Semipalatinsk Test Site, *Proceedings of 13th DARPA/PL Seismic Research Symposium, 8-10 Oct 1991, Keystone, CO.* (Eds J. Lewkowicz and J. McPhetres), *Report PL-TR-91-2208,* Phillips Laboratory, Hanscom Air Force Base, MA. **(ADA241325)**

Jih, R.-S. (1991). m_b-yield regression with uncertain data: a Monte-Carlo approach with applications to Semipalatinsk explosions *(manuscript submitted).*

Jih, R.-S., C. S. Lynnes, D. W. Rivers, and I. N. Gupta (1989). Simultaneous modeling of teleseismic and near regional phases with linear finite-difference method (abstract), *EOS, Trans. A.G.U.*, **70-43**, 1189.

Jih, R.-S., K. L. McLaughlin and Z. A. Der (1988). Free boundary conditions of arbitrary polygonal topography in a 2-D explicit elastic finite difference scheme, *Geophysics,* **53,** 1045-1055.

Jih, R.-S. and R. A. Wagner (1990). m_b bias between Balapan and Degelen test sites, U.S.S.R., as revealed by direct regression of WWSSN data on Soviet-released censored and uncensored yields (abstract), *EOS, Trans. A.G.U.*, **71-43,** 1477.

Jih, R.-S. and R. A. Wagner (1991a). Azimuthal variation of m_b residuals of E. Kazakh explosions and assessment of the path effects (abstract), *EOS, Trans. A.G.U.*, **72-17**, 193.

Jih, R.-S. and R. A. Wagner (1991b). A refined network m_b determination scheme incorporating near-source effects, in *Report PL-TR-91-2212 (=TGAL-91-05),* Phillips Laboratory, Hanscom Air Force Base, MA.

Jih, R.-S., R. A. Wagner, and T. W. McElfresh (1990). Magnitude-yield relationship at various nuclear test sites, in *Report GL-TR-90-0107 (=TGAL-90-03),* Geophysics Laboratory, Hanscom Air Force Base, MA. **(ADA223490)**

Jih, R.-S., and R. H. Shumway (1989). Iterative network magnitude estimation and uncertainty assessment with noisy and clipped data, *Bull. Seism. Soc. Am.*, **79,** 1122-1141.

Marshall, P. D., D. L. Springer, and H. C. Rodean (1979). Magnitude corrections for attenuation in the upper mantle, *Geophys. J. R. astr. Soc.*, **57,** 609-638.

Murphy, J. (1981). Body wave coupling theory, in *"A technical assessment of seismic yield estimation", Report DARPA-NMR-81-01, Appendix,* DARPA/NMRO,

Arlington, VA.

Murphy, J. R. (1990). A new system for seismic yield estimation of underground explosions, in *Proceedings of the 12th DARPA/GL Seismic Research Symposium, (18-20 Sept 1990, Key West, FL.)* (Eds J. Lewkowicz and J. McPhetres), *Report GL-TR-90-0212,* Geophysics Laboratory, Hanscom Air Force Base, MA. **(ADA226635)**

Nuttli, O. W. (1987). L_g magnitudes of Degelen, East Kazakhstan, underground explosions, *Bull. Seism. Soc. Am.*, **77,** 679-681.

Patton, H. J. (1988). Application of Nuttli's method to estimate yield of Nevada Test Site explosions recorded on Lawrence Livermore National Laboratory's digital seismic system, *Bull. Seism. Soc. Am.*, **78,** 1759-1772.

Ringdal, F. (1976). Maximum likelihood estimation of seismic magnitude, *Bull. Seism. Soc. Am.*, **66,** 789-802.

Ringdal, F. (1990). NORSAR detection and yield estimation studies, in *Proceedings of the 12th DARPA/GL Seismic Research Symposium, (18-20 Sept 1990, Key West, FL.)* (Eds J. Lewkowicz and J. McPhetres), *Report GL-TR-90-0212,* Geophysics Laboratory, Hanscom Air Force Base, MA. **(ADA226635)**

Ringdal, F. and R. A. Hansen (1989). NORSAR yield estimation studies, *Proceedings of AFTAC/DARPA 1989 Seismic Research Review* (28-29 Nov 1989, Patrick AFB, Florida), 145-156.

Ringdal, F. and B. K. Hokland (1987). Magnitude of large Semipalatinsk explosions using *P* coda and L_g measurements at NORSAR, Semiannual Technical Summary, 1 April 1987 - 30 Sept 1987, *NORSAR Scientific Report No. 1-87/88,* NTNF/NORSAR, Kjeller, Norway.

Ringdal, F. and P. D. Marshall (1989). Yield determination of Soviet underground nuclear explosions at the Shagan River Test Site, Semiannual Technical Summary, 1 Oct 1988 - 31 Mar 1989 (L. B. Loughran ed.), *NORSAR Scientific Report No.2-88/89,* NTNF/NORSAR, Kjeller, Norway.

Sykes, L. R. and S. Ruggi (1989). Soviet nuclear testing, in Nuclear Weapon Databook (Volume IV, Chapter 10), Natural Resources Defense Concil, Washington D. C.

Vergino, E. S. (1989). Soviet test yields, *EOS, Trans. A.G.U.*, Nov 28, 1989.

von Seggern, D. and D. W. Rivers (1978). Comments on the use of truncated distribution theory for improved magnitude estimation, *Bull. Seism. Soc. Am.*, **68,** 1543-1546.

Prof. Thomas Ahrens
Seismological Lab, 252-21
Division of Geological & Planetary Sciences
California Institute of Technology
Pasadena, CA 91125

Prof. Keiiti Aki
Center for Earth Sciences
University of Southern California
University Park
Los Angeles, CA 90089-0741

Prof. Shelton Alexander
Geosciences Department
403 Deike Building
The Pennsylvania State University
University Park, PA 16802

Dr. Ralph Alewine, III
DARPA/NMRO
3701 North Fairfax Drive
Arlington, VA 22203-1714

Prof. Charles B. Archambeau
CIRES
University of Colorado
Boulder, CO 80309

Dr. Thomas C. Bache, Jr.
Science Applications Int'l Corp.
10260 Campus Point Drive
San Diego, CA 92121 (2 copies)

Prof. Muawia Barazangi
Institute for the Study of the Continent
Cornell University
Ithaca, NY 14853

Dr. Jeff Barker
Department of Geological Sciences
State University of New York
at Binghamton
Vestal, NY 13901

Dr. Douglas R. Baumgardt
ENSCO, Inc
5400 Port Royal Road
Springfield, VA 22151-2388

Dr. Susan Beck
Department of Geosciences
Building #77
University of Arizona
Tuscon, AZ 85721

Dr. T.J. Bennett
S-CUBED
A Division of Maxwell Laboratories
11800 Sunrise Valley Drive, Suite 1450
Reston, VA 22091

Dr. Robert Blandford
AFTAC/TT, Center for Seismic Studies
1330 North 17th Street
Suite 1450
Arlington, VA 22209-2308

Dr. G.A. Bollinger
Department of Geological Sciences
Virginia Polytechnical Institute
21044 Derring Hall
Blacksburg, VA 24061

Dr. Stephen Bratt
Center for Seismic Studies
1300 North 17th Street
Suite 1450
Arlington, VA 22209-2308

Dr. Lawrence Burdick
Woodward-Clyde Consultants
566 El Dorado Street
Pasadena, CA 91109-3245

Dr. Robert Burridge
Schlumberger-Doll Research Center
Old Quarry Road
Ridgefield, CT 06877

Dr. Jerry Carter
Center for Seismic Studies
1300 North 17th Street
Suite 1450
Arlington, VA 22209-2308

Eric Chael
Division 9241
Sandia Laboratory
Albuquerque, NM 87185

Prof. Vernon F. Cormier
Department of Geology & Geophysics
U-45, Room 207
University of Connecticut
Storrs, CT 06268

Prof. Anton Dainty
Earth Resources Laboratory
Massachusetts Institute of Technology
42 Carleton Street
Cambridge, MA 02142

Prof. Steven Day
Department of Geological Sciences
San Diego State University
San Diego, CA 92182

Marvin Denny
U.S. Department of Energy
Office of Arms Control
Washington, DC 20585

Dr. Zoltan Der
ENSCO, Inc.
5400 Port Royal Road
Springfield, VA 22151-2388

Prof. Adam Dziewonski
Hoffman Laboratory, Harvard University
Dept. of Earth Atmos. & Planetary Sciences
20 Oxford Street
Cambridge, MA 02138

Prof. John Ebel
Department of Geology & Geophysics
Boston College
Chestnut Hill, MA 02167

Eric Fielding
SNEE Hall
INSTOC
Cornell University
Ithaca, NY 14853

Dr. Mark D. Fisk
Mission Research Corporation
735 State Street
P.O. Drawer 719
Santa Barbara, CA 93102

Prof Stanley Flatte
Applied Sciences Building
University of California, Santa Cruz
Santa Cruz, CA95064

Dr. John Foley
NER-Geo Sciences
1100 Crown Colony Drive
Quincy, MA 02169

Prof. Donald Forsyth
Department of Geological Sciences
Brown University
Providence, RI 02912

Art Frankel
U.S. Geological Survey
922 National Center
Reston, VA 22092

Dr. Cliff Frolich
Institute of Geophysics
8701 North Mopac
Austin, TX 78759

Dr. Holly Given
IGPP, A-025
Scripps Institute of Oceanography
University of California, San Diego
La Jolla, CA 92093

Dr. Jeffrey W. Given
SAIC
10260 Campus Point Drive
San Diego, CA 92121

Dr. Dale Glover
Defense Intelligence Agency
ATTN: ODT-1B
Washington, DC 20301

Dr. Indra Gupta
Teledyne Geotech
314 Montgomery Street
Alexanderia, VA 22314

Dan N. Hagedon
Pacific Northwest Laboratories
Battelle Boulevard
Richland, WA 99352

Dr. James Hannon
Lawrence Livermore National Laboratory
P.O. Box 808
L-205
Livermore, CA 94550

Dr. Roger Hansen
AFTAC/TTR
Patrick AFB, FL 32925

Prof. David G. Harkrider
Seismological Laboratory
Division of Geological & Planetary Sciences
California Institute of Technology
Pasadena, CA 91125

Prof. Danny Harvey
CIRES
University of Colorado
Boulder, CO 80309

Prof. Donald V. Helmberger
Seismological Laboratory
Division of Geological & Planetary Sciences
California Institute of Technology
Pasadena, CA 91125

Prof. Eugene Herrin
Institute for the Study of Earth and Man
Geophysical Laboratory
Southern Methodist University
Dallas, TX 75275

Prof. Robert B. Herrmann
Department of Earth & Atmospheric Sciences
St. Louis University
St. Louis, MO 63156

Prof. Lane R. Johnson
Seismographic Station
University of California
Berkeley, CA 94720

Prof. Thomas H. Jordan
Department of Earth, Atmospheric &
Planetary Sciences
Massachusetts Institute of Technology
Cambridge, MA 02139

Prof. Alan Kafka
Department of Geology & Geophysics
Boston College
Chestnut Hill, MA 02167

Robert C. Kemerait
ENSCO, Inc.
445 Pineda Court
Melbourne , FL 32940

Dr. Max Koontz
U.S. Dept. of Energy/DP 5
Forrestal Building
1000 Independence Avenue
Washington, DC 20585

Dr. Richard LaCoss
MIT Lincoln Laboratory, M-200B
P.O. Box 73
Lexington, MA 02173-0073

Dr. Fred K. Lamb
University of Illinois at Urbana-Champaign
Department of Physics
1110 West Green Street
Urbana, IL 61801

Prof. Charles A. Langston
Geosciences Department
403 Deike Building
The Pennsylvania State University
University Park, PA 16802

Prof. Thorne Lay
Institute of Tectonics
Earth Science Board
University of California, Santa Cruz
Santa Cruz, CA 95064

Dr. William Leith
U.S. Geological Survey
Mail Stop 928
Reston, VA 22092

James F. Lewkowicz
Phillips Laboratory/GPEH
Hanscom AFB, MA 01731-5000

Mr. Alfred Lieberman
ACDA/VI-OA State Department Building
Room 5726
320-21st Street, NW
Washington, DC 20451

Prof. L. Timothy Long
School of Geophysical Sciences
Georgia Institute of Technology
Atlanta, GA 30332

Dr. Robert Masse
Denver Federal Building
Bos 25046, Mail Stop 967
Denver, CO 80225

Dr. Randolph Martin, III
New England Research, Inc.
76 Olcott Drive
White River Junction, VT 05001

Dr. Gary McCartor
Department of Physics
Southern Methodist University
Dallas, TX 75275

Prof. Thomas V. McEvilly
Seismographic Station
University of California
Berkeley, CA 94720

Prof. Art McGarr
U.S. Geological Survey
Mail Stop 977
U.S. Geological Survey
Menlo Park, CA 94025

Dr. Keith L. McLaughlin
S-CUBED
A Division of Maxwell Laboratory
P.O. Box 1620
La Jolla, CA 92038-1620

Stephen Miller & Dr. Alexander Florence
SRI International
333 Ravenswood Avenue
Box AF 116
Menlo Park, CA 94025-3493

Prof. Bernard Minster
IGPP, A-025
Scripps Institute of Oceanography
University of California, San Diego
La Jolla, CA 92093

Prof. Brian J. Mitchell
Department of Earth & Atmospheric Sciences
St. Louis University
St. Louis, MO 63156

Mr. Jack Murphy
S-CUBED
A Division of Maxwell Laboratory
11800 Sunrise Valley Drive, Suite 1212
Reston, VA 22091 (2 Copies)

Dr. Keith K. Nakanishi
Lawrence Livermore National Laboratory
L-025
P.O. Box 808
Livermore, CA 94550

Dr. Carl Newton
Los Alamos National Laboratory
P.O. Box 1663
Mail Stop C335, Group ESS-3
Los Alamos, NM 87545

Dr. Bao Nguyen
AFTAC/TTR
Patrick AFB, FL 32925

Prof. John A. Orcutt
IGPP, A-025
Scripps Institute of Oceanography
University of California, San Diego
La Jolla, CA 92093

Prof. Jeffrey Park
Kline Geology Laboratory
P.O. Box 6666
New Haven, CT 06511-8130

Howard Patton
Lawrence Livermore National Laboratory
L-025
P.O. Box 808
Livermore, CA 94550

Dr. Frank Pilotte
HQ AFTAC/TT
Patrick AFB, FL 32925-6001

Dr. Jay J. Pulli
Radix Systems, Inc.
2 Taft Court, Suite 203
Rockville, MD 20850

Dr. Robert Reinke
ATTN; FCTVTD
Field Command
Defense Nuclear Agency
Kirtland AFB, NM 87115

Prof. Paul G. Richards
Lamont-Doherty Geological Observatory
of Columbia University
Palisades, NY 10964

Mr. Wilmer Rivers
Teledyne Geotech
314 Montgomery Street
Alexandria, VA 22314

Dr. George Rothe
HQ AFTAC/TTR
Patrick AFB, FL 32925-6001

Dr. Alan S. Ryall, Jr.
DARPA/NMRO
3701 North Fairfax Drive
Arlington, VA 22209-1714

Dr. Richard Sailor
TASC, Inc.
55 Walkers Brook Drive
Reading, MA 01867

Donald L. Springer
Lawrence Livermore National Laboratory
L-025
P.O. Box 808
Livermore, CA 94550

Prof. Charles G. Sammis
Center for Earth Sciences
University of Southern California
University Park
Los Angeles, CA 90089-0741

Dr. Jeffrey Stevens
S-CUBED
A Division of Maxwell Laboratory
P.O. Box 1620
La Jolla, CA 92038-1620

Prof. Christopher H. Scholz
Lamont-Doherty Geological Observatory
of Columbia University
Palisades, CA 10964

Lt. Col. Jim Stobie
ATTN: AFOSR/NL
Bolling AFB
Washington, DC 20332-6448

Dr. Susan Schwartz
Institute of Tectonics
1156 High Street
Santa Cruz, CA 95064

Prof. Brian Stump
Institute for the Study of Earth & Man
Geophysical Laboratory
Southern Methodist University
Dallas, TX 75275

Secretary of the Air Force
(SAFRD)
Washington, DC 20330

Prof. Jeremiah Sullivan
University of Illinois at Urbana-Champaign
Department of Physics
1110 West Green Street
Urbana, IL 61801

Office of the Secretary of Defense
DDR&E
Washington, DC 20330

Prof. L. Sykes
Lamont-Doherty Geological Observatory
of Columbia University
Palisades, NY 10964

Thomas J. Sereno, Jr.
Science Application Int'l Corp.
10260 Campus Point Drive
San Diego, CA 92121

Dr. David Taylor
ENSCO, Inc.
445 Pineda Court
Melbourne, FL 32940

Dr. Michael Shore
Defense Nuclear Agency/SPSS
6801 Telegraph Road
Alexandria, VA 22310

Dr. Steven R. Taylor
Los Alamos National Laboratory
P.O. Box 1663
Mail Stop C335
Los Alamos, NM 87545

Dr. Matthew Sibol
Virginia Tech
Seismological Observatory
4044 Derring Hall
Blacksburg, VA 24061-0420

Prof. Clifford Thurber
University of Wisconsin-Madison
Department of Geology & Geophysics
1215 West Dayton Street
Madison, WS 53706

Prof. David G. Simpson
IRIS, Inc.
1616 North Fort Myer Drive
Suite 1400
Arlington, VA 22209

Prof. M. Nafi Toksoz
Earth Resources Lab
Massachusetts Institute of Technology
42 Carleton Street
Cambridge, MA 02142

Dr. Larry Turnbull
CIA-OSWR/NED
Washington, DC 20505

Dr. Gregory van der Vink
IRIS, Inc.
16116 North Fort Myer Drive
Suite 1440
Arlington, VA 22209

Dr. Karl Veith
EG&G
5211 Auth Road
Suite 240
Suitland, MD 20746

Prof. Terry C. Wallace
Department of Geosciences
Building #77
University of Arizona
Tuscon, AZ 85721

Dr. Thomas Weaver
Los Alamos National Laboratory
P.O. Box 1663
Mail Stop C335
Los Alamos, NM 87545

Dr. William Wortman
Mission Research Corporation
8560 Cinderbed Road
Suite 700
Newington, VA 22122

Prof. Francis T. Wu
Department of Geological Sciences
State University of New York
at Binghamton
Vestal, NY 13901

AFTAC/CA
(STINFO)
Patrick AFB, FL 32925-6001

DAARPA/PM
3701 North Fairfax Drive
Arlington, VA 22203-1714

DARPA/RMO/RETRIEVAL
3701 North Fairfax Drive
Arlington, VA 22203-1714

DARPA/RMO/SECURITY OFFICE
3701 North Fairfax Drive
Arlington, VA 2203-1714

HQ DNA
ATTN: Technical Library
Washington, DC 20305

Defense Intelligence Agency
Directorate for Scientific & Technical Intelligence
ATTN: DTIB
Washington, DC 20340-6158

Defense Technical Information Center
Cameron Station
Alexandria, VA 22314 (5 Copies)

TACTEC
Battelle Memorial Institute
505 King Avenue
Columbus, OH 43201 (Final Report)

Phillips Laboratory
ATTN: XPG
Hanscom AFB, MA 01731-5000

Phillips Laboratory
ATTN: GPE
Hanscom AFB, MA 01731-5000

Dr. Michel Bouchon
I.R.I.G.M.-B.P. 68
38402 St. Martin D'Heres
Cedex, FRANCE

Dr. Michel Campillo
Observatoire de Grenoble
I.R.I.G.M.-B.P. 53
38041 Grenoble, FRANCE

Dr. Kin Yip Chun
Geophysics Division
Physics Department
University of Toronto
Ontario, CANADA

Prof. Hans-Peter Harjes
Institute for Geophysics
Ruhr University/Bochum
P.O. Box 102148
4630 Bochum 1, GERMANY

Prof. Eystein Husebye
NTNF/NORSAR
P.O. Box 51
N-2007 Kjeller, NORWAY

David Jepsen
Acting Head, Nuclear Monitoring Section
Bureau of Mineral Resources
Geology and Geophysics
G.P.O. Box 378, Canberra, AUSTRALIA

Ms. Eva Johannisson
Senior Research Officer
National Defense Research Inst.
P.O. Box 27322
S-102 54 Stockholm, SWEDEN

Dr. Peter Marshall
Procurement Executive
Ministry of Defense
Blacknest, Brimpton
Reading FG7-FRS, UNITED KINGDOM

Dr. Bernard Massinon, Dr. Pierre Mechler
Societe Radiomana
27 rue Claude Bernard
75005 Paris, FRANCE (2 Copies)

Dr. Svein Mykkeltveit
NTNT/NORSAR
P.O. Box 51
N-2007 Kjeller, NORWAY (3 Copies)

Prof. Keith Priestley
University of Cambridge
Bullard Labs, Dept. of Earth Sciences
Madingley Rise, Madingley Road
Cambridge CB3 OEZ, ENGLAND

Dr. Jorg Schlittenhaardt
Federal Institute for Geosciences & Nat'l Res.
Postfach 510153
D-3000 Hannover 51, GERMANY

Dr. Johannes Schweitzer
Institute of Geophysics
Ruhr University/Bochum
P.O. Box 1102148
4360 Bochum 1, GERMANY